QUANTIFYING CARBON DIOXIDE SEQUESTRATION AND CONSTRAINING THE POTENTIAL SOURCES OF DISSOLVED METHANE AT THE TABLELANDS, GROS MORNE NATIONAL PARK, NL, CANADA; A SITE OF CONTINENTAL SERPENTINIZATION

By Emily Cumming ©

A Thesis submitted to the School of Graduate Studies in partial fulfillment of the requirements for the degree of

Master of Science

Department of Earth Sciences

Memorial University of Newfoundland

August 2018

St. John's, Newfoundland and Labrador

Abstract

Sites of continental serpentinization demonstrate natural carbon sequestration, which could be enhanced via the injection of atmospheric gas in order to offset anthropogenic greenhouse gas production.. Establishing the baseline geochemical properties of the Tablelands Ophiolite with respect to greenhouse gases (CH_4 and CO_2) required investigation into the production pathway or pathways of CH_4, and the sequestration rates of atmospheric CO_2. This thesis has constrained the source of methane emitted at the Tablelands to low-temperature (<100 ˚C) abiogenic or thermogenic synthesis, and was the first to quantify natural CO_2 sequestration for an actively serpentinizing ophiolite complex as a whole based on measurements made at multiple discrete sites within the ophiolite. Further characterization of the Tablelands Ophiolite is necessary in order to validate Global Carbon Storage (GCS) at this site as a means of mitigating anthropomorphic greenhouse gas contributions to the atmosphere.

Acknowledgements

I would first and foremost like to thank Dr. Penny Morrill for the guidance, support, and inspiration she has provided to me as my supervisor, first as an undergraduate student research assistant, then as an undergraduate honours student, and finally as a M.Sc. candidate. Her dedication to scientific pursuit is endlessly infectious, and her role in my life as a scientist has been, and will continue to be, indispensable. I am eternally grateful for all the help she has given me. I would also like to thank my committee member Dr. Tao Cheng for his encouragement and enthusiasm.

This work was supported by grants from Natural Sciences and Engineering Research Council (NSERC) Discovery Grant and Terra Nova Young Innovator Award awarded to Dr. Morrill, as well as Buchans Scholarship Fund of ASARCO Incorporated awarded to myself. I would also like to acknowledge the financial support of Memorial University of Newfoundland.

I am grateful for the intellectual, field, and analytical contributions of my collaborators, Amanda Rietze, Liam S. Morrissey, Melissa C. Cook, Jeemin H. Rhim, and Shuhei Ono. I would also like to acknowledge the technical expertise of Geert van Biesen, Alison Pye, and David Mercer.

I would like to give my thanks to all current and past members of Dr. Morrill's DELTAS research group for providing, inspiration, feedback, and help over the past five years. It's so wonderful to be part of a group of engaged scientists.

Finally, I would like to thank my friends and family – Michael, Alessandra, Mark, Carrie, and Leanne in particular - for their constant support and love. I would like to

dedicate this Thesis to my mother, Linda Mary Vecchi, as all my accomplishments can be attributed to her love.

Table of Contents

List of Tables

List of Figures

List of Abbreviations and Symbols

α – isotopic fractionation factor

% - parts per hundred

‰ – parts per thousand

°C – degrees Celsius

$\delta^{13}C$ – stable isotope composition of carbon

$\delta^{13}C_{CH4}$ - stable carbon isotope value of methane

$\delta^{2}H_{CH4}$ or δD_{CH4} - stable hydrogen isotope value of methane

$^{13}CH_3D$ - doubly-substituted ("clumped") methane isotopologues

BSC - Barnes Spring Complex

C_{2+} - the sum of ethane, propane, and butane

Ca^{2+} - calcium ion

$CaCO_3$ – calcite

CD - carbon deuterium

$CaMg(CO_3)_2$ - dolomite

CH_4 – methane

CO – carbon monoxide

CO_2 – carbon dioxide

CROMO - Coast Range Ophiolite Microbial Observatory

DIC - dissolved inorganic carbon

E_h – reduction/oxidation potential measurement

$FeCO_3$ – siderite

FID - flame ionization detector

GC – gas chromatograph

GC-C-IRMS - gas chromatography-combustion-isotope ratio mass-spectrometer

GC-PY-IRMS - gas chromatography-micropyrolysis-isotope ratio mass-spectrometer

GCCSS - Geologic Carbon Capture and Storage System

GCS - Global Carbon Storage

GFF - glass fiber filter

H_2 – hydrogen

H_2O – water

HAA - Humber Arm Allochthon

He - helium

Ma – 1 million years ago

$MgCO_3$ - magnesite

MORB - mid-ocean ridge basalts

mL - a thousandth of a litre

mph – miles per hour

mV – a thousandth of a volt

N_2 - nitrogen

N_2O - nitrous oxide

NL – Newfoundland and Labrador

pH – power of hydrogen, measure of hydrogen ion concentration

rRNA – ribosomal ribonucleic acid

TCD - thermal conductivity detector

TIC - total inorganic carbon

TLE - Tablelands East

TILDAS - tunable infrared laser direct absorption spectrometer

UNESCO – The United Nations Educational, Scientific and Cultural Organization

UUC - Unconsolidated Ultramafic Cover

UV - ultraviolet

WHB - Winter House Brook

WHC - Winter House Canyon

List of Appendices

CHAPTER 1: THESIS INTRODUCTION AND OVERVIEW

As the anthropogenic input of carbon into the atmosphere rises, and contributes to climate change, researchers are seeking to mitigate its effects by capturing atmospheric carbon and injecting it deep in the subsurface where it can be stored on a geologic timescale (Kelemen and Matter, 2008). Geological sites conducive to this storage include mid-ocean ridges and sedimentary basins, but engineering offshore carbon storage presents numerous challenges (Snæbjörnsdóttir and Gislason, 2016). Sites of continental serpentinization – or sub-aerial deposits of hydrothermally- altered ultramafic rock (ophiolites) – demonstrate natural carbon sequestration, which could be enhanced via the injection of atmospheric gas (Kelemen et al., 2011). Their geostratigraphy, geochemistry, and aereal extent make them potentially conducive to carbon storage of globally significant volumes (Kelemen et al., 2011). However, the geostratigraphy and geochemistry of individual sites of continental serpentinization must be thoroughly characterized prior to their consideration for enhanced carbon storage.

Characterization of sites of continental serpentinization must include an understanding of reactions occurring within the ophiolite that either produce or consume greenhouse gases. The interaction of subsurface water and serpentinized ultramafic rocks result in geochemical conditions that are potentially conducive to both methane production and carbon dioxide sequestration, and the injection of carbon dioxide can potentially enhance the generation of methane via numerous reaction pathways. The predominant reactions involving greenhouse gases, and the interplay thereof, must therefore be identified for each ophiolite complex prior to their being engineered for the storage of anthropogenic carbon.

1.1 Potential Sources of Methane at Sites of Serpentinization

The surficial occurrence of ultramafic lithologies globally includes subduction zones, mid-ocean ridges, the Precambrian Shield, and ophiolites. Each of these environments promote the exposure of these ultramafic rocks to aqueous hydrothermal alteration (serpentinization). Ophiolites are the most accessible of these geological settings, and are therefore ideal targets for the investigation of methane production associated with sites of serpentinization. Methane is potentially produced via multiple processes that occur within ophiolites undergoing serpentinization. These processes are the abiogenic, thermogenic, and microbial synthesis of hydrocarbons, including methane (Schoell et al., 1988).

Abiogenic hydrocarbons have been detected in ophiolites in the Philippines, Italy, Greece, Turkey, Oman, New Zealand, and Japan (Etiope (2013) and references therein), as well as the Precambrian Shield in Canada (Sherwood Lollar et al., 2008). Their production is enabled by the conditions created during serpentinization, the hydrothermal alteration of the originally anhydrous constituent minerals of an ultramafic rock, namely olivine, orthopyroxene, and clinopyroxene (Barnes et al., 1967). The hydration of these minerals results in the production of serpentine, iron and magnesium hydroxides, and H_2 gas, and in the reduction of Ca-silicates and subsequent production of subsidiary carbonates (Surour, 1997). This, in turn, results in high pH, Ca^{2+}-rich groundwater flowing through fractures in the hydrothermally altered peridotite. The hydrogen gas can potentially react with inorganic carbon to produce methane abiogenically (Sleep et al., 2004), but laboratory experiments that produced methane abiogenically suggest that these reactions may be slow (McCollom, 2016; McCollom and Donaldson, 2016).

The reactions occurring between the ophiolitic ultramafics and groundwater result in the production of ultra-basic (pH equal or greater than 11), reducing (E_h of -500 mV), Ca-rich (~1 mM) water that discharges at the surface in the form of springs (Barnes et al., 1967; Morrill et al., 2013). These reducing serpentinite springs may promote the existence and productivity of methanogenic microorganisms. Microbial methanogenesis can occur through autotrophic organic acid fermentation, such as acetate fermentation, or through heterotrophic CO_2 reduction (Kohl et al., 2016).

Methane on Earth is predominantly microbially produced (Schoell, 1988). Microbial methane has been detected in Canada's Precambrian Shield (Sherwood Lollar et al., 2008) and tentatively at the Lost City Vent Field (Brazelton et al., 2012). There is, however, limited field evidence for microbial methanogenesis associated with sites of terrestrial serpentinization. Multiple approaches are required to definitively source methane, be it microbially-mediated or otherwise. Several lines of evidence indicate that microbial methanogenesis is occurring in The Cedars Ophiolite in California, USA. Genomic methods (rRNA gene sequencing) conducted by Blank et al. (2009) have identified methanogenic archea that are believed to mediate the deposition of secondary dolomites in the Del Puerto Ophiolite, a subset of the California Coast Range, which also includes The Cedars Ophiolite. Through similar methods of rRNA gene sequencing, Suzuki et al. (2014) have identified a single archean strain within the Barnes Spring Complex (BSC) of The Cedars Ophiolite whose global distribution suggests that it is almost exclusively adapted to sites of active, terrestrial serpentinization. rRNA gene sequencing methods applied to the Samail Ophiolite in Oman have also identified a

methanogen strain (Miller et al., 2016). Using geochemical methods (Bernard plots of CH_4/C_{2+} versus $\delta^{13}C$ of CH_4), Morrill et al. (2013) suggested that methane production in the BSC of the Cedars Ophiolite was likely partially microbial, wherein heterotrophic pathways of methanogenesis that utilize organic acids as carbon substrates were plausible. These genomic (Blank et al., 2009; Suzuki et al., 2014) and geochemical (Morrill et al., 2013) studies constitute the indirect evidence of microbially mediated methane production within sites of continental serpentinization. A lab study has demonstrated direct evidence for the potential for microbial methane production at a site of continental serpentinization – The Cedars Ophiolite (Kohl et al., 2016). In that study, a kill-controlled incubation time series with water and sediment collected from the ophiolite, CH_4 production occurred in live incubations while no CH_4 was observed in killed incubations, indicating metabolism by methanogens.

In addition to abiogenic and microbial methanogenesis, methane is also produced via thermal degradation of buried organic matter, or thermogenesis. Ophiolites are commonly surrounded and underlain by a marine metasedimentary mélange that constitutes a formerly subduction-related accretionary wedge that originated as a seafloor sedimentary deposit. The extensive fracturing inherent to subduction, and subsequent obduction and emplacement of the ultramafic unit, means that conduits exist that allow thermogenic gases to be transported from the subsurface to the surface via groundwater flow. Because ophiolites may be emplaced upon an organic-bearing unit, methane produced in ultra-basic springs is potentially thermogenic (or partially thermogenic) in source. Methane produced at the Coast Range Ophiolite Microbial Observatory (CROMO) site of continental serpentinization is tentatively classified as the result of both

microbial and thermogenic methanogenesis reactions. This is based on isotopologue thermometry in conjunction with empirical observations at the site (Wang et al., 2015). Ophiolites possess characteristics that are potentially conducive to all three established pathways of methanogenesis, or a combination thereof. This holds true for the Tablelands Ophiolite.

1.2 Serpentinized Sites as Potential Sites of CO_2 Sequestration

The role of CO_2 contributes to the enigmatic geochemistry associated with the production of methane in some sites of continental serpentinization. CO_2 is consumed during the abiogenic and microbial production of methane. Additionally, the ultra-basic, Ca^{2+}-rich groundwater associated with the water-rock reaction within the ophiolite is conducive to the rapid, sometimes extensive carbonation of ophiolitic peridotite (Kelemen and Matter, 2008; Kelemen et al., 2011), whereby CO_2 is converted to solid calcium or magnesium carbonate. This has made ophiolites attractive prospective targets for Global Carbon Storage (GCS) (Kelemen and Matter, 2008), or, more specifically, the Geologic Carbon Capture and Storage System (GCCSS) (Rajendran et al., 2014).

Ophiolites are made even more attractive as targets for GCS by their relative accessibility. The largest theoretical targets for GCS are the basalts and the actively serpentinizing ultra-mafic lithologies formed continuously, extensively, and globally at mid-ocean ridges (Snæbjörnsdóttir and Gislason, 2016). Spreading creates an estimated 20 km^3 per year of mid-ocean ridge basalts (MORB) (Searle, 2013), comprising abundant reactive divalent metal cations (i.e. Ca, Mg, and Fe) available to react with dissolved CO_2 to form stable carbonate phases. These phases – calcite ($CaCO_3$), dolomite

($CaMg(CO_3)_2$), magnesite ($MgCO_3$), and siderite ($FeCO_3$) – store the reactant CO_2 on a geologic time scale (Gislason et al., 2014). However, the logistics of extensive offshore CO_2 injection are daunting. Trial offshore injections have been conducted off the southwest coast of Iceland (Alfredsson et al., 2013; Gislason et al., 2014), but ultimately engineering MORB for sequestration will require extensive testing onshore, both in a laboratory setting and in continental sites of serpentinization (Snæbjörnsdóttir and Gislason, 2016). A single flood basalt borehole in a related study (McGrail et al., 2011) constitutes the first onshore injection trial of a continental basalt. After two years of monitoring, this borehole has recorded the first observation of in-situ carbonation from CO_2 injections into basalt, and successful containment of the injected CO_2 to permeable, brecciated basalt units by overlaying impermeable units (McGrail et al., 2017). As this trial took place in basalt, the study neither accounted for the influence of serpentinization on ultramafic units, nor for the influence of resulting methanogenesis on CO_2 sequestration.

The role of CO_2 in methanogenesis at sites of serpentinization is not constrained. Likewise, the fluxes of greenhouse gases, namely CH_4 and CO_2, are also poorly constrained for these sites. Due to the ultra-basic nature of the spring water from sites of continental serpentinization, these rocks can sequester CO_2, while simultaneously emitting CH_4 via the multiple pathways associated with ophiolite diagenesis (Morrissey and Morrill, 2016; Szponar et al., 2013). Sites of continental serpentinization thereby potentially act as both a sink and a source for greenhouse gases. In order to understand the cumulative climate effect of these globally distributed sites, and to thereby effectively incorporate them into climate change models, the flux of greenhouse gases at sites of

continental serpentinization must be quantified. Greenhouse gas flux must also be quantified in order to predict whether the sequestered CO_2 will enhance CH_4 production, or precipitate as carbonate. This quantification relies on an understanding of the CH_4 source, and the role of CO_2 in methanogenesis specific to each site of continental serpentinization. These parameters must be defined prior to engineering these sites for GCCSS.

1.3 Methods for Determining the Generation Pathway of CH_4

Multiple lines of evidence are required to characterize methane generation pathways as abiogenic, thermogenic, or microbial at sites of serpentinization (Etiope, 2013; Sherwood et al., 1988). One line of evidence is known as the carbon deuterium (CD) plot, which is a graph of stable hydrogen isotope value of CH_4 (δ^2H_{CH4}) plotted against the stable carbon isotope value of CH_4 ($\delta^{13}C_{CH4}$). On the CD plot, empirically derived fields have been delineated to represent predominantly microbially mediated, thermogenically produced, and predominantly abiogenically produced CH_4, synthesized based on data from multiple laboratory and field-based studies (Sherwood Lollar et al. (2008) (with microbial and thermogenic CH_4 fields based on empirical data from Shoell (1988); Etiope et al. (2013)). However, these fields are not mutually exclusive, and overlap exists. For example, some of the world's most prevalent methanogen strains produce microbial methane whose $\delta^{13}C$ is characteristically diagnostic of thermogenic methane (Valentine et al., 2004). Similarly, the Bernard Plot (the ratio of CH_4 to the sum of ethane, propane, and butane plotted against the $\delta^{13}C_{CH4}$) has been used by oil and gas researchers to source microbial and thermogenic methane, and to demonstrate mixing

ratios when both methane sources are present. However, there is no established abiogenic field on the Bernard Plot, meaning abiogenic pathways cannot be precluded. Neither plot is capable of conclusively characterizing the source of all methane produced on Earth. Discerning the pathway of methane synthesis therefore requires multiple lines of evidence (Etiope et al., 2013).

The isotope values of methane ($\delta^{13}C_{CH4}$ and $\delta^{2}H_{CH4}$) vary considerably. This is the cumulative result of several factors not limited to their respective pathways. Such factors include whether the reaction occurred in an open or closed system, the temperature at which the methane was produced, concentrations of available reactant gases in the system, the stable isotope composition of the original reactant, and the kinetic isotopic effect associated with the formation reaction. Plotting isotopic fractionation factors (α**)** between reactants and products for both carbon and hydrogen mitigates the influence of the isotopic value of the original substrate on the methane produced. Another method used to determine the methane generation pathway at sites of serpentinization is therefore the CD fractionation plot, which graphs the stable isotope fractionation of C between dissolved inorganic carbon (DIC), total inorganic carbon (TIC), or CO_2, and CH_4 versus the stable isotope fractionation of H between water (H_2O) and CH_4 (Kohl et al., 2016; Sherwood Lollar et al., 2008). Plotting isotopic fractionation between methanogenetic reactants and products eliminates the effect of the original carbon-bearing reactants' stable carbon isotope signature.

In conjunction with the traditional approach to methane characterization based on isotope composition, the more recent isotopologue thermometry framework can further

constrain methanogenic pathways (Wang et al., 2015) by adding another dimension to methane sourcing: that of temperature (Ono et al., 2014). The relative abundance of doubly-substituted ("clumped") methane isotopologues (e.g., $^{13}CH_3D$) can further constrain the origin of methane by providing information about the temperature at which the sample of methane was formed or last equilibrated, and by identifying microbial mediation in the reactions via evidence of kinetic isotope effects (Ono et al., 2014; Stolper et al., 2014). Methane clumped isotope analysis can therefore serve as a geothermometer for methane formed in near-equilibrium processes.

1.4 The Tablelands

The Tablelands massif, a subset of the Bay of Islands ophiolite complex, originally formed at a peri-Laurentian spreading center and obducted as a result of the Taconic orogeny, a subset of the Appalachian orogeny taking place from the late Cambrian to early Silurian, and broadly consisting of the accretion of peri-Laurentian arcs onto the Laurentian continental margin (van Staal et al., 2007). The suprasubduction-zone ophiolite complex was emplaced ca. 484 Ma (van Staal et al., 2007). The ophiolite succession is a part of the larger Humber Arm tectonostratigraphic interval, which was emplaced stratigraphically with a potentially syn-metamorphic metasedimanetary mélange (Jamieson, 1981).

Tectonic emplacement of the ultramafic units of the Tablelands included extensive fracturing and hydrothermal alteration. Later glaciation and subsequent isostatic rebound have resulted in further fracturing, which provides conduits for

groundwater flow. These fractures facilitate the present-day serpentinization of the Tablelands Ophiolite (Szponar et al., 2013).

The methane source at the Tablelands Ophiolite has not been conclusively characterized. However, the massif has been extensively studied, particularly the ultra-basic springs therein. The ophiolite possesses characteristics conducive to all three established pathways of methanogenesis. The presence of an organic-bearing unit directly beneath the highly fractured ultramafic rock of the massif means the methane produced in the Tablelands' ultrabasic springs could be partially or completely thermogenic (Szponar et al., 2013). Serpentinization reactions support the abiogenic production of methane, while the anaerobic nature of the ultra-basic springs is conducive to microbial life including methanogens (Szponar et al., 2013). $\delta^{13}C$ values of dissolved methane, ethane, propane, butane, pentane and hexane in ultra-basic spring waters do not plot in established microbial fields of a Bernard plot (Szponar et al., 2013). This tentatively characterizing the methane as non-microbial, but the lack of an abiogenic field on this plot renders this characterization inconclusive. Genomic observations, namely the lack of characteristically methanogenic archean 16S ribosomal RNA (Brazelton et al., 2012), suggest that the microbial community in the Tablelands does not include methanogens. Laboratory microcosms created using materials collected from the spring sites in the Tablelands did not produce methane, and found instead evidence of carbon monoxide utilization, indicative of a non-methanogenic microbial metabolism (Morrill et al., 2014).

While there is a lack of evidence supporting microbial methanogenesis, it has not been conclusively ruled out as a source, nor has there been conclusive evidence to discriminate between thermogenic and abiogenic origins (Morrill et al., 2014; Szponar et

al., 2013). To do so requires further examination of the stable hydrogen isotope composition of the methane (Szponar et al., 2013). Initial efforts to sample for dissolved hydrogen concentrations and isotopic enrichment yielded samples with values below instrumental detection limits (Rietze et al., 2014). A sampling method that collects sufficient concentrations of dissolved hydrocarbon gas while preserving original isotopic values is therefore required.

In order to isotopically analyze dissolved gases for the purposes of sourcing, CH_4 must be extracted from the water, and if its concentration is low then it must be concentrated before isotopic analysis. However, extraction and concentration methods must be tested to ensure that they do not change the isotope values of the CH_4 sample.

Once the pathway of CH_4 synthesis is established, it is vital to understand the role of CO_2 in methanogenesis, and the flux of greenhouse gases, within the ophiolite. The quantification of CO_2 sequestered and CH_4 emitted at one spring discharge location in the Tablelands was achieved using a prototype closed chamber gas sampler and accompanying method (Morrissey and Morrill, 2016). The closed gas chamber consisted of an inverted five gallon plastic bucket, modified with a gas-tight port that facilitated periodic gas sampling from the top of the bucket. The prototype closed chamber gas sampler was inverted over a pool in order to isolate the air-water interface directly overlying an ultra-basic groundwater outlet (labeled WHC2b) for a period of 24 hours. Discrete samples were taken from the chamber atmosphere for the duration of the observation, and subsequently analyzed for their CO_2, CH_4, and nitrous oxide (N_2O) concentrations.

The 24-hour observation of the WHC2b site showed a negligible N_2O flux, and CO_2 sequestration that occurred at a rate 41 times faster than the emission of CH_4 (Morrissey and Morrill, 2016). These fluxes were then used to calculate the net radiative force of greenhouse gases at the Tablelands. In this study, the radiative forcing of CO_2 was -0.22, and that of CH_4 was 0.01, with a cumulative forcing of -0.21 (Morrissey and Morrill, 2016). Morrissey and Morrill (2016) was the first study to consider the net effect of the fluxes of greenhouse gases associated with serpentinizing springs. The study concluded that the methods applied to WHC2b should be applied to other ultra-basic groundwater discharge locations with the potential to sequester and produce greenhouse gases within the massif.

1.5 Thesis Objectives

The first objective of this thesis was to compare two different field sampling techniques for the purpose of methane characterization – vacuum extraction and gas stripping. In order to definitively characterize a methanogenic pathway, sampling methods for methane gas isotopes must not be isotopically fractionating. Both methods were utilized in the field to sample the δ^2H and $\delta^{13}C$ of dissolved hydrocarbons, CO_2, and H_2. Their results were compared in order to determine whether original isotope values were preserved.

The second objective of this thesis was to conduct a meta-analysis of isotope systematics as a means of sourcing methane. CD and CD fractionation plots were created using data from numerous lab and field-based studies, in order to investigate the relative merit of these plots in contributing to methane characterization.

Due to preliminary geochemical and genomic evidence, methanogenesis at the Tablelands is tentatively characterized as non-microbial, but this has yet to be definitively confirmed. The definitive characterization of methane produced at The Tablelands by examining the stable hydrogen isotope composition of the methane constitutes the third objective of this project. The genetic pathway of methane produced in serpentinizing springs in the Tablelands was constrained by plotting the C and/or H isotopic composition on Bernard, CD, and CD fractionation plots, using aqueous geochemistry parameters measured in the Tablelands. Additional consideration was given to the thermal history of the organic matter of sedimentary units underlying the ophiolite, as well as new H isotope and clumped isotopologue data, which provided further stratigraphical, geological, and geochemical context to methane characterization.

The fourth objective of this thesis was to establish the extent of geochemical stability at a site of continental serpentinization – the Tablelands – over the course of multiple sampling trips over several years. This serves to fortify any conclusions made about the ophiolite based on its aqueous geochemistry.

Additionally, the capacity of these sites to sequester CO_2 makes them potential targets for the enhanced storage of anthropogenic emissions, or global carbon storage (GCS). However, understanding greenhouse gas fluxes is essential to validating ophiolites as viable sites for long-term carbon storage. The baseline conditions of these systems must be established before they are engineered for GCS. The fifth and final objective of this thesis was therefore to quantify CO_2 sequestration at multiple locations within the Tablelands massif, and to thereby calculate a net CO_2 flux estimate for the Tablelands massif as a whole.

1.6 Context of Research in Discipline

Sites of continental serpentinization are pertinent to several branches of environmental and planetary geochemistry. In an environmental context, the dynamics of greenhouse gases such as CH_4 and CO_2 at sites of serpentinization have a global bearing on carbon cycling and climate change models. In order to better incorporate sites of continental serpentinization into global climate change and global carbon cycling models, the local fluxes of CH_4 and CO_2 must be defined. Ophiolites and their associated high-pH serpentinizing springs have been identified as potential targets for enhanced GCS, which could offset anthropogenic carbon emissions. It is essential to first understand the natural baseline conditions of these sites before exploring their engineering for the purpose of enhanced carbon sequestration.

Serpentinized rocks and their associated groundwater springs act as analogues to several enigmatic systems; they inform our understanding of submarine processes that we cannot observe, act as a portal to the subsurface biosphere, and act as planetary analogues. The Tablelands, specifically, acts as a terrestrial analogue to Mars and Saturn's moon Endeadus (Szponar et al., 2013). Constraining the source of CH_4 at the Tablelands can inform researchers' understanding of Martian CH_4 production via subsurface processes. Even more relevant is the role of serpentinization as a source of chemical energy for extremophile life in Earth's deep ocean (Brazelton et al., 2012).

1.7 Co-authorship Statement

Dr. Penny Morrill is responsible for the initial conception of this project, the methodology of which was outlined in a grant proposal prior to the start of the Thesis. During the first semester of the Thesis, the first author (Thesis author) completed a literature review. During the second semester of the Thesis, the first author wrote and submitted a research proposal to the Department of Earth Sciences. Modifications to the original research proposal over the course of the Thesis were made based on collaborative consultation between the first author and Dr. Morrill.

This thesis is a compilation of a submitted manuscript (Chapter 2) and a paper that will be prepared for submission to a research journal (Chapter 3). Chapter 2 was submitted to the journal Chemical Geology, and therefore follows the Chemical Geology manuscript submission guidelines:

Cumming, E.A., Rietze, A., Morrissey, L.S., Cook, M.C., Rhim, J.H., Ono, S., Morrill, P.L. In Press. Potential Sources of Dissolved Methane at the Tablelands, Gros Morne National Park, NL, CAN: a Terrestrial Site of Serpentinization. Chemical Geology.

While Chapter 2 is co-authored, the first author conducted all research pertaining to the objective of this investigation, literature review, research methodology, sample collection and analysis (except where stated below), and manuscript writing. Sampling for this thesis was conducted in July 2016 and 2017, with field assistance from Melissa C. Cook and Dr. Penny Morrill. Sampling, analysis, and description of the isotope enrichment of carbon ($\delta^{13}C$) and palynology of sedimentary organic matter found in rock units adjacent to the Tablelands Ophiolite was conducted by Amanda Rietze. Clumped

isotope analysis was conducted by Dr. Shuhei Ono and Jeemin H. Rhim of the Department of Earth, Atmospheric and Planetary Sciences, Massachusetts Institute of Technology. Laboratory testing of methane extraction methods for isotopic analysis was conducted by Liam S. Morrissey.

While Chapter 3 is co-authored, the first author conducted all research pertaining to the objective of this investigation, literature review, research methodology, sample collection and analysis (except where stated below), and manuscript writing. Sampling for this thesis was conducted in July 2016 and 2017, with field assistance from Melissa C. Cook and Dr. Penny Morrill. The first author created geologic maps in Chapters 2 and 3.

The second reader, Dr. Tao Cheng, provided editorial input during the writing of the Thesis. Dr. Morrill provided indispensable guidance on research methodology, discussion of results throughout the research process, and editorial input during the writing of the manuscript and Thesis.

References Cited

Alfredsson, H.A. et al., 2013. The geology and water chemistry of the Hellisheidi, SW-Iceland carbon storage site. International Journal of Greenhouse Gas Control, 12: 399-418.

Barnes, I., LaMarche, V.C., Himmelberg, G., 1967. Geochemical evidence of present-day serpentinization. Science, 156: 830-832.

Blank, J.G. et al., 2009. An alkaline spring system within the Del Puerto Ophiolite (California, USA): a Mars analog site. . Planetary and Space Science, 57: 533-540.

Brazelton, W.J., Nelson, B., Schrenk, M.O., 2012. Metagenomic evidence for H2 oxidation and H2 production by serpentinite-hosted microbial communities. Frontiers in Microbiology, 2: 1-16.

Etiope, G., Tsikouras, B., Kordella, S., Ifandi, E., Christodoulou, D., Papatheodorou, G., 2013. Methane flux and origin in the Othrys ophiolite hyperalkaline springs, Greece. . Chemical Geology, 347: 161-174.

Gislason, S.R. et al., 2014. Rapid solubility and mineral storage of CO_2 in basalt. Energy Procedia, 63: 4561-4574.

Kelemen, P.B., Matter, J., 2008. In situ carbonation of peridotite for CO2 storage. Proceedings of the National Academy of Sciences of the United States of America, 105(45): 17295-17300.

Kelemen, P.B. et al., 2011. Rates and Mechanisms of Mineral Carbonation in Peridotite: Natural Processes and Recipes for Enhanced, in situ CO_2 Capture and Storage. Annual Review of Earth and Planetary Sciences, 39: 545-576.

Kohl, L. et al., 2016. Exploring the metabolic potential of microbial communities in ultra-basic, reducing springs at The Cedars, CA, US: Experimental evidence of microbial methanogenesis and heterotrophic acetogenesis. Journal of Geophysical Research G: Biogeosciences, 121(4): 1203-1220.

McCollom, T.M., 2016. Abiotic methane formation during experimental serpentinization of olivine. Proceedings of the National Academy of Sciences of the United States of America, 113(49): 13965-13970.

McCollom, T.M., Donaldson, C., 2016. Generation of Hydrogen and Methane during Experimental Low-Temperature Reaction of Ultramafic Rocks with Water. Astrobiology, 16(6): 389-406.

McGrail, B.P. et al., 2017. Wallula Basalt Pilot Demonstration Project: Post-injection Results and Conclusions. Energy Procedia, 114: 5783-5790.

McGrail, B.P., Spane, F.A., Sullivan, E.C., Bacon, D.H., Hund, G., 2011. The Wallula basalt sequestration pilot project. Energy Procedia, 4: 5653-5660.

Miller, H.M. et al., 2016. Modern water/rock reactions in Oman hyperalkaline peridotite aquifers and implications for microbial habitability. Geochemica et Cosmochimica Acta, 179: 217-241.

Morrill, P.L. et al., 2014. Investigations of potential microbial methanogenic and carbon monoxide utilization pathways in ultra-basic reducing springs associated with present-day continental serpentinization: the Tablelands, NL, CAN. Frontiers in Microbiology.

Morrill, P.L. et al., 2013. Geochemistry and geobiology of a present-day serpentinization site in California: The Cedars. Geochimica et Cosmochimica Acta, 109: 222-240.

Morrissey, L., Morrill, P.L., 2016. Flux of methane release and carbon dioxide sequestration at Winterhouse Canyon, Gros Morne, Newfoundland, Canada: a site of continental serpentinization. Canadian Journal of Earth Sciences, 54(3): 257-262.

Ono, S. et al., 2014. Measurement of a doubly substituted methane isotopologue, 13CH3D, by tunable infrared laser direct absorption spectroscopy. Analytical Chemistry, 86(13): 6487-6494.

Rajendran, S., Nasir, S., Kusky, T.M., al-Khirbash, S., 2014. Remote sensing based approach for mapping of CO_2 sequestered regions in Samail ophiolite massifs of the sultanate of Oman. Earth-Science Reviews, 135: 122-140.

Rietze, A. et al., 2014. Hydrocarbon Sources at a Site of Active Continental Serpetninization: The Cedars, California, USA, Goldschimdt, Sacramento, CA.

Schoell, M., 1988. Multiple origins of methane in the Earth. Chemical Geology, 71: 1-10.

Schoell, M., Tietze, K., Schoberth, S.M., 1988. Origin of methane in lake Kivu (east central Africa). Chemical Geology, 71: 257-265.

Searle, R. (Ed.), 2013. Mid-Ocean Ridges. Cambridge University Press, Cambridge, UK.

Sherwood, B. et al., 1988. Methane occurences in the Canadian Shield. Chemical Geology, 71: 223-236.

Sherwood Lollar, B. et al., 2008. Isotopic signatures of CH4 and higher hydrocarbon gases from Precambrian Shield sites: A model for abiogenic polymerization of hydrocarbons. Geochimica et Cosmochimica Acta, 72(19): 4778-4795.

Sleep, N.H., Meibom, A., Fridriksson, T., Coleman, R.G., Bird, D.K., 2004. H2-rich fluids from serpentinization: Geochemical and biotic implications. PNAS, 101(35): 12818 -12823.

Snæbjörnsdóttir, S.Ó., Gislason, S.R., 2016. CO_2 Storage Potential of Basaltic Rocks Offshore Island. Energy Procedia, 86: 371-380.

Stolper, D.A. et al., 2014. Combined 13C-D and D-D clumping in methane: Methods and preliminary results. Geochimica et Cosmochimica Acta, 126: 169-191.

Surour, A.A., Arafa, E.H., 1997. Ophicarbonates: calcified serpentinites from Gebel Mohagara, Wadi Ghadir area, Eastern Desert, Egypt. Journal of African Earth Sciences, 24(3): 315-324.

Suzuki, S., Kuenen, J. G., Schipper, K., van der Velde, S., Ishii, S., Wu, A., Sorokin, D. Y., Tenney, A., Meng, X., Morrill, P. L., Kamagata, Y., Muyzer, G., Nealson, K.H., 2014. Physiological and genomic features of highly alkaliphilic hydrogen-utilizing Betaproteobacteria from a continental serpentinizing site. Nature Communications, 5:3900 doi: 10.1038/ncomms4900.Suzuki, S., Ishii, S., Wu, A.,

Cheung, A., Tenney, A., Wanger, G., Kuenen, J. G., Nealson, K. H. 2013. Microbial diversity in The Cedars, an ultrabasic, ultrareducing, and low salinity serpentinizing ecosystem. PNAS, 110(38): 15336-15341.

Valentine, D.L., Chidthaisong, A., Rice, R., Reeburgh, W.S., Tyler, S.C., 2004. Carbon and hydrogen isotope fractionation by moderately thermophilic methanogens. Geochimica et Cosmochimica Acta, 68(7): 1571-1590.

van Staal, C.R. et al., 2007. The Notre Dame arc and the Taconic orogeny in Newfoundland. Geological Society of America Memoirs, 200(March 2016): 511–552.

Wang, D.T. et al., 2015. Clumped isotopologue fingerprinting of methane sources in the environment. Science, 348(6233): 428-431.

CHAPTER 2: POTENTIAL SOURCES OF DISSOLVED METHANE AT THE TABLELANDS, GROS MORNE NATIONAL PARK, NL, CAN: A TERRESTRIAL SITE OF SERPENTINIZATION[1]

[1] *This chapter is based on the following paper:*

Cumming, E.A., Rietze, A., Morrissey, L.S., Cook, M.C., Rhim, J.H., Ono, S., Morrill, P.L. Submitted. Potential Sources of Dissolved Methane at the Tablelands, Gros Morne National Park, NL, CAN: a Terrestrial Site of Serpentinization. *Chemical Geology.*

Abstract

The Tablelands massif in Western Newfoundland is part of a Phanerozoic ophiolite sequence and is currently a terrestrial site of serpentinization. As in other Phanerozoic ophiolite sequences, the Tablelands possess characteristics that are conducive to all three established pathways of methanogenesis – abiogenic, microbial, and thermogenic – or a combination thereof. Sourcing methane from the Tablelands has thus far been limited by the low dissolved methane concentrations. To approve collection, we tested dissolved gas extraction and concentration methods (vacuum extraction and gas stripping) for their effect upon isotopic fractionation, and we later applied these methods to sample dissolved methane for carbon and hydrogen isotopes ($\delta^{13}C_{CH4}$ and δD_{CH4}) as well as doubly substituted "clumped" isotopologue ($^{13}CH_3D$) analyses. Clumped isotope thermometry of methane indicates an apparent temperature of 85 ± 7 °C. The carbon isotope value of methane ($\delta^{13}C_{CH4}$) for samples collected in 2017 was -27.9 ± 0.5 ‰, consistent with previously measured values (-27.3 ± 0.5 ‰) dating back to 2009. The hydrogen isotope value of methane (δD_{CH4}) in 2017 was -175 ± 5 ‰. On a carbon deuterium (CD) plot, the Tablelands methane data lie outside the microbial field, but within an area where abiogenic and thermogenic fields overlap. A conclusive discrimination between abiogenic and thermogenic methanogenic pathways remains challenging. Nevertheless, a combination of sedimentary organic matter characterization of the underlying sedimentary units and comparison of geochemical characteristics with those described in experimental and theoretical studies suggest that the methane extracted from the Tablelands is likely a result of slow production of methane at ~85 °C from background organic sources.

1 Introduction

1.1 Sourcing Methane

Methane can have a microbial, thermogenic, or abiogenic origin. Multiple lines of evidence are required to determine the source of methane (Etiope and Sherwood Lollar, 2013). Stable carbon and hydrogen isotope ratios have been used as one of the lines of evidence. Traditionally, the carbon-deuterium (CD) plot (a diagram of the stable hydrogen isotope values of CH_4 (δD_{CH4}) plotted against the stable carbon isotopes value of CH_4 ($\delta^{13}C_{CH4}$)), and the Bernard Plot (the ratio of CH_4 to the sum of ethane, propane, and butane plotted against the $\delta^{13}C_{CH4}$) have been used by oil and gas researchers to source microbial and thermogenic methane, and to demonstrate mixing ratios when both methane sources are present, respectively. On the CD plot, empirically derived fields have been drawn encompassing data collected from laboratory and field-based studies for microbial (including autotrophic CO_2 reduction, and heterotrophic acetate fermentation, pathways), abiogenic, and thermogenic methane (Etiope and Sherwood Lollar, 2013 and references therein). However, these fields are not mutually exclusive, and overlaps exist.

Another method used to identify the source of methane is the CD fractionation plot, which graphs the stable isotope fractionation factors of carbon between dissolved inorganic carbon (DIC), total inorganic carbon (TIC), or carbon dioxide (CO_2) and CH_4 on one axis and the stable isotope fractionation of hydrogen between water (H_2O) and CH_4 on the other axis (Kohl et bal. (2016) and Sherwood Lollar et al. (2008) and references therein). Plotting the fractionation factors allows a direct comparison among the isotope effects associated with different methanogenic processes, as it removes the

effect of the stable isotope values of substrates or reactants on those of the product methane.

In addition to the compound-specific isotope ratios, the relative abundance of doubly-substituted ("clumped") methane isotopologues (e.g., $^{13}CH_3D$) can further constrain the origin of methane by providing information about the temperature at which the sample of methane was formed or last equilibrated (Ono et al., 2014; Stolper et al., 2014). Methane clumped isotope analysis can therefore serve as a geothermometer for methane formed in near-equilibrium processes.

1.2 Methane Genesis Associated with Continental Serpentinization

The surficial occurrence of ultramafic rocks on Earth takes place at subduction zones, mid-ocean ridges, in the Precambrian Shield, and ophiolites. These occurrences promote serpentinization by exposing ultramafic lithologies to aqueous alteration. Of these geologic settings, ophiolites are the most accessible and are therefore ideal targets for the investigation of methane production at sites of serpentinization. Methane may be produced via abiogenic, thermogenic, and/or microbial synthesis within an ophiolite's geologic setting.

Methane of proposed abiogenic origins has been detected in ophiolites in the Philippines, Italy, Greece, Turkey, Oman, New Zealand, and Japan (Etiope and Sherwood Lollar, 2013 and references therein), as well as the Precambrian Shield in Canada (Sherwood Lollar et al., 2002). The serpentinization process creates an environment conducive to methane production via hydrothermal alterations of the originally anhydrous constituent minerals of an ultramafic rock, namely olivine, orthopyroxene, and clinopyroxene (Barnes et al., 1967). The hydration of these minerals

results in the production of serpentine, iron and magnesium hydroxides, and H_2. The H_2 may react with inorganic carbon to produce methane abiogenically (Sleep et al., 2004) although experimental studies showed that the kinetics may be sluggish (McCollom, 2016; McCollom and Donaldson, 2016).

Another possible source of methane is microbial methanogenesis; the process of serpentinization may result in both favorable and unfavorable environments for biological methane production. The water-rock reactions result in the production of reducing aqueous environments (E_h of $\leq$-500 mV) where methanogens can flourish. In such reducing environments, methanogens can thrive via autotrophic CO_2 reduction, heterotrophic organic acid fermentation or a combination thereof (Kohl et al., 2016 and references therein). For example, a few terrestrial serpentinization sites (e.g., The Cedars and the Samail Ophiolite of Oman) have been suggested to support microbial methanogenesis. Genomic (Suzuki et al., 2013), geochemical (Morrill et al., 2013), and laboratory studies (Kohl et al., 2016) all demonstrated the potential for microbially sourced methane at The Cedars; and 16S ribosomal RNA (rRNA) analysis detected *Methanobacterium* sp. (methanogens that use the CO_2 reduction pathway) from well water associated with the Samail Ophiolite in Oman (Miller et al., 2016). However, other conditions resulting from the serpentinization process such as high pH can be detrimental to methanogens. Indeed, besides the few exceptions mentioned above, there is generally limited evidence of microbial methanogenisis within sites of terrestrial serpentinization associated with Phanerozoic ophiolites (Etiope and Sherwood Lollar, 2013 and references therein).

In addition to abiogenic and microbial methanogenesis, methane is also produced via the thermal degradation of buried organic matter. Ophiolites are commonly underlain by a marine metasedimentary mélange consisting of a formerly subduction-related accretionary wedge that originated as seafloor sedimentary deposits. The extensive fracturing inherent to the subduction, subsequent obduction and emplacement of the ultramafic unit creates conduits that can transport thermogenic gases from the subsurface to the surface via groundwater flow. Because the ophiolites are emplaced upon organic-bearing units, methane found in an ophiolites' ultra-basic springs is potentially thermogenic (or partially thermogenic) in source. Methane produced at the Coast Range Ophiolite Microbial Observatory (CROMO) site of continental serpentinization is tentatively classified as thermogenic based on isotopologue thermometry in conjunction with empirical observations at the site (Wang et al., 2015). Contribution of thermogenic methane is also suggested in Chiamera seep in Turkey (Young et al., 2017).

The source of the methane produced at the Tablelands Ophiolite has not been conclusively characterized. On a Bernard plot, the Tablelands' methane lies outside of the common range of microbial methane with relatively high $\delta^{13}C$ values (-27 ± 0.5 ‰) and low ratios (6 to 10) of methane to the sum ethane, propane, butane (Szponar et al., 2013). This tentatively characterizes the Tablelands' methane as non-microbial. Genomic observations, namely the lack of characteristically methanogenic Archaean 16S rRNA (Brazelton et al., 2013), suggest that the microbial community in the Tablelands does not include known methanogens. Laboratory microcosms created using materials collected from the spring sites in the Tablelands did not produce methane in spite of the favourable conditions for microbial methanogenesis (Morrill et al., 2014). Thus, the geochemical,

genomic, and experimental evidence collectively suggest that the methane at the Tablelands is likely not microbial in origin.

While microbial methanogenisis is unlikely at the Tablelands, the available data were not sufficient to conclusively identify or distinguish between thermogenic and abiogenic origins (Morrill et al., 2014; Szponar et al., 2013). Therefore, additional lines of evidence may aid in our sourcing the methane. These include measuring the stable hydrogen isotope ratios and the clumped isotopologue abundance of the methane, as well as investigating the thermal history (i.e. Thermal Alteration Index) of the organic matter in the sedimentary units beneath the Tablelands. Initial efforts to measure the stable hydrogen isotope ratios of the dissolved methane (δD_{CH4}) were unsuccessful because the sample concentrations achieved with the sampling protocol employed in our previous study were below the analytical quantification limits (Szponar et al., 2013). A sampling method that collects sufficient concentrations of dissolved methane while preserving original isotopic values is therefore required (Morrissey and Morrill, 2016).

1.3 Sampling Methods for Dissolved Methane

Dissolved methane is typically sampled using two methods: gas stripping (Oremland and Des Marais, 1983; Rudd et al., 1974) and vacuum degassing (Sherwood Lollar et al., 1993). Using greater volumes of water and larger vials with these methods may increase the total amount of methane in the gas/headspace to levels above our analytical quantification limits for δD_{CH4} analyses. However, these sampling methods need to be tested to ensure that the isotopic integrity of the methane sample is maintained.

Therefore, the first objective of this study was to test these sampling methods for isotopic fractionation, and apply them to δD_{CH4} as well as methane clumped isotopologue

($^{13}CH^{3}D$) analyses. The second objective was to examine the thermal history of the organic matter in the sedimentary units below the ophiolite to assess their potential of producing thermogenic methane. The final objective was to source the methane at the Tablelands by using new hydrogen isotope and clumped isotopologue data in the context of other geological and geochemical information.

2 Materials and Methods

2.1 Geologic Site Description: the Tablelands Massif of the Bay of Islands Ophiolite

The Tablelands massif, a part of the Bay of Islands ophiolite complex and the Humber Arm Allochthon, originated at a peri-Laurentian marine spreading center that was obducted onto the continental margin as a result of the Taconic orogeny. This orogeny, a subset of the Appalachian orogeny, occurred during the late Cambrian and Ordovician, and it resulted in the accretion of peri-Laurentian marine arcs onto the Laurentian continental margin (van Staal et al., 2007). The suprasubduction-zone ophiolite complex was emplaced ca. 484 Ma (van Staal et al., 2007). The ultramafic units were subjected to extensive fracturing and hydrothermal alteration (serpentinization) during their tectonic uplift and emplacement. Later glaciation and subsequent isostatic rebound have resulted in further fractures, which act as conduits for groundwater flow. These fractures facilitate present-day serpentinization with the Tablelands Ophiolite (Szponar et al., 2013).

Beneath the ophiolite complex are sedimentary rocks that may contain lithology consistent with the Green Point Shale, the principal unconventional oil and gas source rock on the west coast of Newfoundland. Sedimentary units that contain this organically enriched shale exist on the Port au Port Peninsula, through Gros Morne National Park, to Parsons Pond, in the north (Figure 2.1). Green Point Shale formed during the lower Paleozoic in the deeper waters of the Laurentia continental slope and Iapetus ocean floor. Samples from exploratory oil and gas wells drilled north and south of the Park show that thermal maturity increases from South to the North (i.e., trending from oil- to gas-dominated) (see Hinchey et al.(2005) and references therein). However, the data used to create this trend did not include samples from the Park itself, as oil explorations are not allowed in this UNESCO World Heritage Centre.

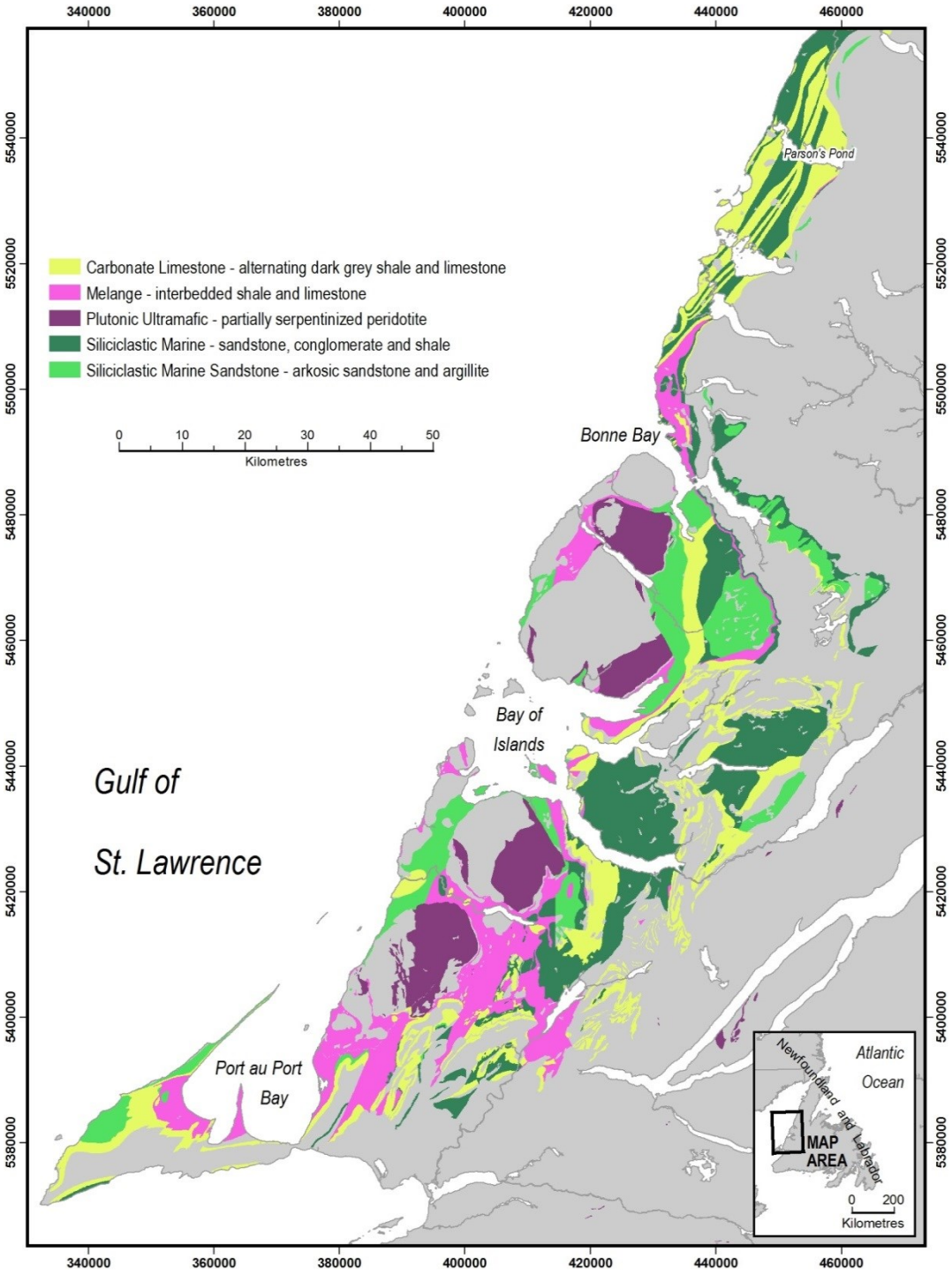

Figure 2.1 A Map of the west coast of Newfoundland from Port au Port to Parson's Pond highlighting the important geologic units. The source data for this map came from NL

survey (http://gis.geosurv.gov.nl.ca/) and the federal Department of Natural Resources (http://geogratis.gc.ca/site/eng/extraction?id=2013_51d579a832fb79.569414).

2.2 Sampling Site Description

Three outcrops of the sedimentary unit below the peridotite within the Humber Arm Allochthon were sampled (Figure 2.2). HAA1 was sampled in Lobster Cove from the Green Point Formation, which contains the Green Point Shale, of the Cow Head Group which consisted of deep water sedimentary rocks belonging to the lower structural slices of the Humber Arm Allochthon. HAA2 was sampled from the Crolly Cove mélange by the Trout River Small Pond. This mélange consisted of sedimentary and ophiolitic rocks that were part of the higher structural slices of the Humber Arm Allochthon, cradling the Tablelands peridotite. HAA3 through HAA6 were sampled along the shoreline of Winter House Brook from the Blow Me Down Brook Formation which were sedimentary and volcanic rocks that were part of the intermediate structural slices of the Humber Arm Allochthon. Sedimentary rocks were scrubbed with distilled water to remove any debris that may have adhered to the surface. The rocks were crushed into fine powder using a cup and mill device which was cleaned thoroughly with ethanol and an air jet in between samples. Samples were stored in sterile plastic containers and kept cold and dark until analysis.

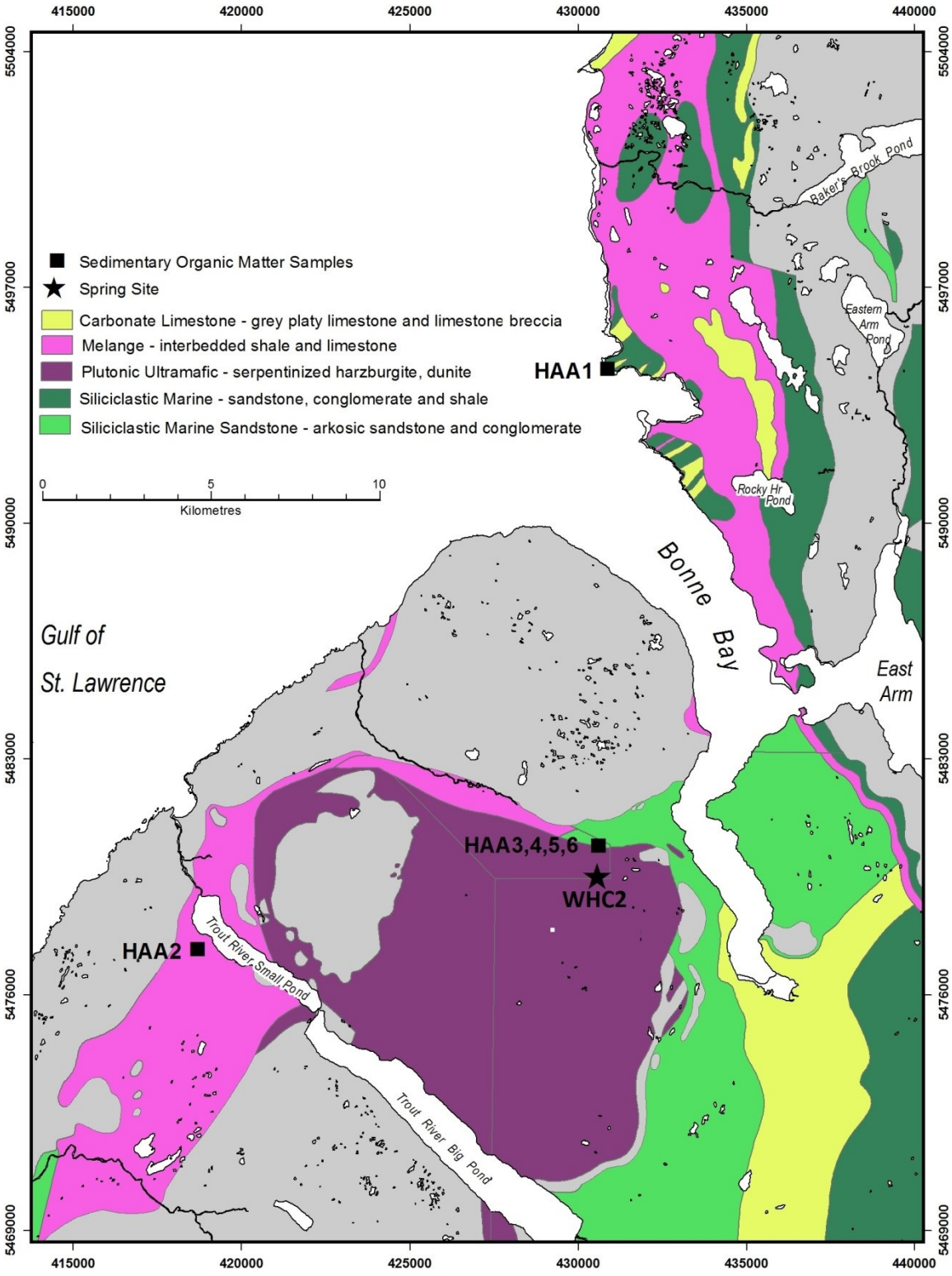

Figure 2.2 Geologic map of the Tablelands highlighting the important geologic units

and approximate sampling locations. The star represents the highly reducing ultra-basic spring, WHC2, located on the partially serpentinized peridotite. Square symbols represent outcrops of the marine sediments and shales that surround the peridotite body where sedimentary organic matter samples were taken. The source data for this map was from NL survey (http://gis.geosurv.gov.nl.ca/) and the federal Department of Natural Resources (http://geogratis.gc.ca/site/eng/extraction?id=2013_51d579a832fb79.569414).

Water and gas samples were taken from a groundwater discharge point in Winter House Canyon (WHC2). At WHC2, the groundwater discharges into the base of a small (1.5 m x 0.75 m) pool that is 3 m west of Winter House Brook (WHB), which flows approximately south to north through Winter House Canyon of the Tablelands. The pool is ultra-basic and reducing, with E_h values becoming more negative towards the bottom of the pool, which was 40 cm deep. Additionally, the discharging groundwater is rich in Ca^+ and OH^- (Szponar et al., 2013). As atmospheric CO_2 reacts with the ultra-basic water carbonate is precipitated as travertine enveloping the pool (Morrissey and Morrill, 2016).

2.3 Field Sampling Methods

In situ measurements of pH, E_h, water temperature, and air temperature were taken prior to taking samples for aqueous geochemistry. Water temperature and pH were measured using a handheld field pH meter (IQ180G GLP, IQ Scientific Instruments, Loveland, CO). The meter was calibrated daily using pH buffer solutions of 4.01, 7.00, and 10.01 (Oakton). Daily calibration checks were conducted using the same solutions. E_h was measured using an OAKTON Waterproof ORPTestr 10 meter. Air temperature was measured using a Kestrel 3000 Pocket Weather Meter.

Water for total inorganic carbon (TIC) and dissolved organic carbon (DOC) analyses was sampled in the field by filling 40 mL amber vials pre-treated with mercuric chloride and phosphoric acid, respectively, and sealed with black butyl rubber septa and tephlon lined silicon septa, respectively. The TIC sample vials were filled and capped with no headspace with unfiltered sample water. The DOC sample vials were filled with 30 mL of water filtered through a glass fiber filter (GFF). Water for the δD_{H2O} analysis was sampled by filling a 4 mL vial with no headspace with unfiltered water. Samples were kept cold and dark until analysis. Water for tritium age dating was sampled by filling a 500 mL Nalgene bottle. Sampling for all parameters was conducted in triplicate

Dissolved gases were sampled for concentration using the gas stripping method used by Szponar et al. (2013) that was adapted from Rudd et al. (1974). In short, 60 mL of sample water was taken up into two 60 mL sterile syringes (30 mL each) pre-filled with the equivalent volume of gas. In samples where H_2 was the target analyte, N_2 gas was used as the stripping gas; for all other analytes He gas was used as the stripping gas. In both cases, the syringes were manually shaken for five minutes to partition the dissolved gas into the gas phase. The gaseous content of both syringes was then injected into an inverted 30 mL glass bottle that was pre-filled with degassed Nano-UV water with no headspace, and sealed with conditioned blue butyl septa and an aluminum crimp seal. A 22-gauge exit needle facilitated the displacement of this water by the sampled gas. Ultimately, the 30 mL bottle was over pressurized with 60 mL of sample gas. A drop of saturated mercuric chloride solution was added to each 30 mL vial to terminate any microorganisms living in residual water within the bottle. Sampling was conducted in duplicate.

Two techniques were used in the field to extract dissolved hydrocarbons and H_2 for δD and $\delta^{13}C$ analyses. The first technique – the vacuum extraction method – was performed by injecting sample water into a pre-evacuated borosilicate vial. Samples extracted for $\delta^{13}C$ analysis consisted of 80 mL of sample water injected into pre-evacuated 160 mL bottles. Samples extracted for δD analysis consisted of 240 mL of sample water injected into pre-evacuated 500 mL bottles. The larger sample volume for the analysis of δD was necessary, as previous sampling of WHC2 using 80 mL of sample in 160 mL bottles had yielded CH_4 concentrations below the quantification limit for δD analysis. A drop of saturated mercuric chloride solution was added to each vial, in order to terminate any microorganisms living in residual water within the bottle. Sampling was conducted in triplicate. Samples were kept cold and dark until analysis.

The second technique – the gas stripping method – was accomplished by filling a 2 L glass bottle with sample water, and capping it with a lid that contained two ports. Two hundred mL of the sample water was displaced by inverting the bottle and forcing 200 mL of He gas through one port. The bottle was then shaken for ten minutes to transfer the dissolved gas phase into the He headspace. To collect the headspace, the bottle was tipped upright and 200 mL of additional sample water was injected through a port while 200 mL of headspace gas was simultaneously removed and injected into an evacuated 160 mL borosilicate vial sealed with a conditioned blue butyl septa. This method was also used to collect samples for clumped isotope analysis, as described in Wang et al. (2015).

2.4 Experimental Validation of Dissolved Gas Sampling Method

The $\delta^{13}C$ and δD values of laboratory CH_4 were determined before testing sampling and concentrating methods for their effect on isotopic fractionation. Two tanks of 99% pure CH_4 were isotopically characterized. CH_4 from the first tank (17 L at 40 psig of 99% CH_4 supplied by Air Liquide) was diluted in He gas by removing 5 mL of tank gas and injecting it into a 35 mL bottle prefilled with He. This sample of CH_4 was then analyzed for its $\delta^{13}C$ and δD values using isotope ratio mass spectrometry. Subsequently, CH_4 from this tank was completely dissolved into water. To dissolve CH_4 in water, a 2 L Kimble glass bottle was completely filled with deionized water and sealed using a black butyl septum conditioned in a NaOH solution. Next, 20 mL of 99% pure CH_4 at 1 atm with known isotopic composition was injected through the septa and allowed to completely dissolve into the water. After 72 hours at 24 °C gas bubbles were gone, ensuring quantitative conversion of gas phase CH_4 to dissolved phase CH_4. CH_4 was then extracted from this solution to test gas extraction methods for their effect on isotope fractionation.Similar to the gas stripping method performed in the field for concentration measurements, 25 mL of He gas was taken up into a 60 mL syringe and an equal volume of water containing dissolved CH_4 was taken up in the same syringe. The two phases were shaken together for 5 minutes whereby the He gas stripped the CH_4 from the water. Next, the gaseous headspace containing the CH_4 was transferred into an inverted 35 mL bottle completely filled with degassed water and sealed using a blue butyl septum. The injected headspace displaced an equal volume of water via an exit needle. The exit needle was removed when the water level approached the top of it, ensuring no gas escape from the bottle. The whole process was then repeated without an exit needle such that 50 mL

of headspace was ultimately injected into a 35 mL bottle, over pressurizing the sample by 15 mL.

To test the vacuum extraction method in the laboratory, 80 mL of water containing dissolved CH_4 was added to a 160 mL evacuated bottle such that an equal ratio of sample to bottle volume was achieved. This procedure was repeated with 125 mL of water and a 250 mL evacuated bottle. The pressure difference caused by the vacuum transferred gases from the liquid to the gas phase in the headspace of the bottle. Larger 250 mL bottles were used for hydrogen isotope analysis due to the greater number of injected moles of hydrogen required for δD measurements.

2.5 Analytical Methods

Hydrocarbon gas (C_1-C_6) concentrations were analyzed using a gas chromatograph (GC, SRI 8610) equipped with a methanizer and a flame ionization detector (FID). The C_2-C_6 hydrocarbons were separated on a Q-bond PLOT column (30 m x 0.32 mm ID, 10 μm film thickness) with a temperature program: 40 °C hold for 4 min, ramp at 12 °C/min to 150 °C, hold for 4 min, ramp at 12 °C/min to 180 °C, hold for 2 min, ramp at 20 °C/min to 225 °C, hold for 3 minutes with helium as the carrier gas. The concentration of CH_4 was analyzed on the same GC system, using a Carboxen 1010 (30 m x 0.32 mm ID, 15 μm film thickness) PLOT column. The temperature program was as follows: 40 °C hold for 6 min, ramp 15 °C/min to 110 °C, hold for 5 min. H_2 gas was measured on a GC (Agilent 6890A) equipped with a thermal conductivity detector (TCD) using the Carboxen 1010 PLOT column with N_2 as the carrier gas. The oven temperature program was isothermal at 40 °C for 6 min. The analytical error for gas concentration analysis was ± 5% RSD.

The $\delta^{13}C$ values of CH_4 were measured by gas chromatography-combustion-isotope ratio mass-spectrometer (GC-C-IRMS) using a GC (Agilent 6890N), connected via a combustion furnace and an open split (Conflo III) Interfaced with an isotope ratio mass spectrometer (Delta V Plus). The GC-C-IRMS was tested using multiple injections, at a 10:1 split ratio, of CH_4 standards with certified $\delta^{13}C$ values of -54.5 ‰ and -38.3 ‰ from Isometric Instruments, Victoria, BC, Canada. The CH_4 gas was separated using a Carboxen 1010 (30 m x 0.32 mm ID, 15 μm film thickness) PLOT column and the following temperature program: 50 °C for 3.5 minutes, ramp at 25 °C/min to 260 °C, 260 °C for 10 min. Other gaseous hydrocarbons (C_2- C_6) were separated using a GS-CARBON (30 m x 0.32 mm ID, 3 μm film thickness) PLOT column and the following temperature program: 50 °C hold for 3.5 min, ramp 25 °C/min to 260 °C, hold for 10 min. The standard analytical error for $\delta^{13}C$ measurements was ± 0.5 ‰.

The δD values of CH_4 and H_2 gases were measured on the same system as the $\delta^{13}C$ but using a Thermo Scientific micropyrolysis furnace (PY), instead of the combustion furnace. The CH_4 and H_2 were separated using a Carboxen 1010 column. The GC-PY-IRMS was calibrated using multiple injections (10:1 split ratio) of CH_4 standards with certified δD values of -266 ‰ and -157 ‰. The gases were separated using a Carboxen 1010 (30 m x 0.32 mm ID, 15 μm film thickness) column and the following temperature program: 110°C hold for 6 minutes, ramp 25 °C/min to 260 °C hold for 10 min. The standard analytical error for δD measurements was ± 5 ‰.

The δD and $\delta^{18}O$ of water were analyzed by a cavity ring down spectrometer (Model L2130-I, IT^2 Isotope Tracer Technologies Inc.). Internal standards used were calibrated with International Atomic Energy Agency Standards (V-SMOW, SLAP, and

GISP, respectively). The typical analytical error for this analysis was ± 0.1 ‰ for $\delta^{18}O$, and ± 1 ‰ for δD. Tritium concentrations were determined using the electrolytic tritium (E^3H) method. Analyses were performed at Isotope Tracer Technologies Inc. in Waterloo, Ontario.

For clumped isotope analysis, methane was purified from collected gas samples by means of cryogenic separation and gas chromatography. Samples were passed through a U-trap cooled to ca. –80 °C to remove H_2O. They were then passed through a second U-trap filled with activated charcoal at liquid nitrogen temperature to freeze CH_4, N_2, CO and CO_2. The trapped gas was heated to ca. 120 °C and injected into a GC equipped with a packed column (Carboxen-1000, 5' x 1/8", Supelco) and a thermal conductivity detector (TCD). Using the temporal separation in the elution of N_2, CH_4, CO_2 and heavier hydrocarbons (in that order), only CH_4 was trapped into a third U-trap filled with silica gel at liquid nitrogen temperature. Trapped pure CH_4 sample was transferred to a sample vial containing silica gel for subsequent introduction into the dual inlet system of the tunable infrared laser direct absorption spectrometer (TILDAS) at Massachusetts Institute of Technology.

TILDAS measures the mid-infrared (~8.6 μm) absorption by each of four methane isotopologues ($^{12}CH_4$, $^{13}CH_4$, $^{12}CH_3D$ and $^{13}CH_3D$) in a multi-pass Herriott absorption cell (76 m pathlength) (Ono et al., 2014; Wang et al., 2015). Using quantum cascade lasers, each absorption line is resolved at a measurement pressure of ca. 1 mm Hg (Ono et al., 2014). The abundance of $^{13}CH_3D$ clumped isotopologues is expressed in a metric noted as $\Delta^{13}CH_3D$, defined according to Ono et al. (2014) as:

$$\Delta^{13}CH_3D = \ln Q, \text{ where } Q = \frac{[^{13}CH_3D][^{12}CH_4]}{[^{13}CH_4][^{12}CH_3D]}$$

Here, Q is the reaction quotient for the isotope exchange reaction among the four methane isotopologues ($^{13}CH_4 + {}^{12}CH_3D \leftrightarrow {}^{13}CH_3D + {}^{12}CH_4$). When methane is formed in equilibrium or re-equilibrates, Q becomes the temperature-dependent equilibrium constant of the reaction (i.e., $Q = K$). Therefore, precise measurements of all four methane isotopologues allow the estimation of the methane formation or equilibrium temperature. The value of $\Delta^{13}CH_3D$ for equilibrium is estimated by:

$$\Delta^{13}CH_3D(T) = -0.1101\left(\frac{1000}{T}\right)^3 + 1.0415\left(\frac{1000}{T}\right)^2 - 0.5223\left(\frac{1000}{T}\right) \quad (1)$$

where T is in Kelvin. This is derived from theoretical calculation based on density function theory (B3LYP) with 6-31G(d) basis set and conventional theory by Urey (1947) (Gruen et al., In press). According to the equation above, the values of $\Delta^{13}CH_3D$ range from 5.7 ‰ at 25 °C to 0.2 ‰ at 1000 °C. The value of $\Delta^{13}CH_3D$ was calibrated by thermally equilibrating methane isotopologues at 250 °C on Pt catalyst. We used methane with δD values from -305 to +244 ‰ (against SMOW) for this purpose.

The $\delta^{13}C$ of the sedimentary organic matter (SOM) was determined by the analysis of CO_2 gas produced by combustion on the Elementar VarioEL III through on-line analysis by continuous-flow with a DeltaPlus Advantage IRMS coupled with a ConFlo II. $\delta^{13}C$ values were reported in standard notation (per mil, ‰) relative to the international reference Vienna Pee Dee Belemnite (V-PDB). The analytical accuracy and

reproducibility for this analysis was ± 0.05 ‰ (1σ) and the reproducibility of field replicates was ± 2 ‰ (1σ).

Palynology slides of the SOM samples were prepared to view their organic maturity using standard palynology processing techniques. In short, the first digestion was in 15 % hydrochloric acid (removal of carbonates) for a minimum of 24 h. Samples were then washed with distilled water a minimum of 3 times before the second digestion in concentrated hydrofluoric acid (removal of silicates) for a minimum of 2 days. The samples were then rinsed and sieved using a 10 μm mesh sieve to further isolate organic compounds. The resultant organic extract was mounted on a glass microscope slide and viewed and photographed using an UV-visible-NIR Microscope Spectrophotometer (QDI 202TM), under transmitted and ultraviolet light sources. The colour of the organics was classified by comparison with a reference colour chart from Pearson (1984).

3 Results

3.1 Testing possible isotope effects associated with CH_4 gas extraction

The average $\delta^{13}C$ value of the laboratory CH_4 extracted using the vacuum extraction method was -40.8 ± 0.1 ‰ (n=3). The average $\delta^{13}C$ value of the laboratory CH_4 extracted using the gas stripping method was -40.2 ± 0.1 ‰ (n=3). The previously determined $\delta^{13}C$ value of the CH_4 used to prepare the solution was -40.1 ± 0.5 ‰. Therefore, neither the vacuum extraction nor the gas stripping method altered the $\delta^{13}C$ value of the CH_4 beyond the ± 0.5 ‰ analytical error.

The average δD value of the laboratory CH_4 extracted using the vacuum extraction method was -162 ± 4 ‰ (n=3). The average δD value of the laboratory CH_4 extracted using the gas stripping method was -163 ± 2 ‰ (n=3). Since the previously determined δD value of the dissolved CH_4 was -167 ± 5‰, neither the vacuum extraction nor the gas stripping method altered the δD value of the CH_4 outside of the ± 5 ‰ analytical error.

In 2015, both the vacuum extraction and gas stripping methods were deployed in the field for $\delta^{13}C$ analysis. The dissolved CH_4 sample extracted from the WHC2 spring in the Tablelands had an average $\delta^{13}C$ value of -27.5 ± 0.1 ‰ (n=5) when the gas was removed using the gas stripping method, compared to an average $\delta^{13}C$ value of -27.7 ± 0.3‰ (n=6) for the vacuum extraction method. In 2016, both the vacuum extraction and gas stripping methods were deployed in the field for $\delta^{13}C$ and δD analyses. However, the gas-to-fluid ratio during gas stripping was modified to 1:10 for the δD of the CH_4 samples. The $\delta^{13}C_{CH4}$ collected via vacuum extraction was -27.6 ± 0.3 ‰ (n=3), while the $\delta^{13}C_{CH4}$ collected via gas stripping in 2016 was -27.7 ± 0.0 ‰ (n=3). δD_{CH4} values for both vacuum extraction and gas stripping were -181 ‰ with standard deviations of ±4 and ±2 ‰, respectively for triplicate samples. Therefore, similar to the laboratory data, the $\delta^{13}C$ and δD values for the gas stripping and the vacuum extraction methods were within analytical error (i.e., ± 0.5 and ± 5 ‰, respectively) of each other.

The δD of H_2 gas extracted using the gas stripping method had an isotope value of -787 ± 0.0 ‰ (n=2), while δD of H_2 gas extracted using the vacuum extraction method had an isotope value of -815 ± 12 ‰ (n=3). Therefore, the results for samples collected using gas stripping and the vacuum extraction methods were not within analytical error

(i.e., ± 5 ‰) of each other. Further laboratory studies are needed to determine which extraction method is causing isotopic fractionation.

3.2 Field Data

Table 2.1 shows a chronology of the aqueous geochemical data collected since 2009 at the WHC2 site. Geochemical data such as water temperature, pH, E_h, CH_4 concentrations and stable carbon isotope ratios of CH_4, stable hydrogen and oxygen isotope ratios of water, have remained relatively constant from year to year. New data such as the δD of CH_4, E^3H, as well as the abundance of methane clumped isotopes ($\Delta^{13}CH_3D$) provide additional information for sourcing the dissolved methane associated with the Tablelands' serpentinization. The measured value of $\Delta^{13}CH_3D$ of 4.17 ± 0.15 ‰ corresponds to an apparent equilibrium temperature of 85 ± 7 °C.

Table 2.1 Summary of geochemical data collected from WHC2 from 2009 to 2017.

	2009[a]	2010[a]	2011	2012	2015	2016	2017	Avg	SD
Water (°C)	16.5	14.4	13.4	-	14.4	13.9	14.7	14.6	1.1
pH	11.6	12.6	12.3	12.2	12.4	12.2	12.2	12.2	0.3
Eh (mV)	-519	-612	-388	-	-	-350	-292	-432	131
[H2] (μM)	129	298	516	529	-	1990	3235	1116	1233
[CH4] (μM)	6.2	15.6	20.0	36.8	56.0	34.4	43.2	30.3	17.3
$\delta^{13}C_{CH4}$ (‰)	-27.4	-26.4	-27.4	-27.0	-27.5	-27.6	-27.9	-27.3	0.5
δD_{CH4} (‰)	-	-	-	-	-	-171	-175	-173	2.8
$\Delta^{13}CH_3D$	-	-	-	-	-	4.17	-	-	-
δD_{H2O} (‰)	-68.3	-72.7	-63.47	-	-	-71.0	-69.3	-69.0	3.5
$\delta^{18}O_{H2O}$ (‰)	-10.4	-11.2	-10.36	-	-	-12.1	-11.0	-11.0	0.7
$\delta^{13}C_{TIC}$ (‰)	-	-13.0	-17.6	-13.9	-	-14.4	-15.9	-14.9	1.8
$\delta^{13}C_{DOC}$ (‰)	-16.9	-23.4	-	-16.2	-	-16.3	-18.8	-18.3	3.0
$CH_4/[C_{2+}]$	5.9	9.5	-	6.9	-	-	-	7.4	1.9
E^3H (TU)	-	-	-	-	-	-	2.6-3.0	-	-

[a] represents data from Szponar (2012). All samples were taken between mid-July and early October. A dash indicates no sample collection. Dissolved gas isotope values collected by vacuum extraction are reported since that was the extraction method used consistently over the years.

3.3 Sedimentary Organic Matter

Rock samples HAA1 to 4 were heavily-cleaved, fine-grained shale that were dark gray in colour. HAA5 was identified as limestone and HAA6 was identified as fine- to medium-grained sandstone. Supplementary Table 1 contains a detailed description of these samples. The most negative $\delta^{13}C$ of the fine grained shale samples was -31.6 ‰ measured from HAA2 and the least negative was -16.3 ‰ measured from HAA4. The $\delta^{13}C$ of HAA1 and HAA3 were -27.4 ‰ and -22.4 ‰, respectively. The limestone sample (HAA5) had a $\delta^{13}C$ value of -4.9 ‰ and the medium-grained sedimentary sample (HAA6) had a $\delta^{13}C$ value of -23.6 ‰.

Microscopic images of organics observed in HAA1 to 4 showed that the organics were heavily degraded and beyond the point of recognition; as a result, no organics could be identified as either phytoclasts or palynomorphs. Organics ranged in colour from dark yellow to dark brown/black. The majority of organics were a dark brown to black colour. Similarly, samples under white transmitted light showed that the organics ranged in colour from dark yellow to dark brown/black under white transmitted light. Under ultraviolet light, the organics observed in slides appeared black in colour and did not fluoresce.

4 Discussion

4.1 Sampling dissolved CH_4 using gas stripping for $\delta^{13}C$ and δD analyses

Vacuum extraction and gas stripping methods for dissolved methane generated δD_{CH4} and $\delta^{13}C_{CH4}$ values that were within analytical error of the initial methane.

Therefore, these methods do not cause significant isotope fractionation during sampling. Likewise, when methods were used to extract dissolved methane from ultra-basic groundwater of the Tablelands, the resulting δD_{CH4} and $\delta^{13}C_{CH4}$ values were within analytical error of each other. These data suggest that either method can be used to extract dissolved methane for stable carbon and hydrogen isotope measurements. However, this is not the general case for all gases. For example, there was an approximately 28 ‰ difference between the δD of H_2 extracted using vacuum extraction and the δD of H_2 extracted using gas stripping. Therefore, the dissolved CH_4 extraction methods used in this study should not be used ubiquitously among other gases without testing.

4.2 Groundwater Geochemistry Associated with the Tablelands Serpentinization

The ^3H data indicate that groundwater discharging from WHC2 is modern, as ^3H values between 2-8 TU for groundwater in coastal regions are considered less than 10 years old (Clark and Fritz, 1997). These data support the conclusion that the groundwater is meteoric in origin and compare favorably with stable hydrogen and oxygen isotopes reported by Szponar et al. (2013).

The collected and compiled aqueous geochemistry, gas concentrations, and isotope values of samples taken from WHC2 since 2009 indicate geochemical stability of the groundwater discharging at that point location. Water temperature, pH, stable carbon and hydrogen isotope values of methane, and stable hydrogen and oxygen isotope values of water remain fairly constant (i.e., all with relative standard errors of less than 10 % RSD; while E_h, concentrations of H_2 and CH_4, and the stable carbon isotope value of TIC

were more variable since 2009. The variations in gas concentrations and E_h are likely from dilution of groundwater by overland flow waters which mix in the WHC2 pool. This dilution would not affect the stable isotopes of the methane because there was no detectable methane in the overland flow. Additionally, this dilution would not affect the isotope ratios of the water, since the groundwater is of meteoric origin (Szponar et al., 2013). However, this water must be well buffered against changes in pH, since the dilution with overland flow did not have a large effect on the pH values.

4.3 Potential Methane Sources

The geologic and geochemical characteristics of the Tablelands Ophiolite are conducive to all three established pathways of methanogenesis (i.e., microbial thermogenic, and abiogenic). All three pathways can occur at the formation/equilibrium temperature of 85 ± 7 °C estimated from the measured $\Delta^{13}CH_3D$ value of 4.17 ± 0.15 ‰. However, this $\Delta^{13}CH_3D$ value does preclude a strong kinetic control by active microbial methanogenesis which has been associated with "anti-clumped" $\Delta^{13}CH_3D$ values (–3‰) observed at The Cedars (Wang et al., 2015). This adds to the mounting evidence that the methane from the Tablelands' ultra-basic spring, WHC2, is not microbial in origin.

Methane formed or equilibrated at 85 ± 7 °C suggests that it was either produced at a predicted depth based on the geothermal gradient, or it was produced within shallower groundwater associated with exothermic serpentinization. From a surface water temperature of 15 °C, 85 °C corresponds to a subsurface depth of 2.3 ± 0.3 km at the standard 30 K/km geothermal gradient. If $\Delta^{13}CH_3D$ reflects the temperature of formation or equilibrium, then the methane could have been generated at these depths below the ultramafic massif. The ultramafic massif at the Tablelands extends to ~0.9 km depth

(Berger et al., 1992). A SOM bearing unit (the Blow Me Down Brook formation) is just below it at ~ 0.9 – 1.5 km from the surface (Berger et al., 1992; Williams and Cawood, 1989). This formation is best represented by our samples HAA2 to HAA6. Below that formation is the Green Point Shale bearing formation, locally known as the McKenzies formation of the Bonne Bay Group. It starts at ~ 1.5 km (Berger et al., 1992; Williams and Cawood, 1989). Sediments from this formation are best represented by our sample HAA1.

On the Bernard Plot the gases from the ultra-basic WHC2 spring of the Tablelands plot in the thermogenic field (Figure 2.3A), and these gases would be considered 'wet' based on their low CH_4/C_{2+} values ranging from 5.9 to 9.5 (Table 2.1). This is consistent with the estimated formation/equilibration temperature, as thermogenic gas that forms at 85 ± 7 °C would be in the oil window and would have a low CH_4/C_{2+} value. However, it must also be noted that there is no abiogenic field on the Bernard Plot. Nevertheless, multiple experimental studies have shown that abiogenic hydrocarbons a low CH_4/C_{2+} ratio of 30 or less (Fu et al., 2007; Lancet and Anders, 1970; McCollom and Seewald, 2006; Taran et al., 2007) overlap with the thermogenic CH_4/C_{2+} range. Therefore, given the lack of an established abiogenic field and the overlapping of abiogenic and thermogenic CH_4/C_{2+} ratios, the Bernard plot cannot be used as a sole diagnostic tool for differentiating thermogenic from abiogenic methane. Consequently, the $\delta^{13}C_{CH4}$ and δD_{CH4} measured in this study were plotted on a CD plot (Figure 2.3B) along with the microbial, thermogenic, and abiogenic fields proposed by Etiope and Sherwood Lollar (2013). Within this plot the Tablelands data lie in the overlapping region of the abiogenic and thermogenic fields.

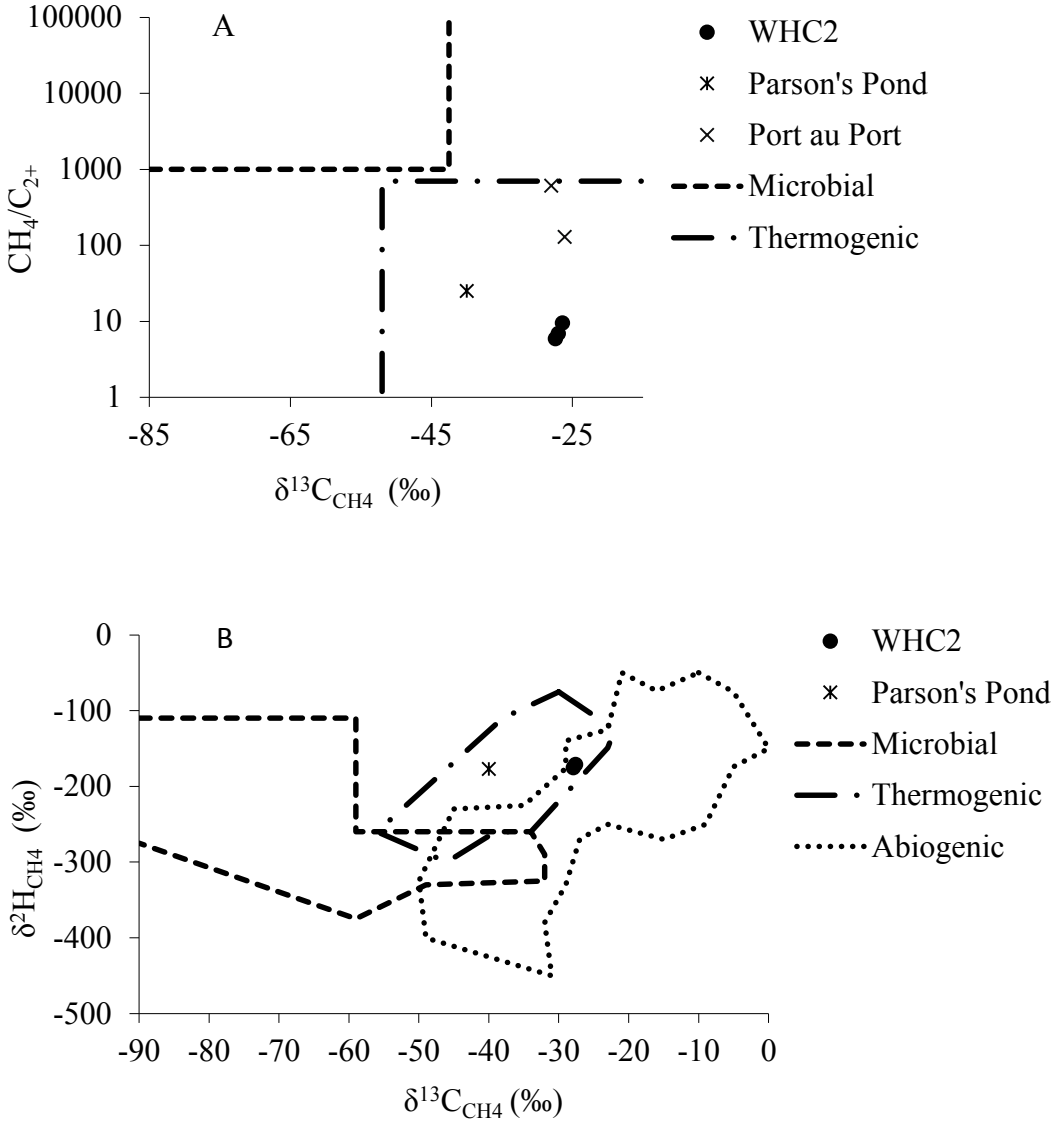

Figure 2.3 A) Hydrocarbons from the Tablelands' WHC2 ultra-basic spring and oil and gas exploration wells near Parson's Pond and Port au Port (Archer, 1996; NALCOR, 2018) graphed on a Bernard Plot. B) Tablelands methane data from WHC2 ultra-basic spring and thermogenic gas sampled from oil and gas exploration wells near Parson's Pond (NALCOR, 2018) graphed on the CD plot with empirically derived fields published

by Etiope and Sherwood Lollar (2013). See Appendix 2 Figure A2.1. for data used in Figure 2.3A, and Appendix 2 Figure A2.2. for data used in Figure 2.3B.

The stable carbon and hydrogen isotope values of methane collected in this study were plotted alongside those of several other laboratory and field-based studies with known methane origins (Figure 2.4A). Data were selected to be plotted on the basis of the diversity of methane sources and the availability of both $\delta^{13}C_{CH4}$ and δD_{CH4} data. Isotope values of methane plotted in Figure 2. 4 were formed in laboratory experiments or naturally in a variety of geologic environments. Laboratory studies produced methane in a range of temperature and pressures to reflect different formational depths (Balabane, 1987; Shuai et al., 2018; Waldron, 1998). Data from field sites were from both sub-aerial and sub-aqueous sites of serpentinization (Kelley and Frueh-Green, 1999; Suda et al., 2014) and hydrocarbon-prone sedimentary basins (Currell, 2017; Ionescu et al., 2017 ; Sherwood et al., 1988). The Tablelands' methane plots adjacent to groundwater springs (Ionescu et al., 2017), and methane gas produced in laboratory experiments using coal collected from mines in southwest and central China as well as shale collected from mines in the midwestern United States (Shuai et al., 2018).

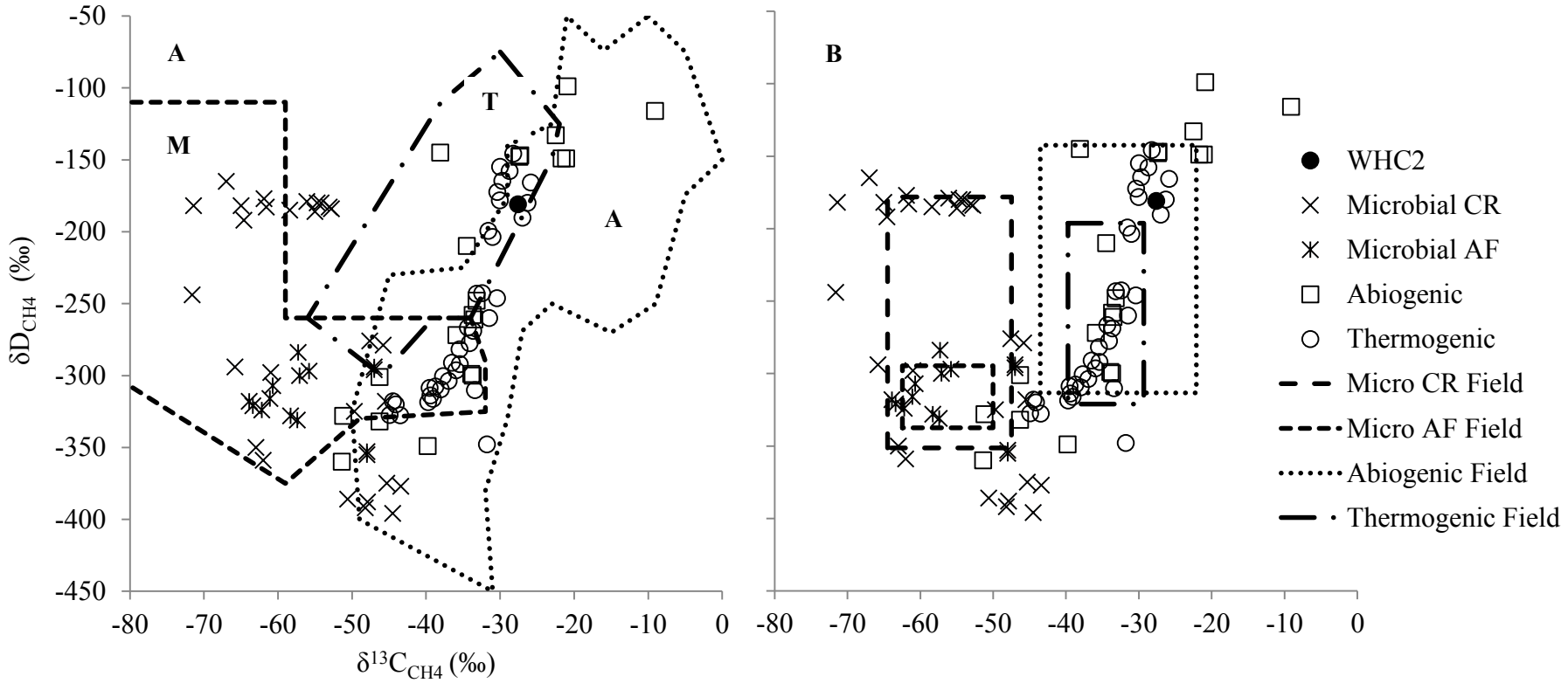

Figure 2.4 CD plot with the stable hydrogen and carbon isotope values of methane classified as Microbial via the CO_2 reduction (CR) pathway (Balabane, 1987; Grossman et al., 1989; Hornibrook, 1997; Waldron, 1998) and the fermentation (AF) pathway (Hornibrook, 1997; Waldron, 1998), Abiogenic (Kelley and Frueh-Green, 1999; Sherwood et al., 1988; Suda et al., 2014) and Thermogenic (Currell, 2017; Ionescu et al., 2017; Shuai et al., 2018). Plot A contains the designated fields (M – microbial, T – thermogenic, and A – abiotic) derived from Etiope and Sherwood Lollar (2013), while the superimposed rectangles in plot B represent one standard deviation (1σ) from the average isotope value calculated for each methanogenic pathway. See Appendix 2 Figure A2.2. for data used in Figure 2.4A, and Appendix 2 Figure A2.3. for data used in Figure 2.4B

The four superimposed fields in Figure 2.4B represent preliminary statistical discrimination between the four pathways of methane production. Fields represent the range of standard deviation from the average value of $\delta^{13}C_{CH4}$ and δD_{CH4} for each of the four pathways. The low and constrained position of the acetate fermentation field in Figure 2.4B depicts a relatively large depletion of deuterium characteristic of acetate fermentation (Schoell, 1988). The relative position of both acetate fermentation and CO_2 reduction fields is in keeping with isotopic depletion as a result of kinetic isotope effects associated with microbial methanogenesis. Conversely, abiogenic and thermogenic fields have relatively less negative $\delta^{13}C_{CH4}$ and δD_{CH4} values. The relative position of these fields is in keeping with that of CD plots in previous studies (Etiope and Sherwood Lollar, 2013 and references therein). However, Figure 2.4B also indicates a considerable overlap between some fields, with the CO_2 reduction field completely encompassing that of acetate fermentation, and the abiogenic field almost completely encompassing that of thermogenic production. However, there remains to be differentiation between the microbial and non-microbial pathways. Methane produced by serpentinizing springs in The Tablelands plots within the non-microbial field, suggesting a non-microbial source, which is in keeping with previous surveys of the spring (Szponar et al., 2013). Furthermore, the geometry of the superimposed fields in Figure 2.4B demonstrates that discrimination between methanogenic pathways based on $\delta^{13}C_{CH4}$ is more conclusive than that based on δD_{CH4}.

As clearly seen in Figure 2.4, the $\delta^{13}C_{CH4}$ and δD_{CH4} values vary considerably. This is the cumulative result of several factors not limited to their respective pathways. Such factors include whether the reaction occurred in an open or closed system, the

temperature at which the methane was produced, concentrations of available reactant gases in the system, the stable isotope composition of the original reactant, and the kinetic isotopic effect associated with the formation reaction. Plotting isotopic fractionation factors (α**)** between reactants and products for both carbon and hydrogen mitigates the influence of the isotopic value of the original substrate.

Figure 2.5 plots the fractionation factor of carbon isotope values between reactant carbon dioxide and product methane ($\boldsymbol{\alpha}^{13}C_{(CO2\text{-}CH4)}$) versus that of hydrogen isotope values between reactant water and product methane ($\alpha D_{(H2O\text{-}CH4)}$) for several laboratory and field-based studies. In a treatment similar to that in Figure 2.4B, the results of these distinct studies were then collated and separated into three methanogenic pathways, and three statistically-derived fields were superimposed in order to discriminate between microbial and abiogenic methane production. A thermogenic field could not be generated due to the lack of data representing that pathway.

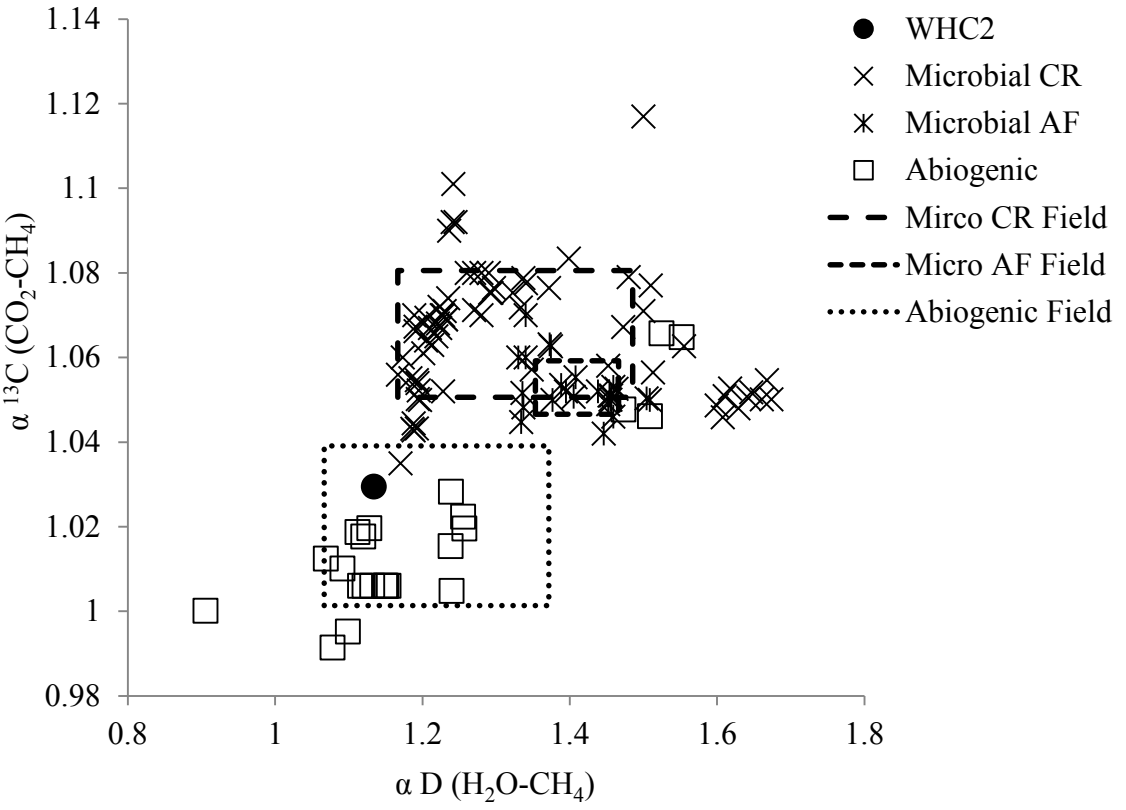

Figure 2.5 Dual fractionation plot showing the fractionation factors between reactants and products for each methanogenic pathway: Microbial via the carbonate reduction (CR) pathway (Balabane, 1987; Chasar, 2000; Claypool, 1973; Friedmann, 1973; Fuchs, 1979; Grossman et al., 1989; Hornibrook, 1997; Kohl et al., 2016; Lansdown et al., 1992; Lien, 1981; Lyon, 1973; Nakai, 1974; Schoell, 1988; Waldron, 1998) and fermentation (AF) pathway (Chasar, 2000; Hornibrook, 1997; Waldron, 1998; Woltemate et al., 1984), and Abiogenic (Fu et al., 2007; Kelley and Frueh-Green, 1999; Proskurowski et al., 2008; Sherwood et al., 1988; Suda et al., 2014; Taran et al., 2010). Superimposed rectangles represent one standard deviation (1σ) from the average isotopic composition calculated for each production pathway. A thermogenic field could not be generated due to the lack of data representing that pathway. Reported $\delta^{13}C_{TIC}$ values were converted to $\delta^{13}C_{CO2}$ as described in Kohl et al. (2016). See Appendix 2 Figure A2.4. for data used in Figure 2.5.

Figure 2.5 exhibits a similar pattern to that observed in Figure 2.4B, with some notable exceptions. As in Figure 2.4B, the superimposed acetate fermentation field is almost entirely encompassed by the CO_2 reduction field, but there is a distinction between microbial and abiogenic fields. This enforces the capacity of the stable isotope composition of CH_4, CO_2, and H_2O in the discrimination between microbial and abiogenic methane sources. However, removing the influence of the isotope values of the substrates did not improve our ability to further differentiate between methane sources. This may be due to other factors, such as system open-ness, original substrate concentration, temperature, and potential similarities between the kinetic isotope effects specific to each methanogenic pathway.

Thermogenic methane is a possibility at the Tablelands, because there are organic-bearing sedimentary units beneath the highly fractured ultramafic rock of the massif. Organic bearing units extend from Port au Port south west of Gros Morne to Parson's Pond north east of Gros Morne as part of the Humber Arm Allochthon (Figure 2.1). We examined the SOM characteristics of the sedimentary units exposed adjacent to the Tablelands massif to determine the type of the thermogenic gas (e.g., wet or dry) that would originate from these units. Using a propriety spore colour comparator generated by Pearson (1984), the colour of organics observed in Humber Arm Allochthon samples corresponded to Thermal Alteration Index (TAI) values that ranged from 3+ to 5. The predominant colour of the observed organics corresponded to a TAI value of 4 which is approximately equal to a vitrinite reflectance (VR) of ca. 3.5 %. A VR this high suggests that the organic thermal maturity of kerogen in source rocks underlying the Tablelands is beyond the oil window and within the dry gas to barren stage. The lack of fluorescent

organics under ultraviolet light further suggests that this source rock has undergone extensive thermal decay. Overall, the SOM characterization suggests that the organic matter in the Humber Arm Allochthon sediments beneath the Tablelands massif is over mature and past the oil window, such that any of the original thermogenic gas generated during the thermal alteration of this source rock would be 'dry' and consist mainly of methane with minor C_{2+} concentrations (i.e., having a high CH_4/C_{2+} value). Therefore it is unlikely that the 'wet' gases sampled from the WHC2 ultra-basic spring originated from the thermal alteration of the SOM in the sedimentary units directly below the massif.

We also examined historical data of the oil and gas exploration wells drilled in the Parsons' Pond and Port au Port areas to determine if the gas at the Tablelands could have migrated there from these other gas producing areas. Near Port au Port, the well logs showed that bottom hole temperatures taken from depths just greater than 3 km did not reach 85 °C, but instead ranged from 47 to 53 °C (Hunt, 1996; Talisman, 1996). While this is a cool basin now, it was once hot during the Acadian orogeny, and it was predicted by Cooper et al. (2001) that the HAA was within the oil window (90 – 150 °C) during the Late Silurian (Cooper et al., 2001). The data from these wells plot in the thermogenic fields of both the Bernard and CD plots (Figure 2.3A&B), and are dissimilar from the gases extracted from the ultra-basic springs of the Tablelands. The observed differences cannot be explained by post genetic alteration processes (e.g., migration oxidation, biodegradation, etc.) because these processes will either enrich the methane in both of the heavy isotopes (i.e., cause the $\delta^{13}C$ and δD to become less negative) or have no measurable effect (Etiope and Sherwood Lollar, 2013). The methane from the Tablelands

is neither more enriched in deuterium compared to the thermogenic methane from Parsons' Pond, nor more enriched in ^{13}C compared to the thermogenic methane from Port au Port. Therefore it is unlikely that the gases sampled from the WHC2 ultra-basic spring in the Tablelands originated from oil and gas producing units north or south of Gros Morne.

An alternative hypothesis is that the gas is abiotic or a mixture of different sources. Since serpentinization is an exothermic reaction, methane may have been formed within groundwaters associated with serpentinization within the ultramafic massif at shallower depths than those predicted by the geothermal gradient through an abiotic process such as inorganic carbon reduction (i.e., abiogenic methane) or hydrocarbon generation from background organic sources. Multiple serpentinization sites report abiogenic methane (Etiope and Sherwood Lollar (2013) and references therein). The extent to which this methane is formed by the reduction of inorganic carbon at low temperatures (i.e., <200 °C) is of interest since recent laboratory experiments showed limited ^{13}C labelled methane production from ^{13}C labelled dissolved inorganic carbon in experiments conducted between 200 – 320 °C without a gas phase present (McCollom, 2016). McCollom (2016) suggested that there were kinetic barriers to abiogenic methane production at low temperature serpentinization sites without a gas phase present, and that the methane that was detected in his experiments, and in other similar experiments, was predominantly derived from background reduced carbon sources rather than abiogenic synthesis. However, McCollom (2016) also observed that ^{13}C labeled methane was observed in similar experiments with a gas phase present, and concluded that shallow serpentinization environments where a separate gas phase is present may be more

favorable for abiogenic synthesis of methane. This may apply to the Tablelands since its ultramafic body is less than 1 km thick; however, the gases within the ultra-basic waters are only found in dissolved phase concentrations. Additionally, the inorganic carbon source at the Tablelands would be atmospheric CO_2 dissolved into rain water ($\delta^{13}C$ = ~-7 ‰), the dissolution of limestone ($\delta^{13}C$ = ~-5 ‰), or a combination of both. Since the ultra-basic waters of WHC are limited in DIC, and if abiogenic methane production consumed most of that DIC, then the $\delta^{13}C$ of the resulting methane would be higher than -27.3 ‰. The $\delta^{13}C$ value of the methane is more similar to that of the SOM (with an average value of -24 ± 5 ‰) than the inorganic carbon sources. While not accounting for all abiogenic hydrocarbons, some putative abiogenic hydrocarbons are well described by a Schulz-Flory distribution and/or an isotope mass balance model (Sherwood Lollar et al., 2008). However, the Tablelands' hydrocarbons are not well described by either of these models (Supplementary Figures 1&2). Considering the potentially slow kinetics and the observed discrepancy in the isotope values of methane and inorganic carbon sources, it is more likely that the methane gas extracted from ultra-basic springs in the Tablelands is a result of slow production of methane at ~85 °C from background organic sources.

4.4 Conclusion

Sourcing methane in the ultra-basic serpentinized springs in the Tablelands was hindered by the inability to measure δD_{CH4} values. We determined that vacuum extraction and gas stripping methods to extract and concentrate dissolved methane are not significantly isotopically fractionationing. The application of these methods enabled the collection of enough CH_4 for the first δD_{CH4} analysis for the Tablelands methane samples

without compromising their isotopic integrity. On a carbon-deuterium plot, the Tablelands methane plotted where thermogenic and abiogenic fields overlap. The SOM in the underlying sedimentary organic unit offer the prospect that, if the methane originated there as thermogenic gas, then the gas would be dry and formed under high temperatures (i.e. >150°C). However, the methane clumped isotope analysis show an apparent temperature of ca. 85°C, leaving open the possibility of other methanogenic pathways. Previous studies have discounted the likelihood of microbial origin of methane in the Tablelands. Low-temperature (<100 ˚C) abiogenic methane formation at this site is a possibility, however data are not well described by existing models of abiogenic methane production. Future study into an abiogenic origin may assess the thermodynamic constraints (e.g., the presence of catalysts, dissolved H_2 concentrations, etc.) relevant for the Tablelands serpentinizing system. Further investigation of the underlying SOM-bearing units and the subsurface hydrogeology will help address a possible thermogenic – either local or remote – source for the Tablelands methane. Lastly, these scenarios are by no means mutually exclusive and future research on the aforementioned possibilities will improve our understanding of the complexity of methanogenic processes.

Acknowledgements

The authors would like to thank Mark Wilson for his inspirational support and great help over the years, and Geert VanBiesen, Elliott Burden, Steve Emberley, and Jamie Warren for their expertise. Geologic maps were created with the diligent support of David Mercer in Memorial University of Newfoundland's Queen Elizabeth II Map Room. This work was supported by grants from Natural Sciences and Engineering Research Council

(NSERC) Discovery Grant awarded to P.I. Morrill, Terra Nova Young Innovator Award awarded to P.I. Morrill, Buchans Scholarship Fund of ASARCO Incorporated awarded to E. Cumming, NSERC Alexander Graham Bell Canada Graduate Scholarship awarded to L. Morrissey, and Chevron Canada Rising Star Scholarship awarded to L. Morrissey. Additionally, we would like to acknowledge Parks Canada for providing access to the site. S. Ono acknowledges support from NASA Astrobiology Institute "Rock-Powered Life" project under cooperative agreement NNA15BB02A and the Alfred P. Sloan Foundation via the Deep Carbon Observatory.

References Cited

Archer, 1996. Geochemical Evaluation of the 1200m to 3650m Interval of the Long Range A-09 Well. , Talisman Energy Inc.

Balabane, M., Galamov, E., Hermann, M., Létolle, R., 1987. Hydrogen and carbon isotope fractionation during experimental production of bacterial methane. Organic Geochemistry, 11: 115-119.

Barnes, I., LaMarche, V.C., Himmelberg, G., 1967. Geochemical evidence of present-day serpentinization. Science, 156: 830-832.

Berger, A.R., Bouchard, A., Brookes, I.A., Grant, D.R., Hay, S.G.,and Stevens, R.K., 1992. Geology, topography, and vegetation, Gros Morne National Park, Newfoundland. Miscellaneous Report 54.

Brazelton, W.J., Morrill, P.L., Szponar, N., Schrenk, M.O., 2013. Bacterial communities associated with subsurface geochemical processes in continental serpentinite springs. Applied and Environmental Microbiology, 79(13): 3906-3916.

Chasar, L.S., Chanton, J.P., Glaser, P.H., Siegel, D.I., 2000. Methane Concentration and Stable Isotope Distribution as Evidence of Rhizospheric Processes: Comparison of a Fen and Bog in the Glacial Lake Agassiz Peatland Complex. Annals of Botany, 86(3): 655-663.

Clark, I., Fritz, P., 1997. Environmental Isotopes in Hydrogeology. Lewis Pubishers, New York, 328 pp.

Claypool, G.E., Presley, B.J., Kaplan, I.R., 1973. Gas analysis in sediment samples from legs 10,11,13,14,15,18,19. Initial Reports Deep Sea Drilling Project, 19: 879-884.

Cooper, M., Weissenberger, J., Knight, I., Hostad, D., Gillespie, D., Williams, H., Burden, E., Porter-Chaudhry, J., Rae, D., and Clark, E., 2001. Basin evolution in western Newfoundland: New insights from hydrocarbon exploration. AAPG Bulletin, 85(3): 393-418.

Currell, M., Banfield, D., Cartwright, I., Cendón, D.I., 2017. Geochemical indicators of the origins and evolution of methane in groundwater: Gippsland Basin, Australia. Environmemtal Science and Pollution Research, 24(15): 13168-13183.

Etiope, G., Sherwood Lollar, B., 2013. Abiotic Methane on Earth. Reviews of Geophysics, 51: 276-299.

Friedmann, I., Hardcastle, K., 1973. Interstial water studies, leg. 15 - Isotopic composition of water. Initial Reports Deep Sea Drilling Project, 20: 901-903.

Fu, Q., Sherwood Lollar, B., Horita, J., Lacrampe-Couloume, G., Seyfried, J., W.E., 2007. Abiotic formation of hydrocarbons under hydrothermal conditions: Constraints from chemical and isotope data. Geochimica et Cosmochimica Acta, 71: 1982-1998.

Fuchs, G.D., Thauer, R., Ziegler, H., Stichler, W., 1979. Carbon isotope fractionation by Methanobacterium thermoautotrophicum. Archives of Microbiology, 120: 135-139.

Grossman, E.L., Coffman, B.K., Fritz, S.J., Wada, H., 1989. Bacterial production of methane and its influence on ground-water chemistry in east-central Texas aquifers. Geology, 17: 495-499.

Gruen, D.S. et al., In press. Experimental investigation on the controls of clumped isotopologue and hydrogen isotope ratios in microbial methane. Geochimica Cosmochimica Acta.

Hinchey, A.M. et al., 2015. The Green Point Shale of Western Newfoundland. A review of its geological setting, its potential as an unconventional hydrocarbon reservoir, and its ability to be safely stimulated using the technique of hydraulic fracturing. In: Department of Natural Resources, G.S. (Editor). Government of Newfoundland and Labrador, , St. John's, pp. 128.

Hornibrook, E.R.C., Longstaffe, F.J., Fyfe, W.S., 1997. Spatial distribution of microbial methane production pathways in temperate zone wetland soils: stable carbon and hydrogen isotope evidence. Geochimica et Cosmochimica Acta, 61(4): 745-753.

Hunt Oil Company., 1996. Final Well Report NHOC/PCP Long Point M16 Appendix IV-1, INV-041414. INV-041414, Hunt Oil Company, Newfoundland.

Ionescu, A., Baciu, C., Kis, B.-M., Sauer, P.E., 2017. Evaluation of dissolved light hydrocarbons in different geological settings in Romania. Chemical Geology, 469: 230-245.

Kelley, D.S., Frueh-Green, G., 1999. Abiogenic methane in deep-seated mid-ocean ridge environments: Insights from stable isotope analyses. Journal of Geophysical Research, 104: 10439-10460.

Kohl, L., Cumming, E. Cox, A. Rietze, A. Lang, S.Q., Richter, A., Suzuki, S. Nealson, K.H. Morrill, P.L., 2016. Exploring the metabolic potential of microbial communities in ultra-basic, reducing springs at The Cedars, CA, US:

Experimental evidence of microbial methanogenesis and heterotrophic acetogenesis. Journal of Geophysical Research G: Biogeosciences, 121(4): 1203-1220.

Lancet, H.S., Anders, E., 1970. Carbon isotope fractionation in the Fischer-Tropsch synthesis of methane. Science, 170: 980-982.

Lansdown, J.M., Quay, P.D., King, S.L., 1992. CH_4 production via CO_2 reduction in a temperate bog: A source of ^{13}C-depleted CH_4. Geochimica et Cosmochimica Acta, 56: 3493-3503.

Lien, Y.Y., Namsaraev, B.B., Trotsyuk, V.Y., Ivanov, M.V., 1981. Bacterial methanogenesis in Holocene sediments of the Baltic Sea. Geomicrobiology Journal, 2: 299-315.

Lyon, G., 1973. Interstitial water studies, leg. 15 - Chemical and isotopic composition of gases from Cariaco Trench sediments. Initial Reports Deep Sea Drilling Project, 20: 773-774.

McCollom, T.M., 2016. Abiotic methane formation during experimental serpentinization of olivine. Proceedings of the National Academy of Sciences of the United States of America, 113(49): 13965-13970.

McCollom, T.M., Donaldson, C., 2016. Generation of Hydrogen and Methane during Experimental Low-Temperature Reaction of Ultramafic Rocks with Water. Astrobiology, 16(6): 389-406.

McCollom, T.M., Seewald, J.S., 2006. Carbon isotope composition of organic compounds produced by abiotic synthesis under hydrothermal conditions. Earth and Planetary Science Letters, 243: 74-84.

Miller, H.M., Matter, J.M, Kelemen, P., Ellison, E.T., Conrad, M.E., Fierer, N., Ruchala, T., Tominaga, M., Templeton, A.S., 2016. Modern water/rock reactions in Oman hyperalkaline peridotite aquifers and implications for microbial habitability. Geochemica et Cosmochimica Acta, 179: 217-241.

Morrill, P.L., Brazelton, W.J., Kohl, L., Rietze, A., Miles, S.M., Kavanagh, H., Schrenk, M.O., Ziegler, S.E., Lang, S.Q., 2014. Investigations of potential microbial methanogenic and carbon monoxide utilization pathways in ultra-basic reducing springs associated with present-day continental serpentinization: the Tablelands, NL, CAN. Frontiers in Microbiology.

Morrill, P.L., Kuenen, J.G., Johnson, O.J., Suzuki, S., Rietze, A., Sessions, A.L., Fogel, M.L., Nealson, K.H., 2013. Geochemistry and geobiology of a present-day serpentinization site in California: The Cedars. Geochimica et Cosmochimica Acta, 109: 222-240.

Morrissey, L., Morrill, P.L., 2016. Flux of methane release and carbon dioxide sequestration at Winterhouse Canyon, Gros Morne, Newfoundland, Canada: a site of continental serpentinization. Canadian Journal of Earth Sciences, 54(3): 257-262.

Nakai, M., Yoshida, Y., Ando, N., 1974. Isotopic studies on oil and natural gas fields in Japan. Chikyakaya, 7/8(1): 87-98.

NALCOR, 2018. In: Morrill, P. (Editor), St. John's NL.

Ono, S., Wang, D.T., Gruen, D.S., Sherwood Lollar, B., Zahniser, M.S., McManus, B.J., Nelson, D.D., 2014. Measurement of a doubly substituted methane isotopologue, 13CH3D, by tunable infrared laser direct absorption spectroscopy. Analytical Chemistry, 86(13): 6487-6494.

Oremland, R.S., Des Marais, D.J., 1983. Distribution, abundance and carbon isotopic composition of gaseous hydrocarbons in Big Soda Lake, Nevada: An alkaline, meromictic lake. Geochimica et Cosmochimica Acta, 47: 2107-2114.

Pearson, D.L., 1984. Pollen/spore colour standard version 2. , Phillips Petroleum Company, Exploration Projects Section.

Proskurowski, G., Lilley, M.D., Seewald, J.S., Früh-Green, G.L., Olson, E.J., Lupton, J.E., Sylva, S.P., Kelley, D.S., 2008. Abiogenic hydrocarbon production at Lost City Hydrothermal Field. Science, 319: 604-607.

Rudd, J.W.M., Hamilton, R.D., Campbell, N.E.R., 1974. Measurement of microbial oxidation of methane in lake water. Limnology and Oceanography, 19(3): 519-524.

Schoell, M., 1988. Multiple origins of methane in the Earth. Chemical Geology, 71: 1-10.

Sherwood, B. et al., 1988. Methane occurences in the Canadian Shield. Chemical Geology, 71: 223-236.

Sherwood Lollar, B. et al., 1993. Evidence for bacterially generated hydrocarbon gas in Canadian Shield and Fennoscandian Shield rocks. Geochimica et Cosmochimica Acta, 57: 5073-5085.

Sherwood Lollar, B. et al., 2008. Isotopic signatures of CH4 and higher hydrocarbon gases from Precambrian Shield sites: A model for abiogenic polymerization of hydrocarbons. Geochimica et Cosmochimica Acta, 72(19): 4778-4795.

Sherwood Lollar, B., Westgate, T.D., Ward, J.A., Slater, G.F., Lacrampe-Couloume, G., 2002. Abiogenic formation of gaseous alkanes in the Earth's crust as a minor source of global hydrocarbon reservoirs. Nature, 416: 522-524.

Shuai, Y., P.M.J. Douglas, Zhang,S., Stolper, D.A, Ellis, G.S., Lawson, M., Formolo, M., Mi, J., He., K., Hu, G., Eiler, J.M., 2018. Equilibrium and non-equilibrium controls on the abundances of clumped isotopologues of methane during thermogenic formation in laboratory experiments: Implications for the chemistry of pyrolysis and the origins of natural gases. Geochimica et Cosmochimica Acta, 223: 159-174.

Sleep, N.H., Meibom, A., Fridriksson, T., Coleman, R.G., Bird, D.K., 2004. H2-rich fluids from serpentinization: Geochemical and biotic implications. PNAS, 101(35): 12818 -12823.

Stolper, D., Sessions, A., Ferreira, A., Santos Neto, E., Schimmelmann, A., Shusta, S., Valentine, D., Eiler, J., 2014. Combined 13C-D and D-D clumping in methane: Methods and preliminary results. Geochimica et Cosmochimica Acta, 126: 169-191.

Suda, K. Ueno,Y. Yoshizaki, M. Nakamura, H. Kurokawa, K., Nishiyama, E., Yoshino, K., Hongoh, Y., Kawachi, K. Omori, S., Yamada, K., Yoshida, N., Maruyama, S. 2014. Origin of methane in serpentinite-hosted hydrothermal systems: The CH4-H2-H2O hydrogen isotope systematics of the Hakuba Happo hot spring. Earth and Planetary Science Letters, 386: 112-125.

Suzuki, S., Ishii, S., Wu, A., Cheung, A., Tenney, A., Wanger, G., Kuenen, J. G., Nealson, K. H. 2013. Microbial diversity in The Cedars, an ultrabasic, ultrareducing, and low salinity serpentinizing ecosystem. PNAS, 110(38): 15336-15341.

Szponar, N., 2012. Carbon Cycling at a Site of Present-Day Serpentinization: The Tablelands, Gros Morne National Park. Thesis - paper based Thesis, Memorial University, St. John's, NL, 156 pp.

Szponar, N. et al., 2013. Geochemistry of a Continental Site of Serpentinization in the Tablelands Ophiolite, Gros Morne National Park: a Mars Analogue. ICARUS, 224: 286-296.

Talisman Energy Incorporated., 1996. Long Range A-09 - Borehole Compensated - Sonic Run 2 - Final - INV-041540. INV-041540, Newfoundland.

Taran, Y.A., Kliger, G.A., Cienfuegos, E., Shuykin, A.N., 2010. Carbon and hydrogen isotopic compositions of products of open-system catalytic hydrogenation of CO2: Implications for abiogenic hydrocarbons in Earth’s crust. Geochimica et Cosmochimica Acta, 74: 6112-6125.

Taran, Y.A., Kliger, G.A., Sevastianov, V.S., 2007. Carbon isotope effects in the open-system Fischer–Tropsch synthesis. Geochimica et Cosmochimica Acta, 71: 4474-4487.

Urey, H.C., 1947. The thermodynamic properties of isotopic substances. Journal of the Chemical Society: 562-581.

van Staal, C.R. et al., 2007. The Notre Dame arc and the Taconic orogeny in Newfoundland. Geological Society of America Memoirs, 200 (March 2016): 511–552.

Waldron, S., Watson-Craik, I.A., Hall, A. J., Fallick, A.E., 1998. The carbon and hydrogen stable isotope composition of bacteriogenic methane: A laboratory study using a landfill inoculum. Geomicrobiology Journal, 15(3): 157-169.

Wang, D.T. et al., 2015. Clumped isotopologue fingerprinting of methane sources in the environment. Science, 348(6233): 428-431.

Williams, H., Cawood, P., 1989. Geology, Humber Arm Allochthon, Newfoundland. Map 1678A. , GS# NFLD/1852. Geological Survey of Canada. .

Woltemate, I., Whiticar, M.J., Schoell, M., 1984. Carbon and hydrogen isotopic composition of bacterial methane in a shallow freshwater lake. Limnology and Oceanography, 29(5): 985-992.

Young, E.D. et al., 2017. The relative abundances of resolved $^{12}CH_2D_2$ and $^{13}CH_3D$ and mechanisms controlling isotopic bond ordering in abiotic and biotic methane gases. Geochimica et Cosmochimica Acta, 203: 235-264.

CHAPTER 3: QUANTIFYING CO_2 SEQUESTRATION AT MULTIPLE SITES WITHIN THE TABLELANDS, GROS MORNE NATIONAL PARK, NL, CANADA; A SITE OF CONTINENTAL SERPENTINIZATION[2]

[2] *This chapter is based on the following paper:*

Cumming, E.A., Morrill, P.L. In Prep. Quantifying CO_2 sequestration at multiple sites within the Tablelands, Gros Morne National Park, NL, Canada; a Site of Continental Serpentinization. *Chemical Geology.*

Abstract

Ophiolites and their associated high-pH serpentinizing springs are potential targets for enhanced Global Carbon Storage (GCS). To eventually validate this potential, and to better incorporate sites of continental serpentinization into global climate change models, rates of sequestration and emission of greenhouse gases such as CO_2 must be constrained at multiple environments within ophiolites. This study examined and sampled the predominant land cover styles at the Tablelands Ophiolite in Western NL. A LI-COR 8100A gas survey chamber and CO_2 gas analyzer was deployed at two sites of flowing high-pH groundwater outlet, one of pooling groundwater outlet, and at a final dry site covered in unconsolidated serpentinized ultramafic cobbles. CO_2 fluxes at both flowing discharge locations were less than analytical reproducibility. A CO_2 flux of -266 μmol m^{-2} min^{-1} was calculated from a pooling groundwater outlet, with another of -2.32 μmol m^{-2} min^{-1} calculated at a dry site. High negative values were indicative of CO_2 sequestration. Two CO_2 fluxes assigned to the vegetated areas of the massif represent the minimum and maximum contribution of the vegetation to net CO_2 sequestration. These discrete values were then collated according to their areal extent, and used to calculate a net CO_2 sequestration rate for the entire massif– a minimum of -118 mol min^{-1} and a maximum of -168 mol min^{-1}. These values suggest that the ophiolite sequesters CO_2. This study constitutes the first attempt to quantify CO_2 flux at multiple sites within the Tablelands, in an effort to quantify the net rate of CO_2 sequestration for the massif as a whole. CO_2 flux is a function of numerous interconnected processes, and as such, more observations of different durations and at different times of year will refine our understanding of annual and seasonal variability in CO_2 flux. This is a necessary step before GCS is considered.

1 Introduction

Serpentinized rocks and their associated groundwater springs act as analogues for several enigmatic systems. They inform our understanding of submarine processes that we cannot observe, act as a portal to the subsurface biosphere, and act as planetary analogues. However, they are also enigmatic themselves.

In exposed serpentinized strata, the fluxes of greenhouse gases, namely methane (CH_4) and carbon dioxide (CO_2), are poorly constrained. Due to the ultra-basic (pH >11-12) nature of spring water within sites of continental serpentinization, they can sequester CO_2, while simultaneously emitting CH_4 via multiple pathways associated with the structural and stratigraphic characteristics of an ophiolite suite (Morrissey & Morrill, 2016.; Szponar et al., 2013). Sites of continental serpentinization thereby act as both a sink and a source for greenhouse gases. In order to understand the net climate effect of such sites, and to thereby effectively incorporate them into climate change models, the flux of greenhouse gases at sites of continental serpentinization must be quantified.

Additionally, the capacity of these sites to sequester CO_2 makes them potential targets for the enhanced storage of anthropogenic emissions, or global carbon storage (GCS). However, understanding greenhouse gas fluxes is essential to validating ophiolites as viable sites for long-term carbon storage. The baseline conditions of these systems must be established before they are engineered for GCS.

A contributing factor to the enigmatic geochemistry associated with the production of methane in some sites of continental serpentinization is the role of CO_2. CO_2 is consumed during the abiogenic and microbial production of methane. Additionally, the ultra-basic, Ca^{2+}-rich groundwater associated with the water-rock reaction within an ophiolite is conducive to the rapid, sometimes extensive carbonation of ophiolitic peridotite (Kelemen & Matter, 2008; Kelemen et al., 2011), whereby CO_2 is converted to solid calcium or magnesium carbonate. This has made ophiolites attractive prospective targets for Global Carbon Storage (GCS) (Kelemen & Matter, 2008), or, more specifically, the Geologic Carbon Capture and Storage System (GCCSS) (Rajendran et al., 2014). However, the role of CO_2 in methanogenesis at sites of serpentinization is not constrained.

Quantification of CO_2 sequestered and CH_4 emitted at one spring discharge location in the Tablelands was achieved using a prototype closed chamber gas sampler (Morrissey & Morrill, 2016) in the summer of 2015. The closed gas chamber consisted of an inverted five gallon bucket, modified with a gas-tight port that facilitated periodic gas sampling from the top of the bucket. For a period of 24 hours, a prototype closed chamber gas sampler was inverted over a pool in order to isolate the air-water interface directly overlying an ultra-basic groundwater outlet (labeled WHC2b). Intermittent discrete samples were taken from the chamber atmosphere for the duration of the observation period, and subsequently analyzed for their CO_2, CH_4, and nitrous oxide (N_2O) concentrations.

The 24-hour observation of site WHC2b saw negligible N_2O flux, and CO_2 sequestration occurred at a rate 41 times faster than the emission of CH_4 (Morrissey & Morrill, 2016). These fluxes were then used to calculate the net radiative force of greenhouse gases at the Tablelands. In this study, the radiative forcing of CO_2 was -0.22, and that of CH_4 was 0.01, with a cumulative forcing of -0.21 (Morrissey & Morrill, 2016). Morrissey and Morrill (2016) was the first study to consider the net effect of fluxes of greenhouse gases associated with serpentinizing springs. The study concluded that the methods applied to WHC2b should be applied to other ultra-basic groundwater discharge locations with the potential to sequester and produce greenhouse gases within the massif.

In this study, in the summer of 2017, instrumental and methodological adjustments were made in order to quantify CO_2 sequestration in the Tablelands. The prototype closed chamber gas sampler developed by Morrissey & Morrill (2016) was replaced by a LI-COR 8100A Automated Soil CO_2 Flux System, a commercial closed chamber gas analyzer capable of continuous, real-time CO_2 measurements. Discrete sampling for CH_4 was also conducted via an in-line commercial trace gas attachment. The power requirements of the commercial gas analyzer limited observation length to 5-6 hours. Three additional sampling sites were monitored for CO_2 concentrations. Figure 3.1 shows the sites where CO_2 sequestration was measured in the summer of 2015 and 2017. Sampling conducted during the summer of 2015 took place at a single area of groundwater discharge and active carbonation within the serpentinized host rock – WHC2b. Sampling conducted during the summer of 2017 took place at three separate

areas of groundwater outlet and active carbonation within the serpentinized host rock – WHC2b, TLE, and WHC500 – and also at a background site of unconsolidated serpentinized ultramafic cobble to boulder cover, UUC.

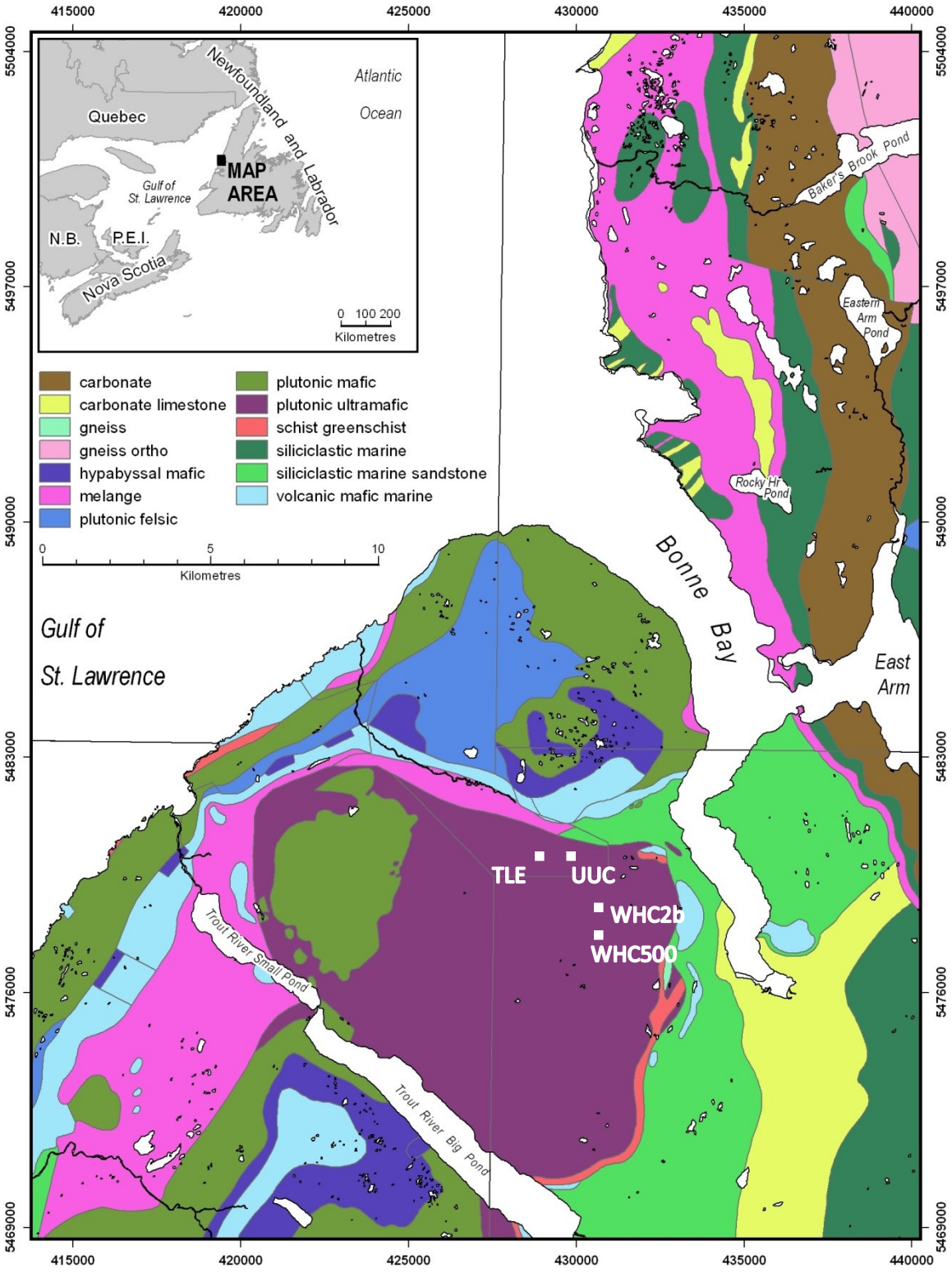

Figure 3.1 Bedrock geologic map, modified after Rietze (2012) of the Tablelands massif and surrounding area. Sampling sites are represented by white squares. Source data from

NL survey (http://gis.geosurv.gov.nl.ca/) and the federal Department of Natural Resources (http://geogratis.gc.ca/site/eng/extraction?id=2013_51d579a832fb79.569414).

Gas concentrations were monitored at three additional sites to account for differences in CO_2 flux associated with different surficial cover. WHC2b represents a pooled groundwater outlet, while TLE and WHC500 both represent flowing high-pH groundwater outlets. These ultra-basic groundwater outlets are conducive to CO_2 sequestration, but their areal extent is small relative to the total lateral extent of the Tablelands massif. UUC was therefore chosen as a background site representative of the massif as a whole, as the majority of the massif surface is comprised of serpentinized ultramafic cobbles and boulders overlying ultramafic bedrock (Figure 3.1). Though mostly barren, some areas of sparse vegetation are found on the Tablelands. Thus, to account for their contribution to the CO_2 sequestration potential of the massif, these areas were defined using satellite imagery of the ophiolite (Figure 3.2).

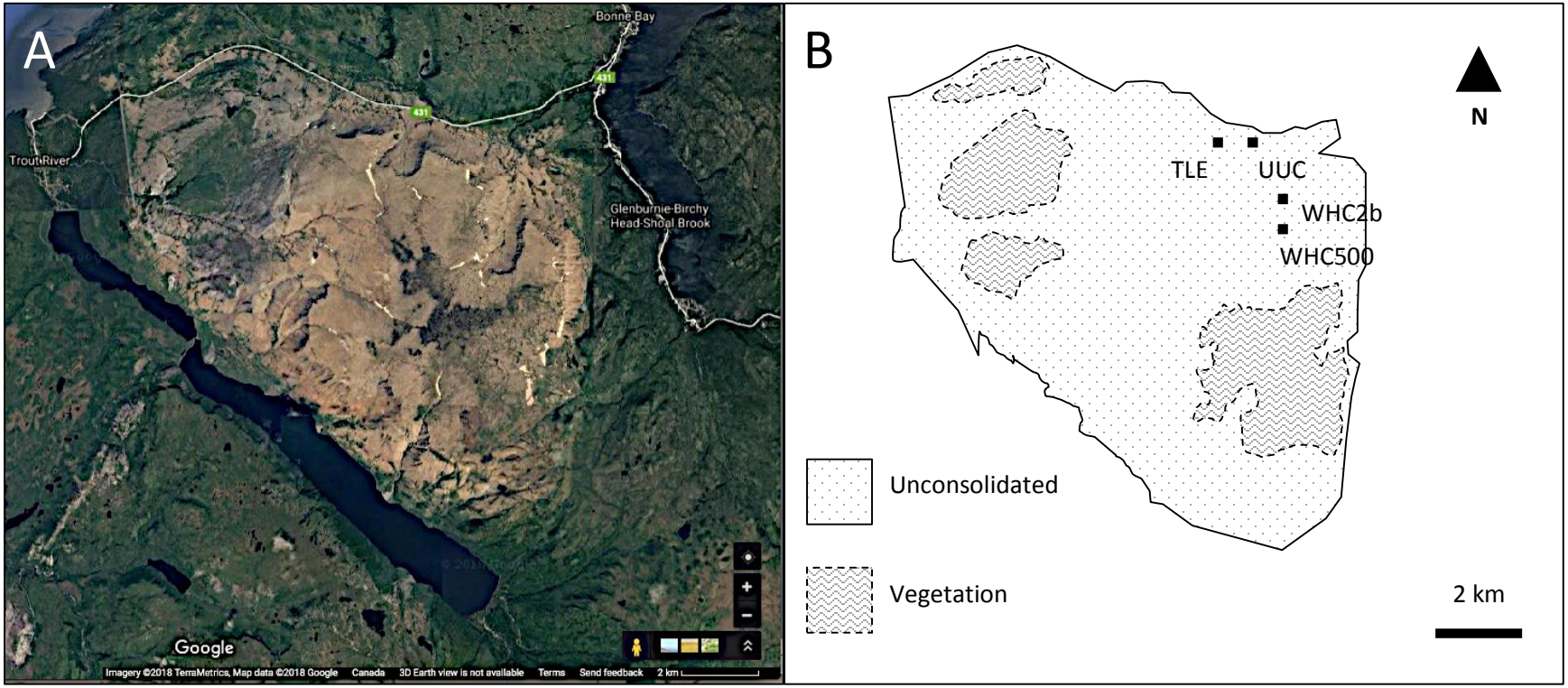

Figure 3.2 (A) Satellite image of the Tablelands massif (obtained from Google Earth on April 9th, 2018), the areal extent of which has been (B) subdivided based on cover style. Sampling sites in 2015 and 2017 are represented by black squares. Note that the areas of serpentinizing springs (WHC2b, WHC500, and TLE) are too small to be represented at this scale.

The main objective of this study was to determine the flux of CO_2 within the Tablelands at multiple sites representative of different end members of CO_2 sequestration potential. An additional outlined objective was to determine the CH_4 flux at WHC2b. Based on the presence of travertine, it was hypothesized that CO_2 sequestration may be observed at groundwater discharge locations. CO_2 sequestration was hypothesized to be non-existent or negligible compared to that at WHC2b. The final objective of this study was to calculate a net CO_2 flux estimate for the Tablelands massif as a whole.

2 Methods

2.1 Description of Sampling Sites

Winter House Canyon – 2b (WHC2b), located at NAD27 0430583'N 5479517'E (UTM 21), was a groundwater discharge point into the base of a small (1.5 m x 0.75 m) ellipsoidal pool 3 m west of Winter House Brook (WHB). This brook runs through the Tablelands flowing approximately south to north. The pool contained ultra-basic and reducing water, with E_h values becoming more negative at the bottom. Values were indicative of an anoxic bottom layer, despite overland flow input into the pool. In addition to being ultra-basic, the discharging groundwater was rich in Ca^+ and OH^- (Szponar et al., 2013), leading to the precipitation of carbonate as a travertine envelope around the pool. Sampling for total inorganic carbon (TIC), dissolved gas, and for the quantification of sequestered CO_2 was completed at this site in 2017.

Figure 3.3 Site photos of (A) WHC500, (B) UUC and the LI-COR 8100a gas survey chamber and CO_2 gas analyzer, and (C) TLE and the LI-COR 8100a gas survey chamber.

Tablelands East (TLE), located at NAD27 0428984'N 5480701'E (UTM 21), and consisting of 3 groundwater discharge locations on the steeply sloping northeastern face of the Tablelands massif, contains a 10 m x 30 m occurrence of scaly to botryoidal travertine. The pH at the springs was 10, while water measured at the base of the travertine was pH 9.5.

A LI-COR gas survey chamber and CO_2 gas analyzer were deployed at the easternmost of the three outlet sites to measure gaseous flux in a flowing system. This outlet was chosen as it was a viable place to deploy the chamber without obstructing spring flow, and because it was the largest and fastest flowing spring. With the exception of pH, no other aqueous geochemistry measurements were taken at TLE.

Winter House Canyon – 500 (WHC500), located at NAD27 0430583'N 5479517'E (UTM 21), contained an array of discharge locations 7 m west of Winter House Canyon on a gentle slope, 500 m upstream from the WHC2b pool, hence its name. The pH at the discharge locations was between 9.5-10, and discharge locations were surrounded by 3 m x 5 m of travertine.

To measure gaseous flux in a flowing system. the LI-COR gas survey chamber and CO_2 gas analyzer were deployed at the topmost of the discharge locations. This discharge location offered a clear place to deploy the chamber without obstructing spring flow, and furthermore contains high pH water. With the exception of pH, no other aqueous geochemistry measurements were taken at WHC500.

Unconsolidated Ultramafic Cover (UUC), located at NAD27 0429397'N 5480973'E (UTM 21), was a flat expanse of unconsolidated serpentinized ultramafic

cobble to boulder cover 100 m south of the Tablelands trail head. Boulder cover depth is variable upon the Tablelands, but based on as assessment of the area, as well as maps detailing local bedrock geology (Figure 3.1), this boulder cover overlies serpentinized ultramafic bedrock.

The LI-COR gas survey chamber and CO_2 gas analyzer were deployed at this site in order to quantify CO_2 sequestration associated with ultramafic lithologies. This area was chosen because it resembled the majority of the Tablelands massif, and could thereby act as a representative background measurement for the entire ultramafic portion of the ophiolite suite.

2.2 Field Sampling Methods

Air temperature and wind speed was measured using a Kestrel 3000 Pocket Weather Meter. This was done in order to account for any discrepancies over the duration of gas flux observation. In summer, and on this matter, conditions remained clear and stable for the duration of fieldwork.

The pH of water was measured before and after deployment of the LI-COR gas survey chamber and CO_2 gas analyzer at TLE, WHC500 and WHC2b. pH was measured at WHC2b with an IQ Scientific Instruments IQ180G GLP handheld field meter. The meter was calibrated prior to the first day of sampling by submerging it in Oakton pH buffer solutions of 4.01, 7.00, and 10.01. Daily calibration checks were conducted

throughout the study period. Water at all other sites was too shallow to use the field probe, and therefore was measured using BDH pH Test strips ranging from 0-14, and EMD colorpHast pH-indicator strips ranging from 6.5-10 and 11.0-13.0.

Water samples for total inorganic carbon (TIC) and dissolved gases were collected before and after deployment of the LI-COR gas survey chamber and CO_2 gas analyzer at WHC2b. Water samples were taken for TIC measurements by filling 40 mL amber vials, containing a single drop of 15% mercuric chloride, to kill microorganisms and fix the sample. Vials were sealed with black butyl septa. On use, duplicate sample vials were filled with no headspace with unfiltered sample water, using a 60 mL syringe. Samples were then kept cold and dark until analysis.

Dissolved methane was extracted from the water using the gas phase equilibration technique described by Szponar et al. (2013). In short, 25 mL of sample water was taken up by two 60 mL sterile syringes already filled with an equivalent volume of He gas. After sealing the syringes they were shaken for five minutes to partition gas dissolved in the sample water to the gas phase. The gaseous content of both syringes was then injected into an inverted 30 mL glass bottle, pre-filled with degassed Nano-UV water with no headspace, and sealed with conditioned blue butyl septa. A 22-gage exit needle facilitated displacement of this water by the sampled gas. Ultimately, the 30 mL bottle was over pressurized with 20 mL of sample gas. A drop of saturated solution of mercuric chloride

was added to each 30 mL vial, to kill the microorganisms living in residual water within the bottle. Sampling was conducted in duplicate.

Gas flux experiments were conducted using a LI-COR LI-8100A Gas Analyzer configured with a 20 cm chamber and in-line trace gas kit. Instrument calibration was conducted by the manufacturer in the month prior to deployment in the field. Prior to deployment in the field, the gas analyzer's zero was set for both CO_2 and H_2O using chemical scrubbers according to the instrument's instruction manual. In order to set the zero for CO_2, a LI-COR Chemical Tube was filled with a soda lime chemical scrubber (LI-COR part number 9964-090), and configured in-line with a particulate filter. This was configured to the survey chamber outflow and the gas analyzer inflow, with the particulate filter separating the chemical scrubber from the analyzer. The LI-COR LI-8100A Gas Analyzer was allowed to pump for 20 minutes, in which time CO_2 values became stable. The zero was then set using the gas analyzer's calibration software. The zero for H_2O was set using the same procedure, configuration, and software, but using a drierite chemical scrubber (LI-COR part number 622-04299).

Once zeroed, continuous, real-time CO_2 concentration values were analyzed in the field by the apparatus's infrared gas analyzer (IRGA) and recorded onto its internal memory. The survey chamber concentration of CO_2 was reported as a mole fraction corrected for water vapor dilution within the chamber.

Discrete sampling for CH_4 gas concentration was facilitated by the in-line trace gas attachment (LI-COR 8100-664 Trace Gas Sample Kit), which consisted of a three-way gas-tight connector, with one port connecting to the chamber outflow port, the second to the intake port of the gas analyzer, and the third allowing sampling access through a rubber septa. Profiles consisted of 8 or 9 measurements taken over the span of 5 or 6 hours, respectively, with the first four measurements occurring in the first hour at twenty-minute intervals, and the final measurements occurring hourly. Each individual sample consisted of two consecutive 50mL volumes of gas collected from the chamber using a 60mL sterile syringe through the connecting port. Sampled gas, totaling 100mL, was then injected into a pre-evacuated 30mL glass vial. This over pressurized the vials, making injection of the sample in its entirety challenging. A trial of this method conducted earlier by Morrissey & Morrill (2016) demonstrated that concentration measurements from duplicate samples were within error of each other. Therefore only single samples were taken in this study.

2.3 Analytical Methods

Concentrations of CH_4 gas were measured using a SRI 8610C gas chromatograph equipped with a flame ionization detector (GC-FID) and a Carboxen 1010 column (30 m x 0.32 mm ID, 15 μm film thickness) subjected to a constant flow of He carrier gas. The detection limit of the GC-FID apparatus was 1 μmol/L for CH_4. The GC-FID was calibrated with consecutive 5 μL, 10 μL, and 15 μL injections at atmospheric pressure of a Scotty gas standard (CO_2 = 5.0%, CO = 5.0%, H = 4.0%, CH_4 = 4.0%, N = 5.0%, O_2 = 5.0%) made with a 25 μL Supelco Pressure-Lok Precision Analytical Syringe. Once the

GC-FID was calibrated, the samples were analyzed by injecting 350 µL of the gas extracted from each bottle with a 500 µL Supelco Pressure-Lok Precision Analytical Syringe. The temperature program used for both calibration and sample injections consisted of a sustained temperature of 40°C for six minutes, followed by temperature increase from 40°C to 110°C for twenty-five minutes, followed by five minutes of sustained temperature at 110°C degrees.

2.4 Calculating Gas Flux

Using gas concentration values obtained from the field, gas flux was calculated using Equation 1:

$$F = V(P_2 - P_1) / RTA(t_2 - t_1) \quad \text{(Equation 1)}$$

where F is flux (mol m^{-2} min^{-1}), V is chamber volume (the LI-COR 20 cm chamber volume is 0.004843 m^3), R is the ideal gas constant (m^3 Pa K^{-1} mol^{-1}), T is air temperature (K), A is the surface area of the chamber mouth (the LI-COR 20 cm chamber area is 0.00043352 m^2), P_1 and P_2 are the gas partial pressures at two different sampling times, denoted by t_1 and t_2.

Equation1 is based on the ideal gas law, and assumes that gas concentration increases or decreases linearly with time. If linearity is invalid, gas flux can be calculated using Equation 2:

$$F = \alpha k (C_{gasw} - C_{sat}) \quad \text{(Equation 2)}$$

where α is a dimensionless coefficient of chemical enhancement (Morrissey and Morrill (2016) calculated a value of 22.7 for CO_2 gas at WHC2b), k is the gas transfer velocity (m s^{-1}), and C_{gasw} and C_{sat} is the gas concentration dissolved in the surface layer of water and dissolved in equilibrium, respectively (mol L^{-1}).

3 Results

3.1 Aqueous Geochemistry

Table 3.1 reports the pH, TIC, and dissolved CH_4 gas concentration measurements taken immediately before and after deploying the LI-COR gas analyzer at WHC2b, TLE, and WHC500.

Table 3.1 Aqueous geochemistry parameters, dissolved gas concentrations, and atmospheric parameters measured before and after gas flux experiments were performed at WHC2b, TLE, and WHC500 in 2017.

	WHC2b		TLE		WHC500	
	Before	After	Before	After	Before	After
pH	12.16[a]	11.96[a]	10[b]	10[b]	9.5-10[b]	9.5-10[b]
TIC (ppm)	0.66±0.01	1.34±0.05	-	-	-	-
$[CH_4]$ (μM)	43.2±1.5	42.8	-	-	-	-
$[CO_2]$ (μM)	159.0±0.5	159.0±6.1	-	-	-	-
Wind Speed (mph)	1.8	3.3	4.3	8.6	3.0	5.9
Air Temp. (°C)	22.2	22.2	28.0	28.0	28.0	28.0

- = parameter not measured at this site; [a] = pH measurements were taken at the base of the pool (WHC2b) using a IQ Scientific Instruments IQ180G GLP handheld field meter; [b] = outlets were prohibitively shallow, so pH measurements were taken directly at outlets using BDH pH Test strips ranging from 0-14, and EMD colorpHast pH-indicator strips ranging from 6.5-10 and 11.0-13.0.

The pH values differed by 0.2, or were within 2% of each other, at WHC2b, and no difference in pH was observed between measurements taken before and after the deployment of the LI-COR gas survey chamber and CO_2 gas analyzer at TLE and WHC500.

3.2 CH_4 Flux at a Serpentinizing Spring

Sampling for the quantification of CH_4 generation associated with the ultra-basic water of a serpentinizing spring was conducted at WCH2b in the summer of 2017. Figure 3.4 depicts the CH_4 concentrations in samples collected in the summer of 2017.

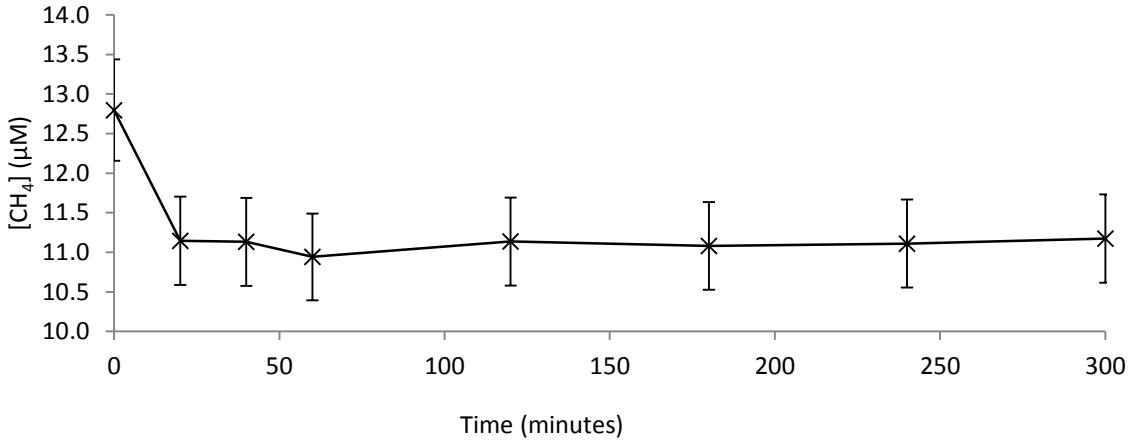

Figure 3.4 CH_4 concentrations in discrete samples taken from the atmosphere of the Licor closed 20 cm chamber, deployed over the air-water interface directly overlying WHC2b in the summer of 2017. Error bars represent a 5% analytical error. See Appendix 3 Figure A3.1. for data used in Figure 3.4.

The measurement taken at Time Zero, immediately after the chamber closed, displays the highest CH_4 concentration. All following concentration values were lower, and did not demonstrate an increase or a decrease in methane within analytical error.

3.3 CO_2 Fluxes within the Tablelands

CO_2 flux associated with the ultra-basic water of serpentinizing springs was quantified at three spring outlets (WHC2b, TLE, WHC500) in the summer of 2017. Additionally, CO_2 flux was quantified at a dry site of unconsolidated serpentinized ultramafic cobble to boulders (UUC), covering serpentinized ultramafic bedrock (see Figure 1 for sampling site location relative to bedrock lithology). Figure 3.5 depicts the concentrations of CO_2 of all four sites over five hours, normalized to their initial concentrations according to Equation 3.

$$(C_x - C_f) / (C_o - C_f) \qquad \text{(Equation 3)}$$

where C_x is the concentration of CO_2 at any time during the five-hour observation, C_o is the concentration of CO_2 at the beginning of the five-hour observation, and C_f is the concentration of CO_2 at the end of the five-hour observation.

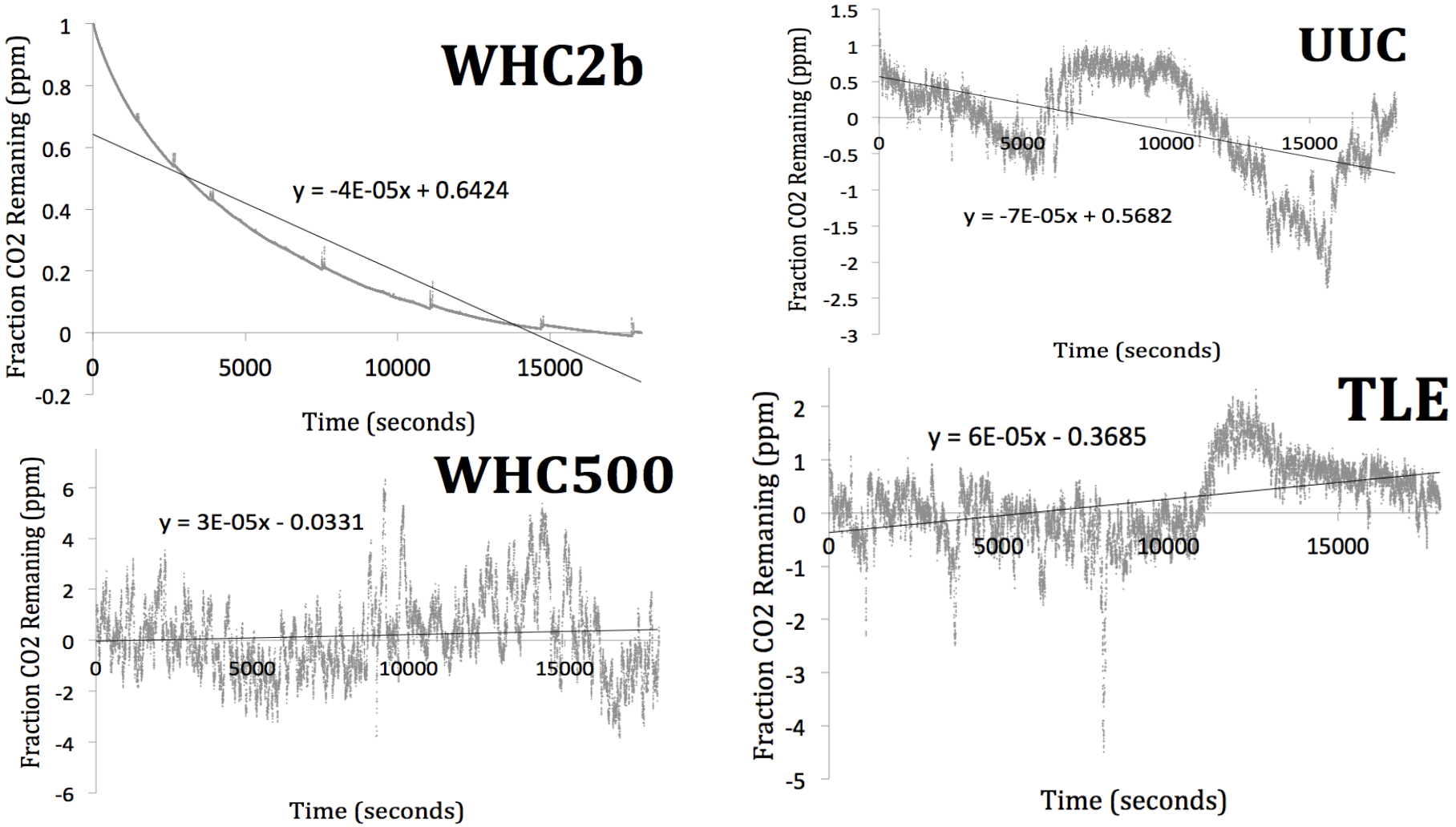

Figure 3.5 Normalized CO_2 concentrations measured continuously over five hours at (A) WHC2b, (B) TLE, (C) WHC500, and (D) UUC using a LI-COR LI-8100A Gas Analyzer. See Appendix 3 for data used in Figure 3.5

The CO_2 concentration values of TLE, WHC500, and UUC fluctuated over the course of the five-hour observation window. As a dry site, UUC was chosen to represent the baseline fluctuations in concentration associated with the LI-COR gas analyzer in the field. The error associated with concentration values at TLE and WHC500 did not exceed that at UUC. As such, the variability of concentrations observed at TLE and WHC500 was attributed to instrumental variability.

The normalized plot depicts the change in concentration in the ultra-basic pool WHC2b compared to the relatively static concentration values over time of the other spring outlets and bare ultramafic rock. It is important to note that the decrease factor of WHC2b was reduced slightly by periodic manual trace gas sampling. The line representing WHC2b in Figure 3.5A displays small upward spikes followed by a slight decrease in normalized CO_2 concentration values relative to those immediately preceding the downward spike. These spikes correspond temporally to manual sampling for trace gas concentrations, conducted every twenty minutes for the first hour of observation, and then hourly for the remaining four hours of observation. The effect of trace gas concentration sampling was minimal, and WHC2b CO_2 concentration values decreased by a factor of nearly 22 over 5 hours.

4 Discussion

Lines of best fit were added to the normalized values in Figure 3.5 in order to demonstrate an increasing or decreasing trend in CO_2 concentration values at each site. Linear trend lines with negative slopes were observed at WHC2b and UUC, suggesting an overall

increase in CO_2 concentration at these sites over five hours. The variability of concentration observed at TLE and WHC500 was attributed to instrumental variability, as it was less than that observed at the background site, UUC.

While these trend lines indicate increasing or decreasing trends, flux is defined more quantitatively using Equation 1. CO_2 fluxes calculated using Equation 1 at WHC2b and UUC were -266 μmol m^{-2} min^{-1} and -2.32 μmol m^{-2} min^{-1}, respectively. Negative flux values at WHC2b and UUC are indicative of CO_2 sequestration. Flux calculated at WHC2b is 115 times greater than that at UUC.

Equation 1 assumes a linear increase or decrease in gas concentration over time. CO_2 concentration profiles obtained by the LI-COR gas analyzer (Figure 3.5) show that gas concentrations do not change linearly over the course of five hours. CO_2 concentration at WHC2b decreased consistently but the concentration profile is curved. CO_2 concentrations at all other sampling sites fluctuated over the five-hour observation period. Therefore, CO_2 flux was also calculated using Equation 2, which is not based on linearity. A CO_2 flux value could only be calculated for WHC2b, as Equation 2 contains parameters that were only sampled for at this site. Additional parameters for Equation 2 – α, k, and C_{sat} of 22.7, 7.9 x 10^{-6} m min^{-1}, and 1.0 x 10^{-1} mol m^{-3}, respectively – were from Morrissey & Morrill (2016). CO_2 flux calculated using Equation 2 at WHC2b was 10.58 μmol m^{-2} min^{-1}. This value was less than both the value of -266 μmol m^{-2} min^{-1} calculated using Equation 1 and the value of -19.0 ± 0.01 μmol m^{-2} min^{-1} calculated by Morrissey and Morrill (2016) from samples collected in September 2015. This

could be indicative of annual variability in CO_2 flux at WHC2b. More annual measurements of CO_2 flux at multiple sites within the massif are needed to define this variability.

With the exception of a concentration decrease within the first 20 minutes of observation, there was no observable change in CH_4 over the course of five hours at WHC2b. An older 24-hour observation at the same spring site (Morrissey & Morrill, 2016) showed CH_4 concentration increased linearly from approximately 2 hours to 20 hours. In this study, observations were limited to 5 hours due to the battery limitations of the LI-COR gas analyzer. The LI-COR experiments therefor only represented the first quarter of the experiments performed by Morrissey and Morrill (2016).

The CO_2 flux calculated at each site is based on the surface area of the LI-COR 20 cm survey chamber. The rate of sequestration of CO_2 for the whole Tablelands massif was calculated according to Equation 4.

(4) $$r_{TBL} = (f_{WHC2b})\,(a_{WHC2b}) + (f_{TLE})\,(a_{TLE}) + (f_{WHC500})\,(a_{WHC500}) + (f_{UUC})\,(a_{UUC}) + (f_{veg})\,(a_{veg})$$

where r is the rate of sequestration (negative values) or emission (positive values) of gas (mol min^{-1}), a is the area of the feature (m^2), and f is the flux associated with that feature (μmol m^{-2} min^{-1}).

The flux values f_{TLE} and f_{WHC500} were assigned values of zero, as variability in concentration values obtained at those field sites were attributed to instrumental variability in the field.

The LI-COR gas survey chamber and CO_2 gas analyzer was not deployed over a vegetated site, so an estimate for f_{veg} was limited to values observed at other sites. Vegetation at the Tablelands is limited (Figure 2), as the species have to tolerate limited soil, high heavy metal concentrations, potentially toxic levels of magnesium, low calcium input, and frequent freeze-thaw (Damman, 1983). The serpentinicolous species that grow on the massif are characterized as peaty fens, and can be further characterized by two heath subassociations – *Lycnetum typicum and Lycnetum adiantetosum*. These subassociations are differentiated from one another based primarily on fen drainage, with the former occurring on quick-draining talus slopes, and the later occurring on in moisture-retaining drainage channels and late snowbed habitats. These subassociations closely resemble heaths in Mt. Albert, Quebec, and Scandinavia (Damman, 1983). As no direct flux measurements were available for the Tablelands vegetation, a CO_2 gas flux value was assigned based on values observed in fens with similar variability in drainage in southern and central Finland (Alm et al., 1999). CO_2 flux values for f_{veg} were made based on a long-term, closed chamber observation in peaty fen habitats that resemble those in the Tablelands (Alm et al., 1999). Of these observations, two were selected that most closely resembled the ecological, geochemical, and hydrogeological conditions at the Tablelands. The flux values observed in two comparable fens in southern Finland, one drained by anthropogenic activity, and one not drained, were 3.94 μmol m^{-2} min^{-1} and 2.21 μmol m^{-2} min^{-1}, respectively.

These values were used as maximum and minimum f_{veg} estimates, respectively, in order to represent the spectrum of fen drainage at the Tablelands.

Minimum and maximum r_{TBL} values of -118 mol min^{-1} and -168 mol min^{-1} were calculated using Equation 4. The negative values indicate that the massif as a whole is sequestering CO_2. As hypothesized, this sequestration can be attributed to water-rock reactions that sequester CO_2 occurring all over the massif (as approximated by f_{UUC}), and especially those occurring at ultra-basic springs such as WHC2b and TLE. There is a paucity of data for CO_2 flux associated with present-day serpentinization with which we can compare r_{TBL}. Chimaera gas seeps in Turkey emit CO_2 at rates between 160 μmol m^{-2} min^{-1} and 1000 μmol m^{-2} min^{-1} (Etiope et al., 2011), which is greater than the rate of sequestration at the Tablelands by a factor of 144 to 901, respectively (see Figure A3.1.). This study is the first to quantify CO_2 emission for an actively serpentinizing ophiolite complex. No CO_2 sequestration was observed at the Chimaera gas seeps.

This study constitutes the first attempt to quantify the net sequestration rate of CO_2 of the Tablelands massif as a whole. In doing so, several assumptions had to be made. The battery life and configuration of the LI-COR gas analyzer dictated that observations were short, only during the day, and only in places where equipment could be secured. As such, a single observation at one site (f_{UUC}) was used to approximate the CO_2 flux of the approximately 100-km^2 non-vegetated portion of the massif. Furthermore, other assumptions were made in order to obtain an f_{veg} value. CO_2 flux in boreal peatlands likely varies considerably according to temperature,

underlying mineralization processes, extent of organic decay and soil respiration, water availability and water table depth, soil pH, and particularly seasonal variability. Gas exchange can also occur through packed snow (Alm et al., 1999), but rates are considerably affected. As such, it should be noted that the value of f_{veg} in the Alm et al (1999) study was calculated upon observations made primarily in winter through snow, with some spring and fall input. In contrast, flux rates in this study were calculated on short-term observations made in the Tablelands in summer. The estimated f_{TBL} value of -1.11×10^{-6} mol m^{-2} min^{-1} could perhaps be further refined with the inclusion of more discrete closed chamber observations.

Alternatively, a more continuous approach, such as remote sensing, could be applied to the ophiolite. Remote sensing is an emerging tool used to monitor CO_2 sequestration globally. More recent hyperspectral ASTER and Landsat remote sensing techniques have been developed for the arid, non-vegetated Samail ophiolite in Oman. These techniques directly show the spectral signature of ultramafic and CO_2-bearing lithologies (Rajendran et al., 2014), thereby providing an unprecedented opportunity to quantify the extent of natural CO_2 storage in ophiolites. This hyperspectral approach could be applied to the mostly barren Tablelands Ophiolite. This approach would also distinguish and separate the effects of the unconsolidated ultramafic talus that covers the majority of the ophiolite and otherwise limits the identification of sites for targeted closed chamber observations. With this technology, observations could also take place at night, and in all seasons. Remote sensing could potentially generate more spatially and temporally sensitive flux profiles. However, remote sensing surveys present logistical and

financial challenges, making the use of discrete CO_2 flux measurements the only viable option for the initial assessment of baseline greenhouse gas flux conditions at sites of serpentinization.

Future surveys of the Tablelands Ophiolite could include multiple measurements at the same sampling site, overnight measurements, and measurements over vegetated areas. This would serve to further delineate the natural CO_2 sequestration potential of ophiolites, the quantification of which is essential prior to their consideration for sites of enhanced GCS.

References Cited

Alm, J., Saarnio, S., Nykänen, H., Silvola, J., & Martikainen, P. J. (1999). Winter CO2, CH4 and N2O Fluxes on Some Natural and Drained Boreal Peatlands. *Biogeochemistry*. Springer. https://doi.org/10.2307/1469562

Damman, A.W.H. 1983. An ecological subdivision of the Island of Newfoundland. In: South, G.R., ed. Biogeography and ecology of the Island of Newfoundland. The Hague: Dr. W. Junk Publishers. 163 – 206

Etiope, G., Schoell, M., & Hosgörmez, H. (2011). Abiotic methane flux from the Chimaera seep and Tekirova ophiolites (Turkey): Understanding gas exhalation from low temperature serpentinization and implications for Mars. *Earth and Planetary Science Letters* (Vol. 310). https://doi.org/10.1016/j.epsl.2011.08.001

Kelemen, Peter B, Matter, J., Kelemen, P. B., & Matter, J. (2008). In situ carbonation of peridotite for CO2 storage. *Proceedings of the National Academy of Sciences of the United States of America*, *105*(45), 17295–17300. https://doi.org/10.1073/pnas.0805794105

Kelemen, P. B., Matter, J., Streit, E. E., Rudge, J. F., Curry, W. B., & Blusztajn, J. (2011). Rates and Mechanisms of Mineral Carbonation in Peridotite: Natural Processes and Recipes for Enhanced, in situ CO 2 Capture and Storage. *Annu. Rev. Earth Planet. Sci*, *39*, 545–76. https://doi.org/10.1146/annurev-earth-092010-152509

Morrissey, L. S., & Morrill, P. L. (n.d.). ARTICLE Flux of methane release and carbon dioxide sequestration at Winterhouse Canyon, Gros Morne, Newfoundland, Canada: a site of continental serpentinization. https://doi.org/10.1139/cjes-2016-0123

Rajendran, S., Nasir, S., Kusky, T. M., & al-Khirbash, S. (2014). Remote sensing based

approach for mapping of CO2 sequestered regions in Samail ophiolite massifs of the Sultanate of Oman. *Earth-Science Reviews*, *135*, 122–140. https://doi.org/10.1016/j.earscirev.2014.04.004

Szponar, N., Brazelton, W. J., Schrenk, M. O., Bower, D. M., Steele, A., & Morrill, P. L. (2013). Geochemistry of a continental site of serpentinization, the Tablelands Ophiolite, Gros Morne National Park: A Mars analogue. *Icarus*, *224*(2), 286–296. https://doi.org/10.1016/j.icarus.2012.07.004

CHAPTER 4: SUMMARY AND FUTURE WORK

Establishing baseline geochemical properties for the Tablelands Ophiolite with respect to greenhouse gases – CH_4 and CO_2 – required investigation into the production pathway or pathways for methane - CH_4, and the sequestration rates of atmospheric carbon dioxide - CO_2. Characterization of the source of methane produced in serpentinizing groundwater springs in the Tablelands is a difficult procedure complicated by our general inability to collect sufficient concentrations of methane for δD_{CH4} and $\Delta^{13}CH_3D$ analysis. This study validated vacuum extraction and gas stripping methods as means of collecting dissolved methane without inducing significant isotopic fractionation. Employing both vacuum extraction and gas stripping methods in the field, sufficient methane was collected from an ultra-basic spring in the massif. Subsequent analysis yielded the first δD_{CH4} and $\Delta^{13}CH_3D$ values for the Tablelands Ophiolite – 173 ± 2.8 ‰ and 4.17 ± 0.15 ‰, respectively - thus facilitating the site's inclusion on traditional methane characterization carbon deuterium (CD) and CD isotopic fractionation plots, as well as the estimation of formation or equilibration temperatures of methane at this site: 85 ± 7 °C.

In order to establish the validity of CD and CD isotopic fractionation plots as a means of characterizing Tablelands methane, a meta-analysis was conducted of both the geochemical stability of the Tablelands, and the use of the stable isotope composition of CH_4, CO_2, and H_2O in discriminating methanogenetic pathways. The stable carbon and hydrogen isotope values of methane, and the stable hydrogen and oxygen isotope values of water remained fairly constant (i.e., all with relative standard errors of less than 10 % RSD) since sampling was first initiated in 2009. In contrast, dissolved concentrations of H_2 and CH_4, and the stable carbon isotope value of TIC were more variable over the years. As the stable isotope composition of the substrates and products were fairly constant at the Tablelands, their use in methane characterization was valid.

The stable carbon and hydrogen isotope values of methane from other studies was collated and plotted according to methanogenetic pathway in order to investigate the application of CD plots in methane characterization. This meta-analysis illustrated that there is considerable overlap in isotope composition between pathways when averages and standard deviations were used, with the CO_2 reduction field completely encompassing that of acetate fermentation, and the abiogenic field almost completely encompassing that of thermogenic production. There remains some apparent differentiation between subsets of microbial and non-microbial pathways. Meta-analysis did demonstrate the efficacy of CD plots in discriminating between microbial and non-microbial pathways, especially based on $\delta^{13}C_{CH4}$, as this plot effectively isolates the isotopic depletion as a result of kinetic isotope effects associated with microbial methanogenesis. A CD isotopic fractionation plot also demonstrated this pattern, but the inability to establish a thermogenic field on this plot due to the paucity of δD_{H2O} data for thermogenic methane rendered characterization based on this plot tentative

Methane extracted from serpentinizing springs in The Tablelands plotted within the non-microbial field of a CD plot, therein indicating a non-microbial source, in keeping with conclusions from earlier surveys (Szponar et al., 2013). The CD plot does not conclusively differentiate between thermogenic and abiogenic sources, nor does the formation/equilibrium temperature of 85 ± 7 °C estimated from the measured $\Delta^{13}CH_3D$ value. However, this formation/equilibrium temperature, in conjunction with the stable carbon and hydrogen isotope values of methane, the thermal characterization of organic matter from sedimentary units adjacent to the massif, and the historical data from oil and gas exploration wells drilled adjacent to the massif, helped contextualize potential thermogenic and abiogenic models for methane production in the Tablelands. The stable carbon and hydrogen isotope values of methane from oil

and gas-producing units north and south of Gros Morne compared to that of springs in the massif eliminated these units as a source of migrated thermogenic methane. Thermogenic gas resulting from the high-temperature thermal alternation of sedimentary units directly underlying the ophiolite was likewise considered unlikely based on SOM characterization. Other local or remote thermogenic methane sources remain a possibility, and models examining how these sources might contribute to thermogenic methane production in the Tablelands warrant further investigation.

While low-temperature (<100 ˚C) abiogenic methane formation at this site is a possibility, existing models of abiogenic methane production do not aptly describe the conditions (e.g., inorganic carbon sources, gas phase and dissolved gas concentrations) within the ophiolite. Future validation of abiogenic models of methane production in the Tablelands relies on the investigation of thermodynamic constraints on low temperature abiogenic methane synthesis. Both abiogenic and thermogenic methane production models require further investigation.

If a methanogenetic pathway is conclusively established, the role of CO_2 in methanogenesis at the Tablelands will require investigation. The ultra-basic nature of the serpentinizing groundwater springs in the massif makes it conducive to natural sequestration of CO_2 from the atmosphere, and subsequent storage on geologic timescales as carbonate rock, spatially associated with groundwater flowpaths and outlets. Ophiolites have been established as potential environments for enhanced Global Carbon Storage (GCS), but the baseline geochemical and hydrogeological conditions of each ophiolite complex must be established prior to their consideration as a GCS site. Additionally, dissolved atmospheric CO_2 is a potential inorganic carbon source in abiogenic and microbial methane synthesis, meaning the injection of supercritical volumes of CO_2 into the massif could enhance methane production at the ophiolite.

As an abiogenic methane synthesis model is possible at the Tablelands, further investigation of natural sequestration rates of atmospheric CO_2 is necessary.

Chapter 3 of this thesis constituted the first attempt to quantify the net sequestration rate of CO_2 of the Tablelands massif as a whole by measuring changing CO_2 concentrations, or fluxes, at multiple discrete sites within the ophiolite. The predominant land cover styles at the Tablelands Ophiolite were identified, and sampling sites within the massif representative of each style were selected. A LI-COR 8100A gas survey chamber and CO_2 gas analyzer was deployed at two sites of high-pH groundwater discharge, one of pooling high-pH groundwater, and at a final dry site covered in unconsolidated serpentinized ultramafic cobbles. The CO_2 flux calculated for this dry site (-2.32 μmol m^{-2} min^{-1}) served as a background value to establish the analytical reproducibility of the instruments used in the field. CO_2 fluxes at both non-pooling discharge locations were less than this established analytical reproducibility. A CO_2 flux of -266 μmol m^{-2} min^{-1} was calculated at the pooling groundwater outlet. Calculations of flux were designed such that negative values were indicative of CO_2 sequestration. The vegetation at the Tablelands was defined as boreal peatlands, consisting of fens presenting variable degrees of drainage. Due to variability in fen drainage, two CO_2 fluxes were assigned to the vegetated areas of the massif (i.e. 3.94 μmol m^{-2} min^{-1} and 2.21 μmol m^{-2} min^{-1}) in order to represent the maximum and minimum contribution of the vegetation, respectively, to net CO_2 sequestration. These discrete values were assigned to their respective land cover styles, then collated based on their areal extent, and used to calculate a net CO_2 sequestration rate for the massif as a whole – a minimum of -118 mol min^{-1} and a maximum of -168 mol min^{-1}. These values suggest that the ophiolite naturally sequesters CO_2. This study is the first to quantify natural CO_2 sequestration for an actively serpentinizing ophiolite complex. As such, no comparison to other ophiolites'

sequestration potential is possible. Chimaera gas seeps in Turkey emit CO_2 at rates between 160 μmol m^{-2} min^{-1} and 1000 μmol m^{-2} min^{-1} (Etiope et al., 2011), which is greater than the rate of sequestration at the Tablelands by a factor of 144 to 901, respectively. As globally-distributed ophiolites are explored as potential sites of enhanced GCS, the natural flux of CO_2 associated with these sites will be quantified and compared.

CO_2 flux in boreal peatlands, such as those in the Tablelands, varies considerably based on temperature, underlying mineralization processes, extent of organic decay and soil respiration, water availability and water table depth, soil pH, and particularly seasonal variability. The Tablelands is covered in snow for a significant portion of each year. While gas exchange through packed snow is possible (Alm et al., 1999), rates are affected considerably. The flux calculated in this study were based on values obtained during short-term observations made in the Tablelands in summer, when snow is either not present, or limited to the topographic highs of the massif. Given that CO_2 flux is a function of numerous interconnected processes, more observations of different durations and at different times of year will refine our understanding of annual and seasonal variability in CO_2 flux. This should include flux measurements over multiple vegetated areas of the Tablelands. This is necessary before GCS is considered.

This thesis has constrained the source of methane emitted at the Tablelands to low-temperature (<100 ˚C) abiogenic or thermogenic synthesis, and was the first to quantify natural CO_2 sequestration for an actively serpentinizing ophiolite complex as a whole based on measurements made at multiple discrete sites within the ophiolite. Further characterization of the Tablelands Ophiolite is necessary in order to validate GCS at this site as a means of mitigating anthropomorphic greenhouse gas contributions to the atmosphere.

Bibliography and References

Alfredsson, H.A. et al., 2013. The geology and water chemistry of the Hellisheidi, SW-Iceland carbon storage site. International Journal of Greenhouse Gas Control, 12: 399-418.

Alm, J., Saarnio, S., Nykänen, H., Silvola, J., & Martikainen, P. J. (1999). Winter CO2, CH4 and N2O Fluxes on Some Natural and Drained Boreal Peatlands. *Biogeochemistry*. Springer. https://doi.org/10.2307/1469562

Archer, 1996. Geochemical Evaluation of the 1200m to 3650m Interval of the Long Range A-09 Well. , Talisman Energy Inc.

Balabane, M., Galamov, E., Hermann, M., Létolle, R., 1987. Hydrogen and carbon isotope fractionation during experimental production of bacterial methane. Organic Geochemistry, 11: 115-119.

Barnes, I., LaMarche, V.C., Himmelberg, G., 1967. Geochemical evidence of present-day serpentinization. Science, 156: 830-832.

Berger, A.R., Bouchard, A., Brookes, I.A., Grant, D.R., Hay, S.G.,and Stevens, R.K., 1992. Geology, topography, and vegetation, Gros Morne National Park, Newfoundland. Miscellaneous Report 54.

Blank, J.G. et al., 2009. An alkaline spring system within the Del Puerto Ophiolite (California, USA): a Mars analog site. . Planetary and Space Science, 57: 533-540.

Brazelton, W.J., Nelson, B., Schrenk, M.O., 2012. Metagenomic evidence for H2 oxidation and H2 production by serpentinite-hosted microbial communities. Frontiers in Microbiology, 2: 1-16.

Brazelton, W.J., Morrill, P.L., Szponar, N., Schrenk, M.O., 2013. Bacterial communities associated with subsurface geochemical processes in continental serpentinite springs. Applied and Environmental Microbiology, 79(13): 3906-3916.

Chasar, L.S., Chanton, J.P., Glaser, P.H., Siegel, D.I., 2000. Methane Concentration and Stable Isotope Distribution as Evidence of Rhizospheric Processes: Comparison of a Fen and Bog in the Glacial Lake Agassiz Peatland Complex. Annals of Botany, 86(3): 655-663.

Clark, I., Fritz, P., 1997. Environmental Isotopes in Hydrogeology. Lewis Pubishers, New York, 328 pp.

Claypool, G.E., Presley, B.J., Kaplan, I.R., 1973. Gas analysis in sediment samples from legs 10,11,13,14,15,18,19. Initial Reports Deep Sea Drilling Project, 19: 879-884.

Cooper, M., Weissenberger, J., Knight, I., Hostad, D., Gillespie, D., Williams, H., Burden, E., Porter-Chaudhry, J., Rae, D., and Clark, E., 2001. Basin evolution in western Newfoundland: New insights from hydrocarbon exploration. AAPG Bulletin, 85(3): 393-418.

Currell, M., Banfield, D., Cartwright, I., Cendón, D.I., 2017. Geochemical indicators of the origins and evolution of methane in groundwater: Gippsland Basin, Australia. Environmemtal Science and Pollution Research, 24(15): 13168-13183.

Damman, A.W.H. 1983. An ecological subdivision of the Island of Newfoundland. In: South, G.R., ed. Biogeography and ecology of the Island of Newfoundland. The Hague: Dr. W. Junk Publishers. 163 – 206

Etiope, G., Sherwood Lollar, B., 2013. Abiotic Methane on Earth. Reviews of Geophysics, 51: 276-299.

Etiope, G., Tsikouras, B., Kordella, S., Ifandi, E., Christodoulou, D., Papatheodorou, G., 2013. Methane flux and origin in the Othrys ophiolite hyperalkaline springs, Greece. . Chemical Geology, 347: 161-174.

Etiope, G., Schoell, M., & Hosgörmez, H. (2011). Abiotic methane flux from the Chimaera seep and Tekirova ophiolites (Turkey): Understanding gas exhalation from low temperature serpentinization and implications for Mars. *Earth and Planetary Science Letters* (Vol. 310). https://doi.org/10.1016/j.epsl.2011.08.001

Friedmann, I., Hardcastle, K., 1973. Interstial water studies, leg. 15 - Isotopic composition of water. Initial Reports Deep Sea Drilling Project, 20: 901-903.

Fu, Q., Sherwood Lollar, B., Horita, J., Lacrampe-Couloume, G., Seyfried, J., W.E., 2007. Abiotic formation of hydrocarbons under hydrothermal conditions: Constraints from chemical and isotope data. Geochimica et Cosmochimica Acta, 71: 1982-1998.

Fuchs, G.D., Thauer, R., Ziegler, H., Stichler, W., 1979. Carbon isotope fractionation by Methanobacterium thermoautotrophicum. Archives of Microbiology, 120: 135-139.

Gislason, S.R. et al., 2014. Rapid solubility and mineral storage of CO_2 in basalt. Energy Procedia, 63: 4561-4574.

Grossman, E.L., Coffman, B.K., Fritz, S.J., Wada, H., 1989. Bacterial production of methane and its influence on ground-water chemistry in east-central Texas aquifers. Geology, 17: 495-499.

Gruen, D.S. et al., In press. Experimental investigation on the controls of clumped isotopologue and hydrogen isotope ratios in microbial methane. Geochimica Cosmochimica Acta.

Hinchey, A.M. et al., 2015. The Green Point Shale of Western Newfoundland. A review of its geological setting, its potential as an unconventional hydrocarbon reservoir, and its ability to be safely stimulated using the technique of hydraulic fracturing. In: Department of Natural Resources, G.S. (Editor). Government of Newfoundland and Labrador, , St. John's, pp. 128.

Hornibrook, E.R.C., Longstaffe, F.J., Fyfe, W.S., 1997. Spatial distribution of microbial methane production pathways in temperate zone wetland soils: stable carbon and hydrogen isotope evidence. Geochimica et Cosmochimica Acta, 61(4): 745-753.

Hunt Oil Company., 1996. Final Well Report NHOC/PCP Long Point M16 Appendix IV-1, INV-041414. INV-041414, Hunt Oil Company, Newfoundland.

Ionescu, A., Baciu, C., Kis, B.-M., Sauer, P.E., 2017. Evaluation of dissolved light hydrocarbons in different geological settings in Romania. Chemical Geology, 469: 230-245.

Kelemen, P.B., Matter, J., 2008. In situ carbonation of peridotite for CO2 storage. Proceedings of the National Academy of Sciences of the United States of America, 105(45): 17295-17300.

Kelemen, P.B. et al., 2011. Rates and Mechanisms of Mineral Carbonation in Peridotite: Natural Processes and Recipes for Enhanced, in situ CO_2 Capture and Storage. Annual Review of Earth and Planetary Sciences, 39: 545-576.

Kelley, D.S., Frueh-Green, G., 1999. Abiogenic methane in deep-seated mid-ocean ridge environments: Insights from stable isotope analyses. Journal of Geophysical Research, 104: 10439-10460.

Kohl, L., Cumming, E. Cox, A. Rietze, A. Lang, S.Q., Richter, A., Suzuki, S. Nealson, K.H. Morrill, P.L., 2016. Exploring the metabolic potential of microbial communities in ultra-basic, reducing springs at The Cedars, CA, US: Experimental evidence of microbial methanogenesis and heterotrophic acetogenesis. Journal of Geophysical Research G: Biogeosciences, 121(4): 1203-1220.

Lancet, H.S., Anders, E., 1970. Carbon isotope fractionation in the Fischer-Tropsch synthesis of methane. Science, 170: 980-982.

Lansdown, J.M., Quay, P.D., King, S.L., 1992. CH_4 production via CO_2 reduction in a temperate bog: A source of ^{13}C-depleted CH_4. Geochimica et Cosmochimica Acta, 56: 3493-3503.

Lien, Y.Y., Namsaraev, B.B., Trotsyuk, V.Y., Ivanov, M.V., 1981. Bacterial methanogenesis in Holocene sediments of the Baltic Sea. Geomicrobiology Journal, 2: 299-315.

Lyon, G., 1973. Interstitial water studies, leg. 15 - Chemical and isotopic composition of gases from Cariaco Trench sediments. Initial Reports Deep Sea Drilling Project, 20: 773-774.

McCollom, T.M., 2016. Abiotic methane formation during experimental serpentinization of olivine. Proceedings of the National Academy of Sciences of the United States of America, 113(49): 13965-13970.

McCollom, T.M., Donaldson, C., 2016. Generation of Hydrogen and Methane during Experimental Low-Temperature Reaction of Ultramafic Rocks with Water. Astrobiology, 16(6): 389-406.

McCollom, T.M., Seewald, J.S., 2006. Carbon isotope composition of organic compounds produced by abiotic synthesis under hydrothermal conditions. Earth and Planetary Science Letters, 243: 74-84.

McGrail, B.P. et al., 2017. Wallula Basalt Pilot Demonstration Project: Post-injection Results and Conclusions. Energy Procedia, 114: 5783-5790.

McGrail, B.P., Spane, F.A., Sullivan, E.C., Bacon, D.H., Hund, G., 2011. The Wallula basalt sequestration pilot project. Energy Procedia, 4: 5653-5660.

Miller, H.M., Matter, J.M, Kelemen, P., Ellison, E.T., Conrad, M.E., Fierer, N., Ruchala, T., Tominaga, M., Templeton, A.S., 2016. Modern water/rock reactions in Oman hyperalkaline peridotite aquifers and implications for microbial habitability. Geochemica et Cosmochimica Acta, 179: 217-241.

Morrill, P.L., Brazelton, W.J., Kohl, L., Rietze, A., Miles, S.M., Kavanagh, H., Schrenk, M.O., Ziegler, S.E., Lang, S.Q., 2014. Investigations of potential microbial methanogenic and carbon monoxide utilization pathways in ultra-basic reducing springs associated with present-day continental serpentinization: the Tablelands, NL, CAN. Frontiers in Microbiology.

Morrill, P.L., Kuenen, J.G., Johnson, O.J., Suzuki, S., Rietze, A., Sessions, A.L., Fogel, M.L., Nealson, K.H., 2013. Geochemistry and geobiology of a present-day serpentinization site in California: The Cedars. Geochimica et Cosmochimica Acta, 109: 222-240.

Morrissey, L., Morrill, P.L., 2016. Flux of methane release and carbon dioxide sequestration at Winterhouse Canyon, Gros Morne, Newfoundland, Canada: a site of continental serpentinization. Canadian Journal of Earth Sciences, 54(3): 257-262.

Nakai, M., Yoshida, Y., Ando, N., 1974. Isotopic studies on oil and natural gas fields in Japan. Chikyakaya, 7/8(1): 87-98.

NALCOR, 2018. In: Morrill, P. (Editor), St. John's NL.

Ono, S., Wang, D.T., Gruen, D.S., Sherwood Lollar, B., Zahniser, M.S., McManus, B.J., Nelson, D.D., 2014. Measurement of a doubly substituted methane isotopologue, 13CH3D, by tunable infrared laser direct absorption spectroscopy. Analytical Chemistry, 86(13): 6487-6494.

Oremland, R.S., Des Marais, D.J., 1983. Distribution, abundance and carbon isotopic composition of gaseous hydrocarbons in Big Soda Lake, Nevada: An alkaline, meromictic lake. Geochimica et Cosmochimica Acta, 47: 2107-2114.

Pearson, D.L., 1984. Pollen/spore colour standard version 2. , Phillips Petroleum Company, Exploration Projects Section.

Proskurowski, G., Lilley, M.D., Seewald, J.S., Früh-Green, G.L., Olson, E.J., Lupton, J.E., Sylva, S.P., Kelley, D.S., 2008. Abiogenic hydrocarbon production at Lost City Hydrothermal Field. Science, 319: 604-607.

Rajendran, S., Nasir, S., Kusky, T.M., al-Khirbash, S., 2014. Remote sensing based approach for mapping of CO_2 sequestered regions in Samail ophiolite massifs of the sultanate of Oman. Earth-Science Reviews, 135: 122-140.

Rietze, A. et al., 2014. Hydrocarbon Sources at a Site of Active Continental Serpetninization: The Cedars, California, USA, Goldschimdt, Sacramento, CA.

Rudd, J.W.M., Hamilton, R.D., Campbell, N.E.R., 1974. Measurement of microbial oxidation of methane in lake water. Limnology and Oceanography, 19(3): 519-524.

Schoell, M., 1988. Multiple origins of methane in the Earth. Chemical Geology, 71: 1-10.

Schoell, M., Tietze, K., Schoberth, S.M., 1988. Origin of methane in lake Kivu (east central Africa). Chemical Geology, 71: 257-265.

Sherwood, B. et al., 1988. Methane occurences in the Canadian Shield. Chemical Geology, 71: 223-236.

Sherwood Lollar, B. et al., 1993. Evidence for bacterially generated hydrocarbon gas in Canadian Shield and Fennoscandian Shield rocks. Geochimica et Cosmochimica Acta, 57: 5073-5085.

Sherwood Lollar, B. et al., 2008. Isotopic signatures of CH4 and higher hydrocarbon gases from Precambrian Shield sites: A model for abiogenic polymerization of hydrocarbons. Geochimica et Cosmochimica Acta, 72(19): 4778-4795.

Sherwood Lollar, B., Westgate, T.D., Ward, J.A., Slater, G.F., Lacrampe-Couloume, G., 2002. Abiogenic formation of gaseous alkanes in the Earth's crust as a minor source of global hydrocarbon reservoirs. Nature, 416: 522-524.

Shuai, Y., P.M.J. Douglas, Zhang,S., Stolper, D.A, Ellis, G.S., Lawson, M., Formolo, M., Mi, J., He., K., Hu, G., Eiler, J.M., 2018. Equilibrium and non-equilibrium controls on the abundances of clumped isotopologues of methane during thermogenic formation in

laboratory experiments: Implications for the chemistry of pyrolysis and the origins of natural gases. Geochimica et Cosmochimica Acta, 223: 159-174.

Sleep, N.H., Meibom, A., Fridriksson, T., Coleman, R.G., Bird, D.K., 2004. H2-rich fluids from serpentinization: Geochemical and biotic implications. PNAS, 101(35): 12818 -12823.

Snæbjörnsdóttir, S.Ó., Gislason, S.R., 2016. CO_2 Storage Potential of Basaltic Rocks Offshore Island. Energy Procedia, 86: 371-380.

Stolper, D., Sessions, A., Ferreira, A., Santos Neto, E., Schimmelmann, A., Shusta, S., Valentine, D., Eiler, J., 2014. Combined 13C-D and D-D clumping in methane: Methods and preliminary results. Geochimica et Cosmochimica Acta, 126: 169-191.

Suda, K. Ueno,Y. Yoshizaki, M. Nakamura, H. Kurokawa, K., Nishiyama, E., Yoshino, K., Hongoh, Y., Kawachi, K. Omori, S., Yamada, K., Yoshida, N., Maruyama, S. 2014. Origin of methane in serpentinite-hosted hydrothermal systems: The CH4-H2-H2O hydrogen isotope systematics of the Hakuba Happo hot spring. Earth and Planetary Science Letters, 386: 112-125.

Surour, A.A., Arafa, E.H., 1997. Ophicarbonates: calcified serpentinites from Gebel Mohagara, Wadi Ghadir area, Eastern Desert, Egypt. Journal of African Earth Sciences, 24(3): 315-324.

Suzuki, S., Kuenen, J. G., Schipper, K., van der Velde, S., Ishii, S., Wu, A., Sorokin, D. Y., Tenney, A., Meng, X., Morrill, P. L., Kamagata, Y., Muyzer, G., Nealson, K.H.

2014. Physiological and genomic features of highly alkaliphilic hydrogen-utilizing Betaproteobacteria from a continental serpentinizing site. Nature Communications, 5:3900 doi: 10.1038/ncomms4900.

Suzuki, S., Ishii, S., Wu, A., Cheung, A., Tenney, A., Wanger, G., Kuenen, J. G., Nealson, K. H. 2013. Microbial diversity in The Cedars, an ultrabasic, ultrareducing, and low salinity serpentinizing ecosystem. PNAS, 110(38): 15336-15341.

Szponar, N., 2012. Carbon Cycling at a Site of Present-Day Serpentinization: The Tablelands, Gros Morne National Park. Thesis - paper based Thesis, Memorial University, St. John's, NL, 156 pp.

Szponar, N. et al., 2013. Geochemistry of a Continental Site of Serpentinization in the Tablelands Ophiolite, Gros Morne National Park: a Mars Analogue. ICARUS, 224: 286-296.

Talisman Energy Incorporated., 1996. Long Range A-09 - Borehole Compensated - Sonic Run 2 - Final - INV-041540. INV-041540, Newfoundland.

Taran, Y.A., Kliger, G.A., Cienfuegos, E., Shuykin, A.N., 2010. Carbon and hydrogen isotopic compositions of products of open-system catalytic hydrogenation of CO2: Implications for abiogenic hydrocarbons in Earth's crust. Geochimica et Cosmochimica Acta, 74: 6112-6125.

Taran, Y.A., Kliger, G.A., Sevastianov, V.S., 2007. Carbon isotope effects in the open-system Fischer–Tropsch synthesis. Geochimica et Cosmochimica Acta, 71: 4474-4487.

Urey, H.C., 1947. The thermodynamic properties of isotopic substances. Journal of the Chemical Society: 562-581.

Valentine, D.L., Chidthaisong, A., Rice, R., Reeburgh, W.S., Tyler, S.C., 2004. Carbon and hydrogen isotope fractionation by moderately thermophilic methanogens. Geochimica et Cosmochimica Acta, 68(7): 1571-1590.

van Staal, C.R. et al., 2007. The Notre Dame arc and the Taconic orogeny in Newfoundland. Geological Society of America Memoirs, 200(March 2016): 511–552.

Waldron, S., Watson-Craik, I.A., Hall, A. J., Fallick, A.E., 1998. The carbon and hydrogen stable isotope composition of bacteriogenic methane: A laboratory study using a landfill inoculum. Geomicrobiology Journal, 15(3): 157-169.

Wang, D.T. et al., 2015. Clumped isotopologue fingerprinting of methane sources in the environment. Science, 348(6233): 428-431.

Williams, H., Cawood, P., 1989. Geology, Humber Arm Allochthon, Newfoundland. Map 1678A. , GS# NFLD/1852. Geological Survey of Canada. .

Woltemate, I., Whiticar, M.J., Schoell, M., 1984. Carbon and hydrogen isotopic composition of bacterial methane in a shallow freshwater lake. Limnology and Oceanography, 29(5): 985-992.

Young, E.D. et al., 2017. The relative abundances of resolved $^{12}CH_2D_2$ and $^{13}CH_3D$ and mechanisms controlling isotopic bond ordering in abiotic and biotic methane gases. Geochimica et Cosmochimica Acta, 203: 235-264.

Appendices

Appendix 1: Supplementary Information submitted to Chemical Geology accompanying submitted manuscript (Chapter 2)

Potential Sources of Dissolved Methane at the Tablelands, Gros Morne National Park, NL, CAN: a Terrestrial Site of Serpentinization

Emily A. Cumming, Amanda Rietze, Liam S. Morrissey, Melissa C. Cook, Jeemin H. Rhim, Shuhei Ono, and Penny L. Morrill

Supplementary Table and Figures

Table A1.1. Sedimentary Organic Matter sample descriptions.

Outcrop description: Location: N 49°36‘06.84" W 057°57'23.52" ~1.5 m high outcrop, homogeneous dark gray shale.	**HAA1** 	Sample description: Dark gray shale that was heavily cleaved.
Outcrop description: Location: N 49°26'43.46" W 058°07'17.59" ~35 m high outcrop, fairly homogeneous, dominantly dark grey/black shaley melange morphed around entrained blocks and cobbles (0.1-1.5m size).	**HAA2** 	Sample description: Shale is heavily cleaved and very fine grained. Shale collected fell apart very easily and was dark grey in colour.
Outcrop description: Location: N 49°28’28.40" W 057°57’27.85" ~10 m high outcrop exposure, running 50 m along shoreline of Winter House Brook. Outcrop dominantly fine grained black shale/mudstone (4 m thick) interbedded with massive limestone and sandstone (10-40 cm thick). Mudstone was penetratively cleaved and contained many angular fragments of limestone and siltstone. The cleaved shale unit varied from a dark gray to a coal black colour. The shale units cleavage was wavy but bedding was mostly parallel.	**HAA3** 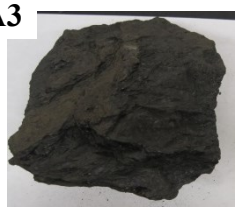	Sample description: Shale was heavily cleaved and very fine grained (1 mm scale). Shale is coal black in colour.
	HAA4 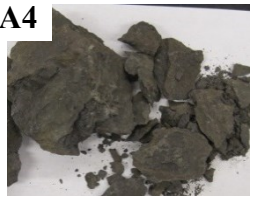	Sample description: Shale was very fine grained and heavily cleaved. Shale is dark grey in colour.
	HAA5 	Sample description: Limestone taken from a thick limestone bed.
	HAA6 	Sample description: Fine to medium grained siltstone/sandstone sample taken from a thick sedimentary bed.

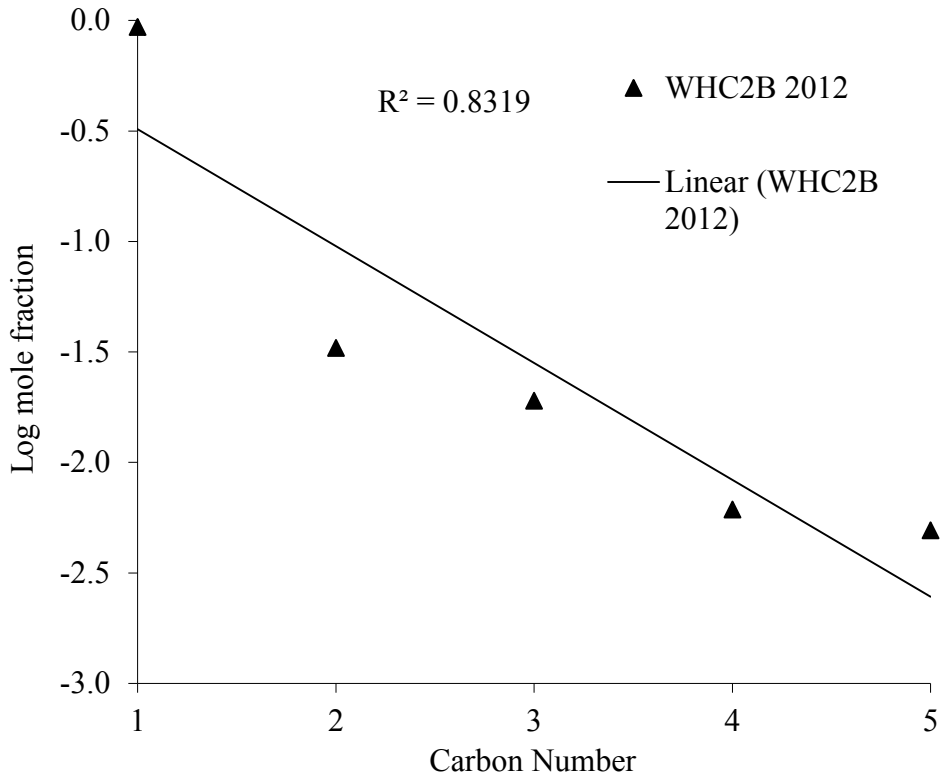

Figure A1.1. A semilog plot of the mole fraction of each n-alkane detected in the Tablelands groundwater discharging from WHC2 versus the number of carbon atoms in each n-alkane. Unbranched alkanes that exhibit a linear decrease on this type of semilog plot are typical of a Fischer Tropsch Type (FTT) reaction and Anderson-Schulz- Flory (ASF) polymerization kinetics. The alkanes extracted from the groundwater discharging at WHC2 were not well described by ASF polymerization kinetics with r^2 value of 0.83.

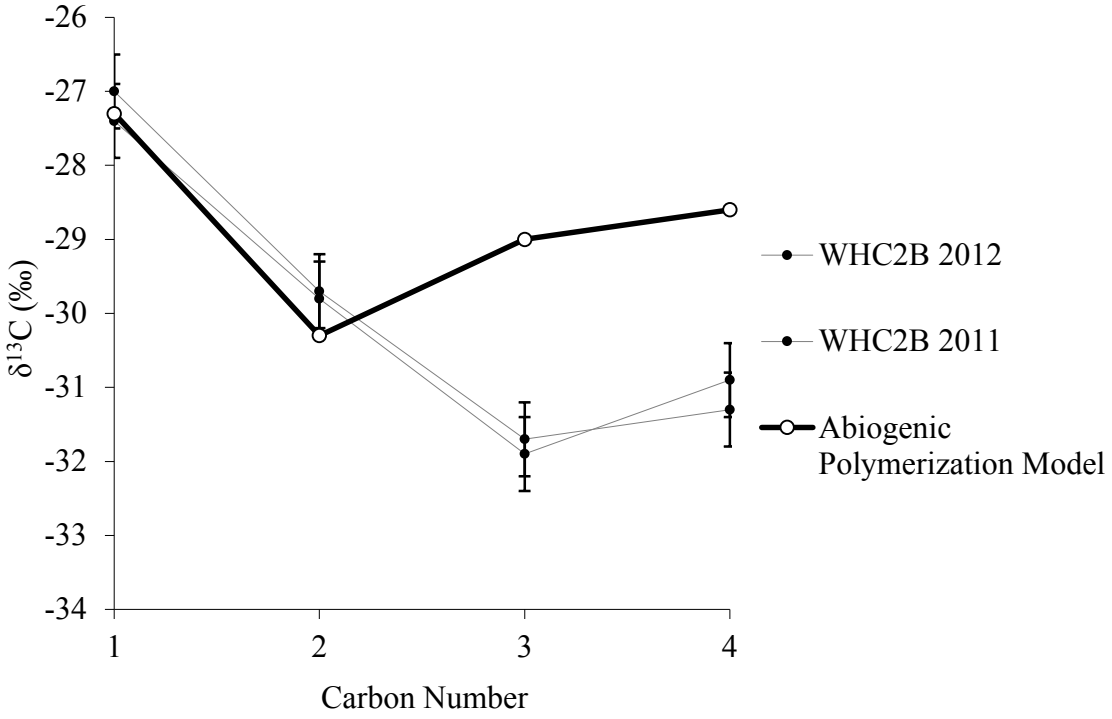

Figure A1.2. Natural gas plot of measured stable carbon isotope values of methane (C_1), ethane (C_2), propane (C_3), and butane (C_4); and the predicted isotope values of the same compounds based on Sherwood Lollar's abiogenic polymerization isotope mass balance model (Sherwood Lollar et al., 2008). The Tablelands data are not well described by the abiogenic polymerization isotope mass balance model.

References Cited

Sherwood Lollar, B. et al., 2008. Isotopic signatures of CH4 and higher hydrocarbon gases from Precambrian Shield sites: A model for abiogenic polymerization of hydrocarbons. Geochimica et Cosmochimica Acta, 72(19): 4778-4795.

Appendix 2: Supporting Information – Chapter 2

Table A2.1. Methane (C1) and sum of ethane, propane, and butane (C_{2+}) values used in Figure 2.3A. Parson's Pond values were obtained from NALCOR (2018), and Port au Port values were obtained from Archer (1996).

	$C1:C_{2+}$	C1(‰)
WHC2	5.9	-27.4
	9.5	-26.4
	6.9	-27
Parson's Pond	25	-40
Port au Port	606.712	-28
	128.767	-26.1
	12011	-38.1
	0.01422	-63.6
	0.01097	-53.2
Thermogenic Field	0.1	-52
	700	-52
	700	-15
Microbial Field	1000	-85
	1000	-42.5
	100000	-42.5

Table A2.2. Carbon and hydrogen isotope values of methane used in Figure2.3B and 2.4A. The vertices of methane production fields were obtained from Etiope et al. (2013), while Parson's Pond values were obtained from NALCOR (2018), and Port au Port values were obtained from Archer (1996).

	d13C(‰)	d2H(‰)		d13C(‰)	d2H(‰)
Abiogenic	-10	-50	Microbial	-90	-110
Field	-5	-75	Field	-59	-110
	0	-150		-59	-260
	-5	-174		-34	-260
	-9	-250		-32	-290
	-15	-270		-32	-325
	-23	-250		-49	-330
	-27	-269		-59	-375
	-29	-330		-90	-275
	-32	-380			
	-31	-450	Thermogenic	-30	-75
	-49	-400	Field	-22	-125
	-50	-325		-23	-149
	-45	-230		-34	-260
	-35	-225		-39	-260
	-29	-176		-46	-300
	-29	-140		-56	-260
	-23	-125		-38	-110
	-21	-50		-30	-75
	-16	-74	WHC2b	-27.6	-171
	-10	-50		-27.9	-175
			Parson's Pond	-40	-177

Table A2.3. Carbon and hydrogen isotope values of methane used in Figure2.4B. The stable hydrogen and carbon isotope values of methane are classified as Microbial via the CO2 reduction (CR) pathway (Balabane, 1987; Grossman et al., 1989; Hornibrook, 1997; Waldron, 1998) and the fermentation (AF) pathway (Hornibrook, 1997; Waldron, 1998), Abiogenic (Kelley and Frueh-Green, 1999; Sherwood et al., 1988; Suda et al., 2014) and Thermogenic (Currell, 2017; Ionescu et al., 2017; Shuai et al., 2018).

Pathway	Source of Data	d13C CH4	d2H CH4	Lab/Field
CO2 Reduction		-61.9	-177	F
		-71.4	-182	F
		-61.6	-183	F
		-65	-182	F
		-67	-165	F
		-54.7	-180	F
		-56.1	-179	F
		-53.1	-183	F
		-52.8	-184	F
		-55	-186	F
		-54.2	-180	F
		-58.4	-185	F
	Grossman et al. (1989)	-64.6	-192	F
		-47.9	-388	L
		-48.2	-392	L
		-50.6	-386	L
		-44.5	-396	L
		-45.3	-375	L
		-43.4	-377	L
		-49.7	-325	L
		-45.5	-318	L
		-47.6	-276	L
	Balabane (1987)	-45.8	-279	L
		-63	-350	L
		-61	-298	L
	Waldron (1998)	-62	-359	L
		-65.8	-294	F
	Hornibrook (1997)	-71.6	-244	F

Acetate Fermentation	Waldron (1998)	-48	-353	L
		-47	-294	L
		-48	-355	L
		-47	-296	L
	Hornibrook (1997)	-57.3	-284	F
		-61.1	-316	F
		-60.7	-307	F
		-63.9	-318	F
		-55.8	-297	F
		-57.1	-300	F
		-57.4	-331	F
		-58.3	-328	F
		-62.2	-324	F
		-63.4	-321	F
Abiogenic	Sherwood et al. (1988)	-51.2	-328	F
		-51.4	-360	F
		-46.3	-301	F
		-46.3	-332	F
		-39.8	-349	F
		-20.9	-99	F
		-9.1	-116	F
		-21.7	-149	F
		-27.3	-147	F
		-27.4	-148	F
	Kelley and Frueh Green (1999)	-21.1	-149	F
		-22.5	-133	F
		-34.5	-210	F
		-33.7	-300	F
		-33.9	-299	F
		-33.2	-248	F
		-33.5	-261	F
		-33.7	-258	F
	Suda et al. (2014)	-38.1	-145	F
		-35.9	-272	F
	This Study	-27.6	-181	F

Thermogenic	Currell (2017)	-31.8	-348	F
		-26.3	-180	F
	Ionescu et al. (2017)	-30	-155	F
		-39.41	-313.8	L
		-38.72	-307.71	L
		-37.71	-300.57	L
		-36.49	-291.14	L
		-35.47	-281.78	L
		-34.35	-266.66	L
		-33.19	-243.21	L
		-31.59	-199.36	L
		-30.37	-172.4	L
		-29.71	-164.6	L
		-39.08	-316.19	L
		-38	-309.59	L
		-36.95	-303.73	L
		-35.94	-296.42	L
		-35.43	-292.05	L
		-33.64	-268.94	L
		-32.41	-242.73	L
		-31.03	-203.66	L
		-30.04	-178.28	L
		-28.71	-157.78	L
		-28.25	-145.83	L
		-34.11	-277.59	L
		-31.48	-260.06	L
		-30.42	-246.17	L
		-27	-190.32	L
		-25.85	-165.78	L
		-44.11	-320.03	L
		-44.48	-318.06	L
		-39.52	-308.74	L
		-43.48	-327.69	L
		-44.92	-327.58	L
		-39.71	-318.63	L
	Shuai et al. (2018)	-33.42	-310.16	L

Table A2.4. Supporting data for Figure 2.5. Fractionation factors between reactants and products for each methanogenic pathway: Microbial via the carbonate reduction (CR) pathway (Balabane, 1987; Chasar, 2000; Claypool, 1973; Friedmann, 1973; Fuchs, 1979; Grossman et al., 1989; Hornibrook, 1997; Kohl et al., 2016; Lansdown et al., 1992; Lien, 1981; Lyon, 1973; Nakai, 1974; Schoell, 1988; Waldron, 1998) and fermentation (AF) pathway (Chasar, 2000; Hornibrook, 1997; Waldron, 1998; Woltemate et al., 1984), and Abiogenic (Fu et al., 2007; Kelley and Frueh-Green, 1999; Proskurowski et al., 2008; Sherwood et al., 1988; Suda et al., 2014; Taran et al., 2010).

Pathway	Source	alpha C	alpha D	Lab/ Field
Acetate Fermentation	Woltemate et al. (1984)	1.05	1.46	F
		1.04	1.45	F
		1.05	1.45	F
		1.05	1.45	F
		1.05	1.46	F
		1.05	1.46	F
		1.05	1.44	F
	Chasar (2000)	1.06	1.33	F
		1.06	1.34	F
		1.07	1.34	F
	Hornibrook (1997)	1.04	1.33	F
		1.05	1.40	F
		1.05	1.38	F
		1.06	1.41	F
		1.05	1.34	F
		1.05	1.34	F
		1.05	1.39	F
		1.05	1.39	F
		1.06	1.37	F
		1.06	1.37	F
	Waldron (1998)	1.05	1.46	L
		1.05	1.50	L
		1.05	1.46	L
		1.05	1.51	L

CO2 Reduction	Claypool, Lyon and Friedman (1973)	1.07	1.23	F
		1.07	1.22	F
		1.07	1.22	F
		1.07	1.23	F
		1.07	1.23	F
		1.07	1.23	F
		1.07	1.22	F
	Schoell (1988)	1.07	1.24	F
		1.07	1.23	F
		1.07	1.22	F
		1.07	1.21	F
		1.06	1.21	F
		1.06	1.20	F
		1.06	1.21	F
		1.05	1.23	F
	Lien (1981)	1.09	1.24	F
		1.09	1.25	F
		1.09	1.24	F
		1.10	1.24	F
	Nakai (1974)	1.05	1.19	F
		1.06	1.17	F
		1.07	1.19	F
	Fuchs (1979)	1.04	1.17	L
	Hornibrook (1997)	1.06	1.35	F
		1.07	1.27	F
	Waldron (1998)	1.06	1.45	L
		1.06	1.51	L
		1.07	1.47	L
	Balabane (1987)	1.05	1.61	L
		1.05	1.61	L
		1.05	1.60	L
		1.05	1.62	L
		1.05	1.67	L
		1.05	1.67	L
		1.05	1.66	L
		1.05	1.63	L
		1.05	1.64	L
		1.05	1.65	L

	Grossman et al. (1989)	1.06	1.18	F
		1.07	1.19	F
		1.05	1.19	F
		1.07	1.19	F
		1.06	1.17	F
		1.04	1.19	F
		1.04	1.19	F
		1.04	1.19	F
		1.05	1.19	F
		1.05	1.20	F
		1.04	1.19	F
		1.05	1.20	F
		1.07	1.21	F
	Lansdown et al. (1992)	1.08	1.29	F
		1.08	1.40	F
		1.08	1.30	F
		1.08	1.32	F
		1.08	1.29	F
		1.08	1.34	F
		1.06	1.56	F
		1.08	1.34	F
		1.08	1.37	F
		1.07	1.33	F
	Chasar (2000)	1.07	1.28	F
		1.08	1.29	F
		1.08	1.28	F
		1.08	1.27	F
		1.08	1.26	F
	Kohl et al. (2016)	1.07	1.50	L
		1.08	1.48	L
		1.08	1.51	L
		1.12	1.50	L

Abiogenic	Fu et al. (2007)	1.00	1.24	L
		1.02	1.24	L
		1.02	1.26	L
		1.02	1.26	L
		1.03	1.24	L
	Taran et al. (2010)	1.05	1.51	L
		1.05	1.47	L
		1.06	1.55	L
		1.07	1.52	L
	Proskurowski et al. (2008)	1.01	1.15	F
		1.01	1.15	F
		1.01	1.15	F
		1.01	1.15	F
		1.01	1.12	F
		1.01	1.12	F
		1.01	1.13	F
	Kelley & Frueh-Green (1999)	1.01	1.07	F
		0.99	1.08	F
		1.00	1.10	F
		1.01	1.09	F
		1.02	1.12	F
		1.02	1.13	F
		1.02	1.11	F
	Suda et al. (2014)	1.00	0.91	F
	Sherwood Lollar et al. (1988)	1.04	1.26	F
		1.04	1.33	F
		1.03	1.29	F
		1.03	1.27	F
		1.02	1.42	F
	This Study	1.03	1.13	F

Appendix 3: Supporting Information – Chapter 3

Table A3.1. Methane concentration concentrations in discrete samples taken from the atmosphere of the Licor closed 20 cm chamber, deployed over the air-water interface directly overlying WHC2b in the summer of 2017

Sample	Peak Area	Concentration Methane (μM)	Time
F1-WHC2-0	84.9	12.80	0
F2-WHC2-20	9.3	11.15	20
F3-WHC-40	8.7	11.13	40
F4-WHC-60	0	10.94	60
F5-WHC-120	8.9	11.14	120
F6-WHC180	6.3	11.08	180
F7-WHC-240	7.7	11.11	240
F8-WHC-300	10.6	11.17	300

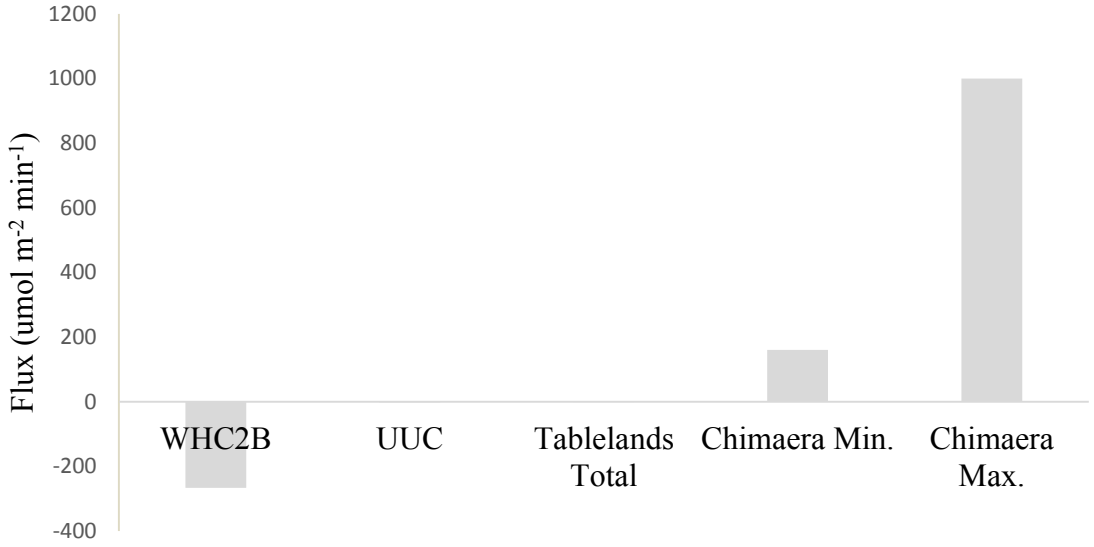

Figure A3.1. Flux at Tablelands sampling sites WHC2B and UUC, and the total flux calculated at the Tablelands Ophiolite, compared to the minimum (Min.) and maximum (Max.) flux values reported for the Chimaera gas seeps (Etiope et al., 2011).